

ON THE NUMERICAL SOLUTION OF NONLINEAR PROBLEMS
IN CONTINUUM MECHANICS

by

Mahmoud Abdel-Ghany Abo-Elkhier, B.Sc., M.Sc.

A Thesis

Submitted to the School of Graduate Studies

in Partial Fulfilment of the Requirements

for the Degree

Doctor of Philosophy

McMaster University

February 1985



ON THE NUMERICAL SOLUTION OF NONLINEAR PROBLEMS
IN CONTINUUM MECHANICS

DOCTOR OF PHILOSOPHY

(Mechanical Engineering)

McMASTER UNIVERSITY

Hamilton, Ontario

TITLE: ON THE NUMERICAL SOLUTION OF NONLINEAR PROBLEMS
IN CONTINUUM MECHANICS

AUTHOR: Mahmoud Abdel-Ghany Abo-Elkhier
(B.Sc. - Cairo University, Egypt)
(M.Sc. - Cairo University, Egypt)

SUPERVISOR: Professor M.A. Dokainish

NUMBER OF PAGES: xvi, 157

ABSTRACT

A critical discussion of the formulation methods for the finite element analysis of nonlinear problems is given, which includes the Lagrangian, the updated Lagrangian, and the Eulerian formulation. It is shown that each formulation is suitable for a specific class of nonlinear problems. In the literature many authors treat updated Lagrangian formulation as an Eulerian formulation. Therefore, the basic differences between the two formulations are critically discussed.

Consistent Lagrangian and updated Lagrangian formulation are derived from the virtual work principle expressed in current configuration, then transformed to the proper reference configuration. A detailed Eulerian formulation in the current configuration is derived by means of the virtual work principle. Explicit forms for the stiffness matrices contributing to the total nonlinear stiffness matrix, for the mass matrix, and for the load increments are presented in each case. Differences between the presented Lagrangian and the updated Lagrangian formulations and similar formulations in the literature are found to exist in the number of the stiffness matrices in the final incremental equilibrium equations as well as in the definition of the load increments. These differences as well as those between the existing formulations in the literature are assessed within the framework of the basic equations of the continuum mechanics. Specific forms of constitutive equations for elastic and elasto-plastic response of the materials are presented. A discussion on the use of the stress-rates to derive acceptable constitutive equations is also given.

For the Lagrangian and the updated Lagrangian formulation two example problems have been solved to demonstrate the applicability of the presented formulations and the effect of the individual stiffness matrices as well as the definition of the follower-load which results from the consistent formulation. These problems are: elastic, large deformation static

analysis of a cantilever under uniformly distributed load and elastic-perfectly plastic dynamic analysis of a pipe-whip problem.

To assess the presented Eulerian formulation and to show the effectiveness of the Eulerian finite element analysis using fixed mesh in space, a metal-extrusion problem has been solved. In this approach, the mesh is maintained fixed in space and the increment of stress tensors for a forward incremental step are added to a set of interpolated stress tensors. Then these stresses are interpolated back to obtain the state of stress of the body-points momentarily occupying the fixed integration points of the mesh.

ACKNOWLEDGEMENTS

The author would like to express his deep appreciation to his supervisor Dr. M.A. Dokainish, for his patient guidance in this endeavour. The valuable supervision, understanding, and encouragement of Dr. Dokainish effectively helped the author to proceed with this work.

Sincere thanks are owed to Dr. G. AE. Oravas, Department of Civil Engineering and Engineering Mechanics, McMaster University, for his very valuable suggestions, extensive discussions, and guidance in every theoretical aspect of this work. The author believes that by adopting the attitude of personal-judgement, which has been developed as a result of the discussions with Dr. Oravas, he has produced a substantially better work than otherwise would have been the case.

Sincere gratitudes are owed to Dr. M.S. Gadala, at Research Division, Ontario Hydro, for his valuable stimulation of the present research, extensive discussions, and the support in every aspect of this work. The author would like to acknowledge Dr. Gadala for bringing this fundamental problem in mechanics to his attention.

The financial assistance of McMaster University and the National Research Council of Canada in the form of scholarships is appreciated.

Thanks are also due to the staff of the Engineering Word Processing Centre for their expert typing of the manuscript.

TABLE OF CONTENTS

	PAGE
Abstract	iii
Acknowledgements	v
Table of Contents	vi
List of Symbols	x
List of Figures	xiii
List of Tables	xvi
CHAPTER I: INTRODUCTION	1
I.1 PREAMBLE	1
I.2 PRELIMINARY REMARKS	1
I.3 STATEMENT OF THE PROBLEM	3
I.4 SCOPE OF THE WORK	4
I.4.1 Survey of Formulation Methods	4
I.4.2 Formulation Methods	4
I.4.2.1 Lagrangian Formulation	4
I.4.2.2 Updated Lagrangian Formulation	5
I.4.2.3 Eulerian Formulation	5
I.4.2.4 Constitutive Equations	5
I.4.3 Numerical Assessment of Different Matrices in Each Formulation	5
CHAPTER II: FORMULATION METHODS OF NONLINEAR PROBLEMS IN CONTINUUM MECHANICS. LITERATURE SURVEY	7
II.1 INTRODUCTION	7

TABLE OF CONTENTS (continued)

	PAGE
II.2 LAGRANGIAN (REFERENTIAL) FORMULATION	9
II.3 UPDATED LAGRANGIAN (RELATIVE) FORMULATION	17
II.4 EULERIAN (SPATIAL) FORMULATION	22
 CHAPTER III: LAGRANGIAN AND UPDATED LAGRANGIAN FORMULATIONS AND APPLICATIONS	 27
III.1 FORMULATION OF THE INCREMENTAL EQUILIBRIUM EQUATIONS	27
III.1.1 ASSUMPTIONS AND BASIC EQUATIONS	27
III.1.1.1 General Assumptions	27
III.1.1.2 Nomenclature	28
III.1.1.3 Deformation Gradient Tensors and Strain Measures	28
III.1.1.4 Displacement Assumption	30
III.1.1.5 Incremental Strain Tensors	31
III.1.1.6 Virtual Work Principle	32
III.1.2 LAGRANGIAN (REFERENTIAL) FORMULATION	33
III.1.3 UPDATED LAGRANGIAN (RELATIVE) FORMULATION	34
III.1.4 CONSTITUTIVE EQUATIONS	43
III.2 APPLICATIONS	48
III.2.1 LARGE DISPLACEMENT STATIC ANALYSIS OF A CANTILEVER	48
III.2.1.1 Analysis Using the Isoparametric Plane Stress Element	48
III.2.1.2 Analysis Using the Isoparametric Beam Element	66

TABLE OF CONTENTS (continued)

	PAGE
III.2.2. DYNAMIC ANALYSIS OF A PIPE-WHIP PROBLEM	75
III.3. DISCUSSION	90
CHAPTER IV: EULERIAN FORMULATION AND APPLICATION	93
IV.1. FORMULATION OF THE INCREMENTAL EQUILIBRIUM EQUATIONS	94
IV.1.1. ASSUMPTION AND BASIC EQUATIONS	94
IV.1.1.1. General Assumptions	94
IV.1.1.2. Nomenclature	94
IV.1.1.3. Kinematics of the Motion	94
IV.1.1.4. Displacement Assumption	97
IV.1.2. EULERIAN FORMULATION	98
IV.1.3. CONSTITUTIVE EQUATIONS	102
IV.2. FINITE ELEMENT ANALYSIS PROCEDURES USING THE EULERIAN FORMULATION (EULERIAN FIXED MESH TECHNIQUE)	103
IV.3. APPLICATION: STRESS AND DEFORMATION ANALYSIS OF METAL-EXTRUSION PROCESS	104
IV.3.1. Problem Description and Solution Procedures	106
IV.3.2. Boundary Conditions for Fixed Mesh Metal-Extrusion Analysis	111
IV.3.3. Interpolation Techniques	113
IV.3.4. Incompressibility Constraint	115
IV.3.5. Numerical Results	119
CHAPTER V. CONCLUSIONS	129

TABLE OF CONTENTS (continued)

	PAGE
REFERENCES	133
APPENDIX A TRANSFORMATION OF THE VIRTUAL WORK PRINCIPLE	144
APPENDIX B SHAPE FUNCTIONS AND SHAPE FUNCTION DERIVATIVES OF THE ISOPARAMETRIC 8-NODE PLANE ELEMENT	147
APPENDIX C THE RELATION BETWEEN HOOKEAN TENSOR AND STRESS-STRAIN MATRIX.	150
APPENDIX D SHAPE FUNCTIONS AND SHAPE FUNCTION DERIVATIVES OF THE ISOPARAMETRIC 3-NODE BEAM ELEMENT.	153
APPENDIX E TRANSFORMATION OF THE SHAPE FUNCTION DERIVATIVES FROM THE GLOBAL AXES TO THE LOCAL AXIS.	156

LIST OF SYMBOLS

The following is a list of frequently used symbols. For a brief comment on the adopted system of notation, the reader is referred to page 28 of this document.

\bar{a}	acceleration vector
A	area of the loading surface
\bar{b}	body force vector
C	configuration of a body
\bar{D}	rate of deformation tensor
\bar{D}	fourth order tensor relating stresses to strains
\bar{e}	unit base vector
\bar{e}	deformation tensor
E	Young's modulus
\bar{E}	Green-Lagrange strain tensor
\bar{F}	force vector
\bar{F}	deformation gradient tensor
h_k	interpolation functions
H	strain-hardening modulus
I	identity matrix
J	Jacobian matrix
K	element stiffness matrix
M	element mass matrix
r,s,t	local coordinate system of the element
\bar{R}	generalized force vector
\bar{S}	second Piola-Kirchhoff stress tensor

LIST OF SYMBOLS (continued)

t	time
$\bar{\bar{T}}$	first Piola-Kirchhoff stress tensor
\bar{u}	displacement vector
$\bar{\bar{u}}$	displacement gradient tensor
\bar{v}	velocity vector
\bar{V}_s	unit vector in s direction
\bar{V}_t	unit vector in t direction
$\bar{\bar{w}}$	spin tensor
X	body-point
\bar{x}	current or spatial position vector
\bar{X}	reference or Lagrangian position vector
Y	yield stress
$\bar{\bar{I}}$	identity tensor
δ	variation operation
Δ	prefix indicating a finite increment
Σ	prefix indicating summation
σ	effective stress
$\bar{\sigma}$	Cauchy stress tensor
$\bar{\tau}$	nominal or Kirchhoff stress tensor
ξ	effective strain
$\bar{\bar{\epsilon}}$	Euler-Almansi strain tensor
ρ	mass density
ν	Poisson's ratio
ψ	displacement interpolation function

LIST OF SYMBOLS (continued)

SUBSCRIPTS

Right Subscripts

- i direction
- j direction
- K number of nodes per element

Left Subscripts

- 0, 1, 2 configuration to which the quantity is referred

SUPERSCRIPTS

Right Superscripts

- T transpose of a matrix, or of a tensor
- 1 inverse of a matrix, or of a tensor


Left Superscripts

- 0,1,2 configuration at which the quantity is measured

LIST OF FIGURES

FIGURE	DESCRIPTION	PAGE
II.1	Geometry of the motion from configuration C_0 to C_1 to C_2	14
III.1	Cantilever under uniformly distributed load	50
III.2	Finite element mesh for the cantilever	50
III.3	Two-dimensional element undergoing large deformation	51
III.4	A three-dimensional element showing an infinitesimal surface area as a vector normal to the face	54
III.5	Large displacement analysis of a cantilever using Lagrangian formulation	56
III.6	Large displacement analysis of a cantilever using Lagrangian formulation	57
III.7	Large displacement analysis of a cantilever using Lagrangian formulation	59
III.8	Large displacement analysis of a cantilever using updated Lagrangian formulation	61
III.9	Large displacement analysis of a cantilever using updated Lagrangian formulation	64
III.10	Large displacement analysis of a cantilever using updated Lagrangian formulation	65
III.11	Large displacement analysis of a cantilever using updated Lagrangian formulation	67
III.12	Beam element undergoing large displacements and rotations	68
III.13	Large displacement analysis of a cantilever using Lagrangian formulation	71
III.14	Large displacement analysis of a cantilever using updated Lagrangian formulation	73

LIST OF FIGURES (continued)

FIGURE	DESCRIPTION	PAGE
III.15	 Large displacement analysis of a cantilever	74
III.16	Pipe whip problem	77
III.17	Finite element modelling of the pipe-whip problem	77
III.18	Pipe beam element undergoing large displacements and rotations	78
III.19	Predicted displacement response in the pipe-whip analysis	85
III.20	Beam response at neutral axis at $t = 0.002$ seconds	86
III.21	Beam response at neutral axis at $t = 0.003$ seconds	87
III.22	Beam response at neutral axis at $t = 0.006$ seconds	88
III.23	Beam response at neutral axis at $t = 0.012$ seconds	89
III.24	Predicted displacement response in the pipe-whip analysis	91
IV.1	Continuous medium moving through a fixed region R in space	95
IV.2	Finite element mesh for the extrusion problem	108
IV.3	Configuration of the plastic region in the steady state	109
IV.4	The stress-strain relation for the aluminum which is used in the analysis	110
IV.5	A part of the mesh showing the imaginary mesh	114
IV.6	The distribution of the longitudinal stress σ_{xx} at steady state	121
IV.7	The distribution of the shear stress σ_{xy} at steady state	122
IV.8	The distribution of the normal stress σ_{yy} at steady state	123
IV.9	The distribution of the longitudinal stress σ_{xx} at steady state (Yamada et al. [106])	124
IV.10	The distribution of the shear stress σ_{xy} at steady state (Yamada et al. [106])	125

LIST OF FIGURES (continued)

FIGURE	DESCRIPTION	PAGE
IV.11	The distribution of the normal stress σ_{yy} at steady-state (Yamada et al. [106]).	126
IV.12	The distribution of the longitudinal stress σ_{xx} at steady-state (Lee et al. [99]).	127
IV.13	The distribution of the shear stress σ_{xy} at steady-state (Lee et al. [99]).	128

LIST OF TABLES

TABLE	TITLE	PAGE
III.1	Number of equal load increments required to obtain identical solutions for different Lagrangian formulations	58
III.2	Number of equal load increments required to obtain identical solutions for different updated Lagrangian formulations	63
III.3	Step-by-step solution using Newmark method	82

CHAPTER I INTRODUCTION

I.1 PREAMBLE

During recent years an increasing demand for the solution of various engineering problems with geometric and/or material nonlinearity has arisen, and, consequently, an intensive research effort has been devoted to the development of efficient solution procedures for such problems. The increasing importance of nonlinear analysis is largely due to the emphasis placed by various agencies in more realistic modelling and accurate analysis of critical structural components which arise, for example, in the safety consideration of strategic structures and nuclear reactor components, and in the design of satellites. Lately, the finite element method has proven to be very effective in linear analysis, and by means of it solutions have been obtained to some rather complex nonlinear problems, yet most problems are still very difficult and computationally very expensive to analyze. Recently, much research is underway to improve the theory of continuum mechanics, the constitutive equations of the material experiencing large deformation, the finite element formulation, the numerical integration procedures, and the computer implementations. Presently, various large scale computer programmes and smaller special purpose codes are used which offer various capabilities for analysis. Although these codes can be used effectively to solve a large number of problems, they still have serious limitations.

I.2 PRELIMINARY REMARKS

The solutions of nonlinear problems in continuum mechanics mainly contain two types of nonlinearity: the geometric and the material nonlinearity. Geometric nonlinearity

arises from nonlinear strain-displacement relations, whereas material nonlinearity arises from the material response as in inelastic, elasto-plastic, and creep behaviour of the material. The main aspects in the formulation of such problems are: the choice of proper formulation for specific applications, the proper modelling of physical problems, the construction of the proper constitutive equations, the introduction of an incompressibility constraint, and the use of proper numerical techniques for solving the nonlinear equilibrium equations. In what follows, the formulation methods are briefly discussed. In Chapter II a more detailed discussion will be given. The other aspects of the formulation will be discussed later.

Four types of kinematic description of motion are in common use in continuum mechanics. According to Truesdell's definition [1,2], these four types are: the material, the referential, the spatial, and the relative description.

1. In the material description, the independent variables are the body-point X and the time t . This description is the most natural one from the point of view of the general principles of motion and is used exclusively in analytical dynamics.
2. In the referential description, the independent variables are the position \bar{x} of the body-point X in an arbitrarily chosen reference configuration and the time t .
3. In the spatial description, the independent variables are the current position \bar{x} of the body-point X and the time t .
4. In the relative description, the independent variables are the position \bar{x} of the body-point X in the present configuration and a variable time t .

In finite element applications, only three descriptions of motion are in common use: the referential (Lagrangian), the spatial (Eulerian), and the relative (updated Lagrangian) description. The relative description (updated Lagrangian) is introduced to overcome some disadvantages of the referential (Lagrangian) description. The formulation of the Finite

element theory based on these three descriptions are called the referential (Lagrangian), the spatial (Eulerian), and the relative (updated Lagrangian) formulation.

1.3 STATEMENT OF THE PROBLEM

In nonlinear analysis of problems involving large deformation and material nonlinearity, it is necessary to rely on the incremental formulation of the equations of motion. Most of the researches which have been done in formulating the equations of motion in the finite element solutions start with the virtual work principle, or the energy balance equation, in the deformed configuration and then transform it either to the (referential) undeformed configuration in the Lagrangian formulation, or to the present (the last calculated) configuration in the updated-Lagrangian formulation. On the other hand, in the Eulerian (spatial) formulation these equations should be considered in the current configuration.

It appears that most of the work done on finite element formulations of nonlinear continua is based on the Lagrangian formulation and only relatively small amount of research use the updated Lagrangian formulation, whereas very little effort has been made concerning a detailed Eulerian formulation.

In the Lagrangian and the updated Lagrangian formulation, it appears that the inconsistent transformation of the virtual work principle leads to incorrect definition of the load increment and the stiffness matrices [15, 21-24, 45, 52-56, 61-74]. It also appears that during the linearization process of the kinematic relations within the increment some non-linear terms have been omitted when they appear with other incremental quantities [11, 23]. Also, some of the existing formulations introduce an implicit final form for the stiffness matrices contributing to the total stiffness matrix of the element [14, 44, 45, 67, 71]. More-

over, some of the updated Lagrangian formulations have been mistakenly named Eulerian formulations [72, 80, 81, 83].

In the Eulerian formulation mentioned above many authors treat the updated Lagrangian formulation as an Eulerian formulation. Hence, relatively little effort has been devoted to the development of a consistent and detailed Eulerian formulation [51, 85, 86].

1.4 SCOPE OF THE WORK

1.4.1 Survey of Formulation Methods

In this section, the different formulation methods for the finite element analysis of nonlinear problems and their pertinent characteristics are critically discussed, and the differences between the existing formulations in the literature are examined. These differences may be due to the simplifying assumptions imposed upon the nonlinear kinematic relations within the linear increment, to the different uses of stress measures and their conjugate strain definitions, and to the interpretations of the virtual work principle in the undeformed Lagrangian configuration. The basic differences between the updated Lagrangian and Eulerian formulation are explained. Finally, the choice of the proper formulation for specific applications is discussed.

1.4.2 Formulation Methods

1.4.2.1 Lagrangian Formulation

A consistent Lagrangian formulation is derived from the virtual work principle established with respect to the current configuration; and then transformed to the Lagrangian undeformed configuration. For comparison, explicit forms for the individual stiffness matrices contributing to the total stiffness matrix of the element are given. For numerical convenience, the form of the total stiffness matrix of the element has been

rearranged. Differences between the derived formulation and similar formulations [5, 14-21, 31, 44, 45] in the literature are discussed.

1.4.2.2 Updated Lagrangian Formulation

An updated Lagrangian formulation is derived on a basis similar to the development of the Lagrangian formulation. The form of the individual stiffness matrices are presented. The final form of the total stiffness matrix has been rearranged as it was done in the Lagrangian formulation. Once again, differences between the present formulation and similar formulations [16-21, 31] in the literature are discussed.

1.4.2.3 Eulerian Formulation

A detailed Eulerian formulation in the current configuration has been derived by means of the virtual work principle. Specific approximations which make Eulerian formulation suitable for numerical applications are examined. The distinctions between the presented formulation and those existing [85,86] in the literature are discussed.

1.4.2.4 Constitutive Equations

The constitutive equations for linearly elastic response, and infinitesimal strains are only considered. Discussion on the use of stress rates which are invariant with respect to rigid body rotations for the derivation of acceptable constitutive equations is presented.

1.4.3 Numerical Assessment of the Different Stiffness Matrices in Each Formulation

For the Lagrangian and the updated Lagrangian formulation two example problems have been solved to demonstrate the applicability of the presented formulations and the effect of the individual matrices on the accuracy of the analysis. The two problems are:

elastic, large displacement analysis of a cantilever under uniformly distributed load and elastic-perfectly plastic analysis of a pipe-whip problem.

To assess the presented Eulerian formulation and to demonstrate the numerical procedures which can be used to solve nonlinear problems based on the Eulerian formulation, a metal-extrusion problem has been solved. In general, some metal-forming processes, such as extrusion, rolling, and drawing, operate under steady-state condition. Therefore, the analysis of such processes is facilitated by the use of an Eulerian type mesh which is fixed in space.

CHAPTER II
FORMULATION METHODS OF NONLINEAR PROBLEMS IN CONTINUUM
MECHANICS: LITERATURE SURVEY

II.1 INTRODUCTION

For the description of the motion of a body, there exist four methods of formulation; Truesdell [1,2] calls them: the material, the referential, the spatial, and the relative formulation.

1. In the material description, the independent variables are the body-point X , and the time t . This description is the most natural one with respect to general principles of motion, and is the one exclusively used in analytical dynamics. However, it is rarely used in formulating problems in continuum mechanics, and especially so in the finite element method of solution.
2. In the referential description, the independent variables are the position \bar{x} of the body-point X in an arbitrarily chosen reference configuration, and the time t . It should be noticed that the choice of the reference configuration is arbitrary, and such a choice should not affect the results of the analysis. A particular referential description was introduced by Euler in which the reference configuration is taken as the configuration of the body at $t=0$, which means that the position \bar{X} of the body-point X at the particular time $t=0$ is used to describe the subsequent motion of the body-point. This particular description is often called Lagrangian description in the literature. Thus, the motion $\bar{x} = \bar{x}(\bar{X}, t)$ gives the position occupied by the body-point X at time t in the Lagrangian description.

3. In the spatial description, the independent variables are the current position \bar{x} of the body-point X , and the time t . In the spatial description, attention is focussed on what is happening in a fixed region in space as the time progresses instead of on a given element of the body. This description seems to be ideally suited for the analysis of the flow problems. It was introduced by Daniel Bernoulli, and later used by D'Alembert and Euler in hydrodynamics, but in the literature it is usually called the Eulerian description. It is important to emphasize the fact that the independent variable \bar{x} is a function of the Lagrangian position \bar{X} and the time t , i.e. $\bar{x} = \bar{x}(\bar{X}, t)$. In the spatial description, for example, the velocity field is a function of the current position \bar{x} and the time t , $\bar{v} = g(\bar{x}, t)$, where the function g is unique. Thus, while there are infinitely many referential descriptions for any given motion, there is only one unique spatial description. Owing to the explicit dependence of the current position \bar{x} on the time in tracing the motion of a body-point, X , all material time derivatives are more complicated in the spatial description.
4. In the relative description, the independent variables are the position \bar{x} in the present configuration and the time t , whereas the present configuration itself depends upon the time. Since the present configuration is taken as the reference configuration, the past and the future configurations are described relative to the present configuration. The variable time t is the time relative to the present configuration when the body-point X occupied the position $\bar{\xi} = \bar{\xi}(\bar{x}, t)$. It is important to observe that, instead of using \bar{X} at time $t=0$ in the referential description, the position \bar{x} at time t is used in the relative description, which justifies the assignment of the referential nature to the relative description. This description in Finite Element analysis is usually called the updated Lagrangian

description; and it is introduced to avoid some of the disadvantages of the Lagrangian description which will be discussed in the following sections.

As mentioned above, only the last three descriptions are in common use for finite element formulations of problems in nonlinear continuum mechanics. In the following sections, an assessment of different finite element formulations available in the literature within the framework of the definitions given above is presented. The simplifying assumptions and the reasons for the differences between the existing formulations are also examined. Finally, the choice of the proper formulation for specific nonlinear problems is discussed.

II.2 LAGRANGIAN (REFERENTIAL) FORMULATION

Lagrangian formulation is the most natural one and, also, is the most widely used formulation in finite element analysis of nonlinear problems, see for example references [11, 14-28] among many others. The main advantage of the Lagrangian formulation which refers the motion to a fixed reference configuration is that: the treatment of most of the kinematic questions in such configuration is relatively simple. This advantage exists actually for all integrated quantities since in the Lagrangian formulation the integration is taken over the initial configuration. Another advantage of the Lagrangian formulation is the simplicity with which material time derivatives can be calculated. However, the use of the Lagrangian formulation entails some disadvantages which come from the requirement of a continuous updating of the boundary conditions as, for example, in contact problems, metal-forming problems, and crack-propagation problems, all of which are difficult to handle in the Lagrangian formulation. In addition, the requirement that the stresses which act in the instantaneous configuration have to be referred to the initial configuration is physically quite artificial yet mathematically consistent. The continuous deformation of the

body tends to distort the original finite element mesh, and such distortion might affect the accuracy and the reliability of the solution.

Most of the Lagrangian finite element formulations utilize an incremental method based on linear increments. The general approach to the incremental Lagrangian formulation is to consider complete nonlinear kinematic relations within a linear increment. The differences between the existing formulations are due to simplifying assumptions imposed upon the nonlinear kinematic relations within the increment, to the interpretation of the virtual work principle in the initial Lagrangian configuration, and to the use of different stress measures and their conjugate strain definitions. In the incremental theory, the incremental equilibrium equations may be formulated by using the virtual work principle [13-27, 29-33, 36-45] or the energy balance equation [46-49, 51, 85], and then variations in the variables are imposed. In the rate-type theories of continuum mechanics, the incremental equilibrium equations may be formulated by utilizing rates of the variables within the increment [72, 97-99, 104-109].

In this work, the Lagrangian formulation is based on the virtual work principle referred to the current configuration (see Chapter III). When fully nonlinear kinematic relations are used within a linear increment, it is found that there are three stiffness matrices contributing to the nonlinear element stiffness matrix [4,5]. These are: the usual small displacement or the incremental stiffness matrix, the initial stress or the geometric stiffness matrix, and the initial displacement or the initial rotation stiffness matrix. Also, it is found from the consistent development of the incremental equilibrium equations that a fourth stiffness matrix: the load-correction matrix, or the initial load matrix contributes to the total stiffness matrix. Many authors, however, differ in considering the load-correction matrix as will be discussed later.

As stated above, one of the main reasons for the differences between the existing formulations is the simplifying assumptions imposed on the kinematics relations. Much of the earlier literature on finite element applications to geometrically nonlinear problems neglected the initial displacement, or the initial rotation stiffness matrix and used the initial stress stiffness matrix to correct the usual small displacement or the incremental stiffness matrix at the end of each load increment. As discussed by Oden [4] and Oden et al. [41], unless a new frame of reference is established in the deformed element at the end of each increment, as is done, for example, by Stricklin et al. [33, 36] and Murray et al. [43], this procedure is incorrect. Also, for higher order elements, this convected coordinate system may be inadequate since finite rotations within the element may take place. The importance of including the initial displacement stiffness matrix in certain nonlinear analysis is discussed by Marcal [54]. Martin [58] makes an early attempt to develop the incremental Lagrangian formulation for geometrically nonlinear problems by including the higher order terms in the strain tensor, and presents an expression for the initial displacement stiffness matrix for some elements. In reference [59] Kawai follows a similar approach with application to elastic plates. Wunderlich [23] has introduced a consistent development of an incremental Lagrangian formulation. However, he omits specific nonlinear terms for the intended linearization process within the increment, when they appear with incremental quantities. In reference [24] and [65] a similar simplified approach is applied to the plate and shell problems. Larsen et al. [44] present an incremental Lagrangian formulation by means of subtracting the virtual work principle referred to two consecutive configurations. However, they present an implicit form for the incremental equilibrium equations. In a similar treatment, Felippa et al. [67] also introduce an incremental Lagrangian formulation and present an implicit form for the individual stiffness matrices contributing to the total nonlinear stiffness matrix. Jones et al. [69, 70] develop a different Lagrangian formulation in

which they use the variation of the incremental strain tensor in the current configuration instead of the present configuration, and, consequently, obtain an expression for element total stiffness matrix which is unsymmetric. Jones et al. [69, 70] eliminate the initial stress, or the geometric stiffness matrix, while its contribution is included in the generalized load term through an estimation of the next incremental displacements.

Cescotto et al. [25, 26] and Frey et al. [27] introduce generalized incremental equilibrium equations for the Lagrangian formulation based on the virtual work principle. They assume a nonlinear displacement field within the element. The final incremental equilibrium equations include an additional initial stress matrix and a symmetric initial load matrix which, in general, have non-zero values. However, it should be noticed that in the usual isoparametric finite element formulation, the shape functions are linearly dependent on the generalized displacements, and therefore, these two additional matrices will identically vanish. Carey [28] presents a Lagrangian formulation based on the strain energy for geometrically nonlinear problems. He shows that various early approximations for geometric nonlinear formulation may be obtained by introducing or neglecting specific terms in the complete strain energy expression.

Fully nonlinear kinematic relations are used by Oden [4] and Oden et al. [39-41], Marcal [53, 55], Hibbit et al. [52], and followed by many authors. Bathe [14,15], Bathe et al. [16-21], and Ishizaki et al. [31] also follow the generalized consistent approach for deriving the Lagrangian formulation but they present an implicit form for the final incremental equilibrium equations. Also, Ramm [22], Nagarajan et al. [68], Brockman [45], and Mondkar et al. [64] have used the same approach as in references [17-21] to develop their formulations and they also present an implicit form for the final incremental equilibrium equations. Gadala [51] and Gadala et al. [46-49] use a different approach to develop their formulation which is based on the energy balance equation, and then by utilizing increments of the

variables within a linear increment to derive explicit forms for the element stiffness matrices and the increment of the load vector. We may state concerning this particular discussion that none of the stiffness matrices contributing to the total stiffness matrix of the element should in general be omitted.

The second point which may be one of the reasons for the differences existing between the various formulations is the transformation of the virtual work principle from the current (incremented) configuration to the initial (undeformed) configuration. Most of the works done in the Lagrangian as well as in the other formulations start with the virtual work principle expressed in the current configuration. If we consider three different configurations of the body; the initial (undeformed) configuration C_0 at time 0, the present (the last calculated) configuration C_1 at time t , and the current (the incremented) configuration C_2 at time $t + \Delta t$, see Figure (II.1), then we may express the virtual work principle in the current configuration C_2 as

$$\int_{2V} {}^2\bar{\sigma} : \delta {}^2\bar{e} \, d^2V + \int_{2V} {}^2\rho {}^2\bar{a} \cdot \delta {}^2\bar{u} \, d^2V = \int_{2V} {}^2\rho {}^2\bar{b} \cdot \delta {}^2\bar{u} \, d^2V + \int_{2A} d^2A \cdot {}^2\bar{\sigma} \cdot \delta {}^2\bar{u} \quad (\text{II.1})$$

where the left superscripts indicate the configuration at which the quantity is measured.

${}^2\bar{\sigma}$ is the Cauchy stress tensor,

$$\delta {}^2\bar{e} = \frac{1}{2} \left(\frac{\partial \delta {}^2\bar{u}}{\partial {}^2x} + \frac{\delta {}^2\bar{u}}{\partial {}^2x} \right)$$

is the variation of the deformation tensor,

2V is the current volume,

${}^2\rho$ is the material density,

${}^2\bar{a}$ is the current acceleration vector,

$\delta {}^2\bar{u}$ is the variation of the displacement vector,

${}^2\bar{b}$ is the body force per unit mass,

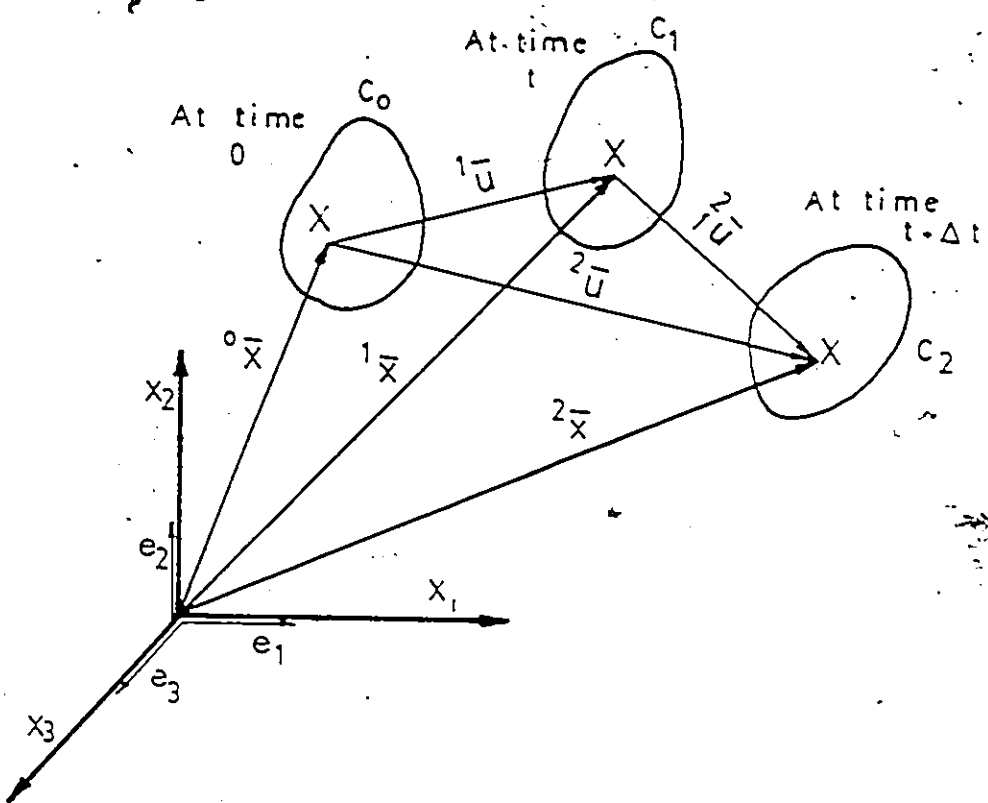


Figure (II 1) Geometry of the motion from configuration C_0 to C_1 to C_2

2A is the current loaded areas.

${}^2\bar{\sigma}:\delta^2\bar{e}$ means the double dot-product of the two second order tensors ${}^2\bar{\sigma}$ and $\delta^2\bar{e}$ (i.e. ${}^2\bar{\sigma}:\delta^2\bar{e} = {}^2\bar{\sigma}_{ij}\delta^2e_{ij}$).

A consistent transformation of eqn. (II.1) from the current deformed configuration to the initial configuration gives [4, 39, 41] (also see Appendix A).

$$\int_{0V} {}^2\bar{S}:\delta^2\bar{E} d^0V + \int_{0V} {}^0\rho {}^2\bar{a} \cdot \delta^2\bar{u} d^0V = \int_{0V} {}^0\rho {}^2\bar{b} \cdot \delta^2\bar{u} d^0V + \int_{0A} d^0\bar{A} \cdot {}^2\bar{S} : {}^2\bar{F}^T \cdot \delta^2\bar{u} \quad (\text{II.2})$$

where the left subscripts indicate the configuration to which the quantity is referred,

${}^2\bar{S}$ is the second Piola-Kirchhoff stress tensor,

$\delta^2\bar{E}$ is the variation of the Green-Lagrange strain tensor,

0V is the initial volume,

${}^0\rho$ is the material density in the initial configuration,

${}^2\bar{F}^T$ is the transpose of the deformation gradient tensor.

In the previous work, it appears that many authors differ in their treatment of the surface traction term in eqn. (II.2). Bathe and his coworkers [14-21, 31] drop the transpose of the deformation gradient tensor ${}^2\bar{F}^T$ from the surfaces traction term. Also, ${}^2\bar{F}^T$ has been dropped in references [22, 23, 44, 52-56, 64]. White, in reference [52] Hibbit et al. introduce a rather intuitive argument by setting $\Delta\bar{F} = \Delta_{\text{load}}\bar{F} + \Delta_{\text{geom.}}\bar{F}$ where \bar{F} is the surface traction or the body force vector to obtain the form of the load-correction matrix which has zero value in some loading cases. In [17] Bathe et al. consider a similar treatment to that given by Hibbit et al. [52] for the deformation-dependent loading. Also, in reference [68] a similar consideration for the load-correction matrix is presented. The load-correction matrix derived here is obtained through consistent transformation of the virtual work principle with no

reference to the type of loading. The development of the load-correction matrix presented here is similar to the procedures given by Oden [4], and Oden et al. [39,41] even though, their form of the load-correction matrix does not coincide with the form derived here. However, Oden et al. pointed out the importance of including the load-correction matrix in the incremental formulations. In conclusion, we suggest that the introduction of the load-correction matrix is important both in large strain and in infinitesimal strain analysis with finite rotations. The effect of including this matrix on the accuracy of the solution is dependent on the nature of the application.

Finally, we make some critical remarks about the choice of the compatible stress and strain measures. Within the framework of the definitions given by Hill [127, 128] and based on the virtual work of stresses per unit current volume expressed as $\bar{\sigma} \delta \bar{e}$, the conjugate pairs of the stress and strain can be expressed as follows

$$[\bar{\sigma}, \delta \bar{e}], [\bar{\tau}, \delta \bar{e}], [\bar{T}, \delta F], [\bar{S}, \delta E] \quad (11.3)$$

where $\bar{\sigma}$ and \bar{e} are defined above, and

$$\bar{\tau} = [\bar{F}] \bar{\sigma} \quad (11.4)$$

is the nominal or Kirchhoff stress tensor,

$$\bar{F} = \frac{\bar{\sigma}}{\partial X} \quad (11.5)$$

is the deformation gradient tensor,

$$[\bar{F}] = (\bar{F} \bar{F}^{\times} \bar{F})/3! \quad (11.6)$$

is the third scalar invariant of the deformation gradient tensor, and \bar{F}^{\times} represent double-dot and double cross products of tensors, respectively,

$$\bar{T} = [\bar{F}] \bar{F}^{-1} \bar{\sigma} \quad (11.7)$$

is the unsymmetric first Piola-Kirchhoff stress tensor, \bar{F}^{-1} is the inverse of the deformation gradient tensor \bar{F} ,

$$\bar{S} = [\bar{F}] \bar{F}^{-1} \bar{\sigma} (\bar{F}^{-1})^T = \bar{T} [\bar{F}^{-1}]^T \quad (11.8)$$

is the symmetric second Piola-Kirchhoff, also known as the Kirchhoff-Trefftz stress tensor,

$$\bar{\bar{E}} = \frac{1}{2} [\bar{\bar{F}}^T \cdot \bar{\bar{F}} - \bar{\bar{I}}] \quad (\text{II.9})$$

is the Green-Lagrange, or the Euler-Lagrange strain tensor and, finally, $\bar{\bar{I}}$ is the identity tensor.

In finite element formulations, the last two conjugate pairs are in common use, especially the last pair. It can be seen from eqns. (II.1) and (II.2) that the transformation of the virtual work principle from the current to the undeformed configuration leads to an expression of virtual work of stresses in terms of $\bar{\bar{S}}$ and $\bar{\bar{E}}$ which is used by many authors [14-27, 31-33, 34-41, 44-58]. Owing to the symmetry of the second Piola-Kirchhoff stress tensor $\bar{\bar{S}}$, the formulation identically satisfies the moment equilibrium equations. The use of the conjugate pair $\{\bar{\bar{T}}, \delta\bar{\bar{F}}\}$ arises mainly in formulating the incremental equilibrium equations based on the complementary energy principle. This will not be discussed in this work since we are concerned with the displacement-based finite element formulation, which at present is regarded to be the most effective method of analysis.

II.3 UPDATED LAGRANGIAN (RELATIVE) FORMULATION

As discussed above, the reference configuration in the relative description is taken at a variable time t . In the relative description, we describe the past and the future configuration with respect to the present. In the updated Lagrangian the independent variables are \bar{x} and τ , where \bar{x} is the position occupied by the body-point X at time t . This indicates that the present configuration is dependent on the time t , a feature which makes the relative formulation referential in nature. It should be noticed that, in updated Lagrangian formulation we still follow the deformation of the body-point X , yet, the deformations are referred to the present configuration. This is different from the Eulerian formulation in which we are concerned with what is happening in a fixed region in the space. This particular

point is usually ignored in the finite element literature, and many authors [72, 80, 81, 83, 84] describe the updated Lagrangian (relative) formulation under the name of Eulerian formulation.

Owing to the nature of the updated Lagrangian, it has certain advantages compared to the Lagrangian formulation. For example, the continuous updating of the boundary conditions and the mesh distortion will be relatively easy to handle in the updated Lagrangian formulation. Also, in the updated Lagrangian formulation the stresses will be referred to the present configuration which represents the true stress state. On the other hand, since the reference configuration is variable it may lead to some difficulties in carrying out the integration over the present configuration. Also, in the updated Lagrangian formulation, special attention should be devoted to the transformation of the stress and strain tensors in each increment.

As in the Lagrangian formulation, the differences between the existing updated Lagrangian formulations basically lie in the simplifying assumptions imposed on the kinematic relations, the interpretation of the transformed virtual work principle in the present configuration, and the use of different stress measures and conjugate strains. Once again, we base the updated Lagrangian formulation on the virtual work principle written in the current configuration, eqn (II.1). In a procedure similar to that given in Appendix A, the virtual work principle referred to the present configuration may be expressed in the form

$$\int_{1V} {}_1^2 \bar{S} : \delta {}_1^2 \bar{E} d^1V + \int_{1V} {}_1 \rho^2 \bar{a} \cdot \delta {}_1^2 \bar{u} d^1V - \int_{1V} {}_1 \rho^2 \bar{b} \cdot \delta {}_1^2 \bar{u} d^1V + \int_{1A} d^1 \bar{A} \cdot {}_1^2 \bar{S} \cdot {}_1^2 \bar{F}^T \cdot \delta {}_1^2 \bar{u} \quad (II.10)$$

As shown in Chapter III, the use of the fully nonlinear kinematic relations within a linear increment gives the same number of stiffness matrices contributing to the nonlinear

element stiffness matrix as the Lagrangian formulation. However, there exist some differences in the expression of the incremental equilibrium equations.

Concerning the simplifying assumptions, Murray et al. [43] utilize a local coordinate system which translate and rotate with each element, and also refine the subdivisions of the structure. By this means, they assumed that the displacement and the displacement gradients are small with reference to the local axes. Their approach tackles the nonlinearity in the strain-displacement relationships through a geometric transformation. However, the local coordinate system may not be adequate for higher order elements. Yaghmai [62], and Yaghmai et al. [61] introduce an updated Lagrangian formulation based on the virtual work principle. The incremental virtual work-expression is obtained as the difference between the virtual work expression for two consecutive configurations. They neglect the nonlinear terms in the strain increment. Sharifi and Popov [63] extend the formulation given by Yaghmai et al. [61] to elasto-plastic analysis involving infinitesimal strains but finite rotations. In the work by Felippa and Sharifi [67] based on the Lagrangian approach, they refer to the above work and the updated Lagrangian formulation by Yaghmai et al. [61] as Eulerian formulation. In a similar procedure to that given by Yaghmai et al., Hofmeister et al. [30] present their updated Lagrangian formulation. In reference [33] Stricklin et al. follow the work by Yaghmai and Popov [61]. However, their formulation is restricted to small strains. Gunasekera et al. [75] follow a general approach to develop their formulation. They indicate that under proper updating of the coordinates of the system, the initial displacement, or the initial rotation stiffness matrix can be conveniently discarded. Wilson et al. [76] follow a systematic approach to develop the updated Lagrangian formulation, but they do not introduce a clear definition of the constitutive equations.

McMeeking and Rice [72] introduce another updated Lagrangian formulation based on the rate of the virtual work principle for the incremental deformation given by Hill

[132] under the name of the Eulerian formulation. It can be seen that their analysis follows the deformation of the body, which formulation is referential in nature, rather than, considering what is happening in a fixed region in space. Also, they discuss some previous relative formulations under the name of the Eulerian formulation. Wunderlich [23] presents a consistent development for the updated Lagrangian formulation. However, as in his Lagrangian formulation, he omits specific nonlinear terms in the linearization process within the increment. Bathe et al. [16-21, 31] follow a similar approach to present their formulation. Similar to the Lagrangian formulation, they introduce an implicit form for the incremental equilibrium equations. A similar approach is used in references [29, 71, 73, 74]. Argyris and Chan [13] give another updated Lagrangian formulation. They do not, however, give a clear definition of their stress and strain measures. Argyris et al. [12] introduce a distinct updated Lagrangian formulation on the basis of Kleiber's work [95], in which they utilize the intermediate stress-free state as a reference configuration. This configuration is obtained by the hypothetical removal of stresses without causing further plastic deformation. Since infinitesimal increments of the independent variables are used, they neglect the nonlinear terms in the incremental strain. However, the use of the natural approach which is based on stress-free state makes it difficult to compare the final equilibrium equations of Argyris's work with the corresponding ones in the literature. Cescotto et al. [25, 26] develop an updated Lagrangian formulation similar to their development of the Lagrangian formulation. In their analysis, only small displacement increments are used and it is shown that the displacement field is a linear function in the discretized parameters and, consequently, the additional initial stress matrix and symmetric load-correction-matrix vanish, whereas the unsymmetric displacement dependent, load-correction matrix will not vanish. Gadala [51] and Gadala et al. [46-49] present a consistent development of the updated Lagrangian formulation based on the energy balance equation. They also show that the most general approach for the updated

Lagrangian formulation is to consider fully nonlinear kinematic relations within a linear increment, where none of the stiffness matrices should be omitted.

Lee et al. [97-99] introduce an updated Lagrangian formulation based on the rate of the virtual work principle given by Hill [132]. Their formulation leads to a development of stress-dependent stiffness terms in case of curved boundary conditions. They present an implicit form for the final equilibrium equations. Yamada [104] and Yamada et al. [105-108] present an updated Lagrangian formulation utilizing rate quantities on the basis of Hill's work [132]. They employ stress-rates in the constitutive equations therefore their formulation leads to a development of a geometric stiffness matrix which is symmetric or unsymmetric depending on the stress-rate utilized. Therefore, the final expression of the incremental equilibrium equations is dependent on the stress-rate used in the constitutive equations. Yamada et al.'s formulation leads to a development of a load-correction factor for cases in which coupling exists between the stresses and the boundary velocities. The expression of the load-correction matrix is based on specifying the load vector associated with the updated surface area. The expression of the load vector depends on the state of deformation. Yamada et al. [105-108] suggest the use of an infinitesimal form of the strain rate-velocity relationship. This procedure eliminates the initial displacement stiffness matrix from the final incremental equilibrium equations.

Considering the virtual work principle in the present configuration, eqn. (II.10), it can be seen that the surface traction term is dependent on the relative deformation gradient tensor between the present and the current configuration. It is shown in Chapter III that this term leads to the development of the initial load, or the load correction matrix which depends on the increment of the surface traction from the present to the current configuration. As in the Lagrangian formulation, many authors differ in treating the surface traction term in eqn

(II.10). We may conclude this section with the same remarks given or discussed in the Lagrangian formulation.

The final point to discuss in the updated Lagrangian formulation is the choice of the compatible stress and strain measures. Let us refer to the definition of the conjugate pairs given by eqn. (II.3). As in the Lagrangian formulation, it can be seen from eqn. (II.10) that the last conjugate pair comes from the consistent transformation of the virtual work principle. This pair is used by many analysts [17-21, 23, 25, 26, 31, 33, 46-49, 51].

As mentioned above, Argyris and Chan [13] do not define what measures of either stress or strain are intended in their work. It is not clear that their stress measure is a member of the conjugate family.

McMeeking and Rice [72], Lee and his coworker [97-101], and Yamada and his coworkers [104-109] utilize the rate form of the virtual work principle, which has been cited by Hill [132]. Referring to the definition of the conjugate pairs, eqn. (II.3), Hill uses the rate of the third conjugate pair $\{\bar{T}, \bar{SF}\}$.

II 4 EULERIAN (SPATIAL) FORMULATION

As discussed above, the main difference between the Eulerian formulation and other formulations is that the deformation of the material moving through a fixed region in space is determined as a function of time instead of determining the deformation of the material element by following its motion in space. Furthermore the independent variables in the Eulerian description are the current position \bar{x} of the body-point X and the time t . For the material motion, \bar{x} itself becomes dependent on the time t , which fact complicates material time derivatives in the spatial description.

In the finite element analysis based on the Eulerian formulation, the above points are usually overlooked, or ignored, and many authors describe the updated Lagrangian

formulation under the name of the Eulerian formulation (see for example, Hartzman [81], McMeeking and Rice [72], and Fengels [83]). On the other hand, there has been little effort made concerning the development of a consistent Eulerian formulation (see for example, Gadala, Oravas and Dokainish [85], Nemat-Nasser and Shatoff [82], and Key [79]).

Hartzman and Hutchinson [80] make an early attempt of the Eulerian formulation in which the geometric and the material nonlinearity are considered. They utilize the proper material time derivative for the acceleration term, point out its complications and provide a lumped mass approximation to overcome the computational difficulties. The governing partial differential equations of the system are reduced to a set of simultaneous nonlinear ordinary differential equations. They present an implicit form for the incremental equilibrium equation. Hartzman and Hutchinson [80] introduce a system of local coordinates that translate and rotate with each element, which, strictly speaking, imposes a referential nature on the analysis and makes it similar to the updated Lagrangian formulation. Furthermore, it can be seen that the transformation of the stress, the strain, and the constitutive equations introduced in [80], are identical to the procedures used in the updated Lagrangian formulation.

In [82] another treatment of the Eulerian formulation is given by Nemat-Nasser and Shatoff. They utilize an absolute minimum principle for small deformation superimposed on a finitely-deformed, stable configuration of an elastic solid. An incremental formulation in the solution of problems involving geometric and material nonlinearities is given. They present an accurate discussion of the differences between the Lagrangian and the Eulerian formulation. An accurate discussion of the stress and the strain increments, and the constitutive equations in both the Lagrangian and the Eulerian formulation is presented. However, the authors seem to overlook the difficulties in obtaining the material time-

derivatives in the Eulerian formulation. Therefore, the final equations they present are only applicable to the Lagrangian formulation.

Another attempt on the subject is made by Key [79]. He gives an accurate discussion of the basic differences existing between various formulations, points out that if the mechanics are carried out properly and the numerical procedures are sound, the differences in the results should be minor when translated to a common frame of reference. Based on the work of Truesdell and Noll [130], Key [79] presents a brief discussion of the kinematics of the problem. He gives a careful treatment of the constitutive models and the time-integration schemes and a proper transformation between the second Piola-Kirchhoff and the Cauchy stress tensor. In the Lagrangian formulation, an interpolation functions fixed in the coordinates of the reference configuration are employed making the material time-derivatives straightforward, whereas, in the Eulerian formulation the interpolation functions are function of the current configuration making the material time-derivatives rather awkward. To remedy this difficulty, Key [79] restricts his analysis to the isoparametric elements in which the coordinates and the displacement have the same interpolation. The isoparametric coordinates effectively become material coordinates and play a similar role to the coordinates of the reference configuration. However, the solution procedure and the transformation of the stress seems to be identical to the procedure used in the updated Lagrangian formulation.

Fengels [83] introduces another Lagrangian and Eulerian formulation for solving large deformation problems which include material as well as geometric nonlinearities. He employs two types of references: the first is the Lagrangian formulation in which the small deformation resulting from incremental loading is referred to the undeformed configuration and superimposed on a finitely-deformed, stable configuration; the second is called the Eulerian formulation in which the small deformation is referred to the present deformed

configuration and superimposed on the same deformed configuration. The second formulation is actually the updated Lagrangian formulation, but it is referred to as the Eulerian formulation.

A different approach to the Eulerian formulation is given by Derbalian et al. [86]. In this approach, they utilize an updated Lagrangian formulation relative to a fixed mesh in space by adding the incremental stresses obtained in a forward Lagrangian step to a set of interpolated stresses to determine new set of stresses at the fixed mesh points. The interpolation technique used seems to be inconsistent and computationally expensive. Derbalian et al. [86] discuss the advantages of the fixed mesh finite element analysis, which is Eulerian in nature, compared to the updated Lagrangian one.

Gadala, Oravas and Dokainish [85] discuss the basic differences between the Eulerian, the Lagrangian, and the updated Lagrangian formulation. They introduce a general approach for developing Eulerian formulation on the basis of the energy balance equation in the current configuration. Gadala et al. utilize fully nonlinear kinematic relations within a linear increment. When such analysis is carried out, it is found that only two stiffness matrices contribute to the total nonlinear stiffness matrix of the element. They also point out that a comparison between the Eulerian and other formulations may not be strictly logical, owing to the particular nature of each formulation. On the other hand, to obtain an expression for the velocity of the body-point X , Gadala et al. [85] apply the general form of the material time derivative in the spatial description which leads to an expression dependent on the deformation gradient. When they utilize the proper time derivative for the acceleration, a complicated and highly nonlinear expression is obtained. Therefore, they suggest replacing this complicated expression for the acceleration by an equivalent expression associated with a lumped-mass approximation. They do not give any application

to support their formulation and to show the numerical procedures that can be used to make Eulerian formulation suitable for numerical applications.

A consistent Eulerian formulation is developed in this work, based on the virtual work principle referred to the current deformed configuration. As shown in Chapter IV, utilizing the fully nonlinear kinematic relations within linear increments, specific simplifying assumptions have to be imposed in order to obtain the final incremental equilibrium equations in a form suitable for numerical applications. It is also found that only two stiffness matrices contribute to the total nonlinear stiffness matrix. As discussed by Gadala et al. [85], owing to the nature of each formulation, a strict comparison may be not logical between the spatial formulation on one side and the referential formulations on the other side. However, the two stiffness matrices in the Eulerian formulation correspond to the usual small displacement, or the incremental stiffness matrix and to the initial displacement, or initial rotation stiffness matrix of the two Lagrangian formulations. The load-vector increment is independent of the deformation gradient tensor contrary to the Lagrangian and the updated Lagrangian formulation. This fact eliminates the initial load or the load-correction matrix in the Eulerian formulation. As discussed above, this formulation is perfectly suited to the study of fluids and some of the metal forming processes which operate under steady-state condition.

CHAPTER III

LAGRANGIAN AND UPDATED LAGRANGIAN FORMULATIONS AND APPLICATIONS

As previously mentioned, only the Lagrangian, the updated Lagrangian, and the Eulerian formulation are used in finite element applications to continuum mechanics problems. In this chapter, we will discuss the simplifying assumptions and the basic equations for the Lagrangian and the updated Lagrangian formulation whereas, the Eulerian formulation will be considered in the next chapter. On the basis of these basic equations, we will develop consistently the final incremental equilibrium equations in an explicit form in each case. We will also examine the basic differences between the derived formulations and similar formulations in the literature. Finally, two example problems will be solved to show the applicability and effectiveness of the derived formulations. These problems are: large displacement static analysis of a cantilever beam and a dynamic analysis of pipe whip. Comparisons are made with available analytical solutions as well as of other known numerical analyses.

III.1 FORMULATION OF THE INCREMENTAL EQUILIBRIUM EQUATIONS

III.1.1 ASSUMPTIONS AND BASIC EQUATIONS

III.1.1.1. General Assumptions

A general body which occupies a finite region of Euclidean space as shown in Figure (II.1) is considered. Subjected to prescribed surface tractions and body forces the body undergoes the motion $\bar{x} = \bar{x}(\bar{X}, t)$. A fixed rectangular frame with Cartesian coordinate system in three-dimensional space is established to describe the motion of the body. Three

configurations of the body are considered. These are: the initial configuration C_0 at time 0, the present configuration C_1 at time t , and the current configuration C_2 at time $t + \Delta t$. Assume that the complete solution of the problem for all time steps Δt from time 0 to time t , inclusive, has been obtained, and that the solution for time $t + \Delta t$ is required next. In order to formulate the equilibrium equations, complete nonlinear kinematic relations within a linear increment will be used throughout the formulation. The second order incremental variables will be neglected. We will consider only perfect mechanical systems which take no account of thermodynamical effects. Further simplifying assumptions will be introduced where required.

III.1.1.2 Nomenclature

It is useful at this point to set the notations which will be employed in all formulations. A Cartesian coordinate system fixed in three dimensional space is established to describe the motion of the body. We adopt the direct method of tensor analysis in which the tensor can be referred to its basis. The order of the tensors is identified by a number of superposed bars which equals the order of the tensor. All repeated indices are to be summed over their admissible range. Right subscripts in upper case refer to nodal points, whereas lower case right Greek scripts refer to generalized displacements. Left superscripts (numbers) indicate the configuration at which the quantity is measured whereas, left subscripts (numbers) indicate the configuration to which the quantity is referred.

III.1.1.3 Deformation Gradient Tensors and Strain Measures

Referring to Figure (II.1), the position-vector \bar{x} of the body-point X at configuration C_1 and C_2 may be written as follows.

$${}^1\bar{x} = {}^0\bar{X} + {}^1\bar{u} \quad (III.1)$$

$${}^2\bar{x} = {}^0\bar{X} + {}^2\bar{u} = {}^1\bar{x} + {}^2\bar{u} \quad (\text{III.2})$$

The deformation gradient tensor at configuration C_1 referred to configuration C_0 is defined as

$${}^1_0\bar{F} = \frac{{}^1\bar{x} \partial}{\partial {}^0\bar{X}} \quad (\text{III.3})$$

Substituting from eqn. (III.1) into eqn. (III.3), ${}^1_0\bar{F}$ may be written in the form

$${}^1_0\bar{F} = \bar{1} + \frac{{}^1\bar{u} \partial}{\partial {}^0\bar{X}} = \bar{1} + {}^1_0\bar{u} \quad (\text{III.4})$$

where $\bar{1}$ is the identity tensor and ${}^1_0\bar{u}$ is the displacement gradient tensor. Similarly, other deformation gradient tensors may be formed

$${}^2_0\bar{F} = \frac{{}^2\bar{x} \partial}{\partial {}^0\bar{X}} = \bar{1} + \frac{{}^1\bar{u} \partial}{\partial {}^0\bar{X}} + \frac{{}^2\bar{u} \partial}{\partial {}^0\bar{X}} = {}^1_0\bar{F} + \frac{{}^2\bar{u} \partial}{\partial {}^0\bar{X}} = {}^1_0\bar{F} + {}^2_1\bar{u} \quad (\text{III.5})$$

and

$${}^2_1\bar{F} = \frac{{}^2\bar{x} \partial}{\partial {}^1\bar{x}} = \bar{1} + {}^2_1\bar{u} \quad (\text{III.6})$$

When the components of the displacement gradient tensor are not small compared to the components of the identity tensor such as in the case of finite strains, the problem of characterizing the strains is more difficult than in the case of small strains. Several different kinds of finite strain measures have been proposed, the majority of which can be computed from the deformation gradient tensor. In what follows, however, we will be mainly using the Green-Lagrange strain tensor, which can be written in configuration C_2 but referred to configuration C_0 as follows:

$${}^2_0\bar{E} = \frac{1}{2} ({}^2_0\bar{F}^T \cdot {}^2_0\bar{F} - \bar{1}) = \frac{1}{2} \left[\frac{\partial^2\bar{u}}{\partial {}^0\bar{X}} + \frac{{}^2\bar{u} \partial}{\partial {}^0\bar{X}} + \frac{\partial^2\bar{u}}{\partial {}^0\bar{X}} + \frac{{}^2\bar{u} \partial}{\partial {}^0\bar{X}} \right] \quad (\text{III.7})$$

Substituting ${}^2\bar{u} = {}^1\bar{u} + {}^2_1\bar{u}$, eqn. (III.7) takes the form:

$${}^2_0\bar{E} = {}^1_0\bar{E} + \Delta_0^1\bar{E} \text{ (linear)} + \Delta_0^1\bar{E} \text{ (nonlinear)} \quad (\text{III.8})$$

where

$${}^1\bar{E} = \frac{1}{2} \left[\frac{\partial^1 \bar{u}}{\partial^0 \bar{X}} + \frac{{}^1 \bar{u} \partial}{\partial^0 \bar{X}} + \frac{\partial^1 \bar{u}}{\partial^0 \bar{X}} \cdot \frac{{}^1 \bar{u} \partial}{\partial^0 \bar{X}} \right] \quad (III.9)$$

$$\Delta_0^1 \bar{E} \text{ (linear)} = \frac{1}{2} \left[\frac{\partial^2 \bar{u}}{\partial^0 \bar{X}} + \frac{{}^2 \bar{u} \partial}{\partial^0 \bar{X}} + \frac{\partial^2 \bar{u}}{\partial^0 \bar{X}} \cdot \frac{{}^1 \bar{u} \partial}{\partial^0 \bar{X}} + \frac{\partial^1 \bar{u}}{\partial^0 \bar{X}} \cdot \frac{{}^2 \bar{u} \partial}{\partial^0 \bar{X}} \right] \quad (III.10)$$

and

$$\Delta_0^1 \bar{E} \text{ (nonlinear)} = \frac{1}{2} \left[\frac{\partial^2 \bar{u}}{\partial^0 \bar{X}} \cdot \frac{{}^2 \bar{u} \partial}{\partial^0 \bar{X}} \right] \quad (III.11)$$

For the updated Lagrangian

$${}^2\bar{E} = {}^1\bar{E} + \Delta_1^1 \bar{E} \text{ (linear)} + \Delta_1^1 \bar{E} \text{ (nonlinear)} \quad (III.12)$$

where

$${}^1\bar{E} = \frac{1}{2} \left[\frac{\partial^1 \bar{u}}{\partial^1 \bar{x}} + \frac{{}^1 \bar{u} \partial}{\partial^1 \bar{x}} + \frac{\partial^1 \bar{u}}{\partial^1 \bar{x}} \cdot \frac{{}^1 \bar{u} \partial}{\partial^1 \bar{x}} \right] \quad (III.13)$$

$$\Delta_1^1 \bar{E} \text{ (linear)} = \frac{1}{2} \left[\frac{\partial^2 \bar{u}}{\partial^1 \bar{x}} + \frac{{}^2 \bar{u} \partial}{\partial^1 \bar{x}} + \frac{\partial^2 \bar{u}}{\partial^1 \bar{x}} \cdot \frac{{}^1 \bar{u} \partial}{\partial^1 \bar{x}} + \frac{\partial^1 \bar{u}}{\partial^1 \bar{x}} \cdot \frac{{}^2 \bar{u} \partial}{\partial^1 \bar{x}} \right] \quad (III.14)$$

and

$$\Delta_1^1 \bar{E} \text{ (nonlinear)} = \frac{1}{2} \left[\frac{\partial^2 \bar{u}}{\partial^1 \bar{x}} \cdot \frac{{}^2 \bar{u} \partial}{\partial^1 \bar{x}} \right] \quad (III.15)$$

III.1.1.4 Displacement Assumption

In the Lagrangian formulation, usually the displacement assumption within any given element is assumed in the form

$${}^1 u_i = \psi_{i\alpha}({}^0 \bar{X}) {}^1 u_{i\alpha} \quad (III.16)$$

and

$${}^2 u_i = \psi_{i\alpha}({}^0 \bar{X}) {}^2 u_{i\alpha} \quad (III.17)$$

In the updated Lagrangian, we have

$${}^1 u_i = \psi_{i\alpha}({}^1 \bar{x}) {}^1 u_{i\alpha} \quad (III.18)$$

and

$$\underline{u}_i = \psi_{i\alpha}(\underline{x}) \underline{u}_\alpha \quad (III.19)$$

where, in general, a displacement vector can be expressed as $\underline{u} = u_i \bar{e}_i$, \bar{e}_i ($i = 1, 2, 3$) are the Cartesian base vectors, $\psi_{i\alpha}$ are the finite element shape functions, and \underline{u}_α is the nodal displacements vector.

III.1.1.5 Incremental Strain Tensors

Substituting the displacement assumptions, eqns. (III.16, III.17) into the increment of the Green-Lagrange strain tensor eqns. (III.10, III.11), we obtain

$$\begin{aligned} \Delta_0^1 \bar{\bar{E}}(\text{total}) &= \Delta_0^1 \bar{\bar{E}}(\text{linear}) + \Delta_0^1 \bar{\bar{E}}(\text{nonlinear}) \\ &= \frac{1}{2} \left\{ \left[\frac{\partial \psi_{i\alpha}}{\partial^0 X_j} + \frac{\partial \psi_{j\alpha}}{\partial^0 X_i} + \frac{\partial^1 u_k}{\partial^0 X_i} \frac{\partial \psi_{k\alpha}}{\partial^0 X_j} + \frac{\partial^1 u_k}{\partial^0 X_j} \frac{\partial \psi_{k\alpha}}{\partial^0 X_i} + \frac{\partial \psi_{k\alpha}}{\partial^0 X_i} \frac{\partial \psi_{k\beta}}{\partial^0 X_j} \right] \underline{u}_\alpha \right\} \bar{e}_i \bar{e}_j \end{aligned} \quad (III.20)$$

Since we are considering the nonlinear kinematic equations within a linear increment, eqn.

(III.20) may be written as

$$\Delta_0^1 \bar{\bar{E}} = \frac{1}{2} \left\{ \left[\frac{\partial \psi_{i\alpha}}{\partial^0 X_j} + \frac{\partial \psi_{j\alpha}}{\partial^0 X_i} + \frac{\partial^1 u_k}{\partial^0 X_i} \frac{\partial \psi_{k\alpha}}{\partial^0 X_j} + \frac{\partial^1 u_k}{\partial^0 X_j} \frac{\partial \psi_{k\alpha}}{\partial^0 X_i} \right] \underline{u}_\alpha \right\} \bar{e}_i \bar{e}_j \quad (III.21)$$

In a similar manner, we may write the incremental strain tensor in the updated Lagrangian formulation in the form

$$\Delta_V^1 \bar{\bar{E}} = \frac{1}{2} \left\{ \left[\frac{\partial \psi_{i\alpha}}{\partial^1 X_j} + \frac{\partial \psi_{j\alpha}}{\partial^1 X_i} + \frac{\partial^1 u_k}{\partial^1 X_i} \frac{\partial \psi_{k\alpha}}{\partial^1 X_j} + \frac{\partial^1 u_k}{\partial^1 X_j} \frac{\partial \psi_{k\alpha}}{\partial^1 X_i} \right] \underline{u}_\alpha \right\} \bar{e}_i \bar{e}_j \quad (III.22)$$

At this point, we should emphasize that the referential nature of the analysis is implied in the obtaining of eqns. (III.21, III.22). In the Lagrangian formulation, the derivatives are taken with respect to the initial (undeformed) configuration and the displacement 1u is a function of the relative time t ; whereas, in the updated Lagrangian formulation, the derivatives are taken with respect to the present configuration.

Substitution of displacement assumptions, eqns. (III.16-III.19), into the deformation gradient tensors, eqns. (III.4, III.6), yield

$${}^1_0 \bar{\bar{F}} = {}^1_0 F_{ij} \bar{e}_i \bar{e}_j = \frac{\partial {}^1 x_i}{\partial {}^0 X_j} \bar{e}_i \bar{e}_j = \left(\delta_{ij} + \frac{\partial \psi_{ia}}{\partial {}^0 X_j} {}^1 u_a \right) \bar{e}_i \bar{e}_j \quad (\text{III.23})$$

$${}^2_1 \bar{\bar{F}} = {}^2_1 F_{ij} \bar{e}_i \bar{e}_j = \frac{\partial {}^2 x_i}{\partial {}^1 X_j} \bar{e}_i \bar{e}_j = \left(\delta_{ij} + \frac{\partial \psi_{ia}}{\partial {}^1 X_j} {}^2 u_a \right) \bar{e}_i \bar{e}_j \quad (\text{III.24})$$

where δ_{ij} denotes the Kronecker delta.

III.1.1.6 Virtual Work Principle

Since the solution is assumed to be known at all discrete time intervals $0, \Delta t, \dots, t$, i.e. until configuration C_1 , see Figure (II.1), the basic aim of the formulation is to establish the incremental equilibrium equations from which the unknown solution in the configuration C_2 at time $t + \Delta t$ can be obtained. We start with the virtual work principle referred to the current configuration given above in eqn. (II.1) in Chapter II. Equation (II.1) cannot be solved directly since the configuration C_2 at time $t + \Delta t$ is unknown. A solution can be obtained by referring all variables to a previously known calculated equilibrium configuration. As discussed above, in the Lagrangian formulation, the virtual work principle is transformed to the initial configuration C_0 (see Appendix A). For a quick reference, the transformed equation is reported here:

$$\int_{0_V} {}^2_0 \bar{\bar{S}} : \delta {}^2_0 \bar{\bar{E}} d^0 V + \int_{0_V} {}^0 \rho {}^2_a \bar{u} \cdot \delta {}^2 \bar{u} d^0 V = \int_{0_V} {}^0 \rho {}^2_b \bar{u} \cdot \delta {}^2 \bar{u} d^0 V + \int_{0_A} d^0 \bar{A} \cdot {}^2_0 \bar{\bar{S}} \cdot {}^2_0 \bar{\bar{F}}^T \cdot \delta {}^2 \bar{u} \quad (\text{III.25})$$

In the updated Lagrangian formulation the virtual work principle is transformed to the updated, that is to the variable Lagrangian reference configuration C_1 . Similar to the development given in Appendix A, the virtual work principle referred to configuration C_1

may be written in the form

$$\int_{1_V} {}^2\bar{\mathbb{S}} : \delta_1^2 \bar{\mathbb{E}} d^1V + \int_{1_V} {}^1p {}^2\bar{a} \cdot \delta^2 \bar{u} d^1V = \int_{1_V} {}^1p {}^2\bar{b} \cdot \delta^2 \bar{u} d^1V + \int_{1_A} d^1\bar{A} \cdot {}^2\bar{\mathbb{S}} \cdot {}^2\bar{\mathbb{F}}^T \cdot \delta^2 \bar{u} \quad (\text{III.26})$$

III.1.2 LAGRANGIAN (REFERENTIAL) FORMULATION

The development of the Lagrangian formulation to follow is based on the virtual work principle transformed to the initial (undeformed) configuration C_0 , eqn. (III.25). The integral on 0V extends over the volume of the continuum and that on 0A over the surface areas subjected to surface traction. In the development of the formulations, it is convenient to consider only a single finite element, and then the total incremental equilibrium equations can be obtained by superimposing the contributions from all the elements inside the continuum. With this in mind, then considering the left hand side and the right hand side of the virtual work principle, eqn. (III.25), as follows:

$$\text{L.H.S.} = \int_{0_V} {}^2\bar{\mathbb{S}} : \delta_0^2 \bar{\mathbb{E}} d^0V + \int_{0_V} {}^0p {}^2\bar{a} \cdot \delta^2 \bar{u} d^0V$$

substituting for the displacement assumption, eqn. (III.17), and the incremental strain tensor given by eqn. (III.21), we obtain

$$\begin{aligned} \text{L.H.S.} &= \int_{0_V} {}^2\bar{S}_{ij} \delta_0^2 E_{ij} d^0V + \int_{0_V} {}^0p {}^2\bar{a} \cdot \psi_{i\alpha} \bar{e}_i \delta^2 \bar{u}_\alpha d^0V \\ &= \int_{0_V} \left[\frac{1}{2} {}^2\bar{S}_{ij} \left(\frac{\partial \psi_{i\alpha}}{\partial {}^0X_j} + \frac{\partial \psi_{j\alpha}}{\partial {}^0X_i} + \frac{\partial^1 u_k}{\partial {}^0X_i} \frac{\partial \psi_{k\alpha}}{\partial {}^0X_j} + \frac{\partial^1 u_k}{\partial {}^0X_j} \frac{\partial \psi_{k\alpha}}{\partial {}^0X_i} \right) d^0V \right] \delta^2 \bar{u}_\alpha \\ &\quad + \int_{0_V} \left[({}^0p \psi_{i\alpha} \psi_{i\beta}) d^0V \frac{d^2}{dt^2} ({}^1\bar{u}_\beta + {}^2\bar{u}_\beta) \right] \delta^2 \bar{u}_\alpha \end{aligned} \quad (\text{III.27})$$

Now, considering the fact that a second order tensor $(\partial \psi_{i\alpha} / \partial {}^0X_j, \bar{e}_i, \bar{e}_j)$ can be decomposed additively as follows:

$$\frac{\partial \psi_{ia}}{\partial {}^0X_j} \bar{e}_i \bar{e}_j = \left[\frac{1}{2} \left(\frac{\partial \psi_{ia}}{\partial {}^0X_j} + \frac{\partial \psi_{ja}}{\partial {}^0X_i} \right) \bar{e}_i \bar{e}_j \right]_{\text{sym}} + \left[\frac{1}{2} \left(\frac{\partial \psi_{ia}}{\partial {}^0X_j} - \frac{\partial \psi_{ja}}{\partial {}^0X_i} \right) \bar{e}_i \bar{e}_j \right]_{\text{skew}} \quad (\text{III.28})$$

where sym means the symmetric part of the tensor and skew denotes the skew symmetric part.

Double-dotting of this tensor with the stress tensor gives

$$\begin{aligned} {}^2_0\bar{S} : \left(\frac{\partial \psi_{ia}}{\partial {}^0X_j} \bar{e}_i \bar{e}_j \right) &= {}^2_0S_{ij} \frac{\partial \psi_{ia}}{\partial {}^0X_j} \\ &= \frac{1}{2} {}^2_0S_{ij} \left(\frac{\partial \psi_{ia}}{\partial {}^0X_j} + \frac{\partial \psi_{ja}}{\partial {}^0X_i} \right) \end{aligned} \quad (\text{III.29})$$

Since the double-dot product of second order symmetric and skewsymmetric tensors is zero.

By utilizing eqn. (III.29), the L.H.S. of the virtual work principle may be written as

$$\begin{aligned} \text{L.H.S.} &= \left(\int_{0V} {}^2_0S_{ij} \left(\frac{\partial \psi_{ia}}{\partial {}^0X_j} + \frac{\partial^1 u_k}{\partial {}^0X_i} \frac{\partial \psi_{ka}}{\partial {}^0X_j} \right) d^0V \right. \\ &\quad \left. + \int_{0V} \rho(\psi_{i\alpha} \psi_{i\beta}) d^0V \left| \frac{d^2}{dt^2} ({}^1_{\underline{\beta}} u + {}^2_{\underline{\beta}} u) \right| \delta^2_{\underline{\alpha}} \right) \end{aligned} \quad (\text{III.30})$$

Increments of the above equation give

$$\begin{aligned} \Delta(\text{L.H.S.}) &= \left(\int_{0V} \left({}^2_0S_{ij} \frac{\partial \psi_{k\beta}}{\partial {}^0X_i} \frac{\partial \psi_{ka}}{\partial {}^0X_j} {}^2_{\underline{\beta}} u \right) d^0V \right. \\ &\quad \left. + \int_{0V} \left[\left(\frac{\partial \psi_{ia}}{\partial {}^0X_j} + \frac{\partial^1 u_k}{\partial {}^0X_i} \frac{\partial \psi_{ka}}{\partial {}^0X_j} \right) (\Delta {}^2_0S_{ij}) \right] d^0V \right. \\ &\quad \left. + \int_{0V} \rho(\psi_{i\alpha} \psi_{i\beta}) d^0V \left| \frac{d^2}{dt^2} (\Delta^1_{\underline{\beta}} u + \Delta^2_{\underline{\beta}} u) \right| \delta^2_{\underline{\alpha}} \right) \end{aligned}$$

Introducing the assumptions

$$\Delta {}^2_0S_{ij} = \Delta ({}^1_0S_{ij} + \Delta {}^1_0S_{ij}) = \Delta {}^1_0S_{ij} + 0(\Delta(\Delta {}^1_0S_{ij})), \quad (\text{III.31})$$

where 0 signifies "of order"

$$\Delta {}^1_0S_{ij} = {}^0D_{ijkl} \Delta^1 E_{kl}, \quad (\text{III.32})$$

and

$$\frac{d^2}{dt^2} (\Delta^1 \underline{u}_{-B} + \Delta^2 \underline{u}_{-B}) = \underline{\ddot{u}}_{-B}$$

where, in eqn. (III.32) we express the increment of the second Piola-Kirchhoff stress tensor as linear function of the increment of the Green-Lagrange strain tensor using the fourth order tensor ${}^0D_{ijkl}$ of the material. Different forms of ${}^0D_{ijkl}$ will be discussed in a separate section.

Then the increment of the L.H.S. may be put in the form

$$\begin{aligned} \Delta(\text{L.H.S.}) &= \left(\int_{0V} {}^2S_{ij} \left(\frac{\partial \psi_{m\beta}}{\partial {}^0X_i} \frac{\partial \psi_{m\alpha}}{\partial {}^0X_j} \right) d {}^0V \right) \underline{\ddot{u}}_{-B} \\ &+ \left[\int_{0V} \left[\left(\frac{\partial \psi_{ia}}{\partial {}^0X_j} + \frac{\partial^1 u_m}{\partial {}^0X_i} \frac{\partial \psi_{m\alpha}}{\partial {}^0X_j} \right) {}^0D_{ijkl} \left(\frac{\partial \psi_{k\beta}}{\partial {}^0X_l} + \frac{\partial^1 u_n}{\partial {}^0X_k} \frac{\partial \psi_{n\beta}}{\partial {}^0X_l} \right) \right] d {}^0V \right] \underline{\ddot{u}}_{-B} \\ &= \left[\int_{0V} {}^0\rho(\psi_{ia} \psi_{i\beta}) d {}^0V \right] \underline{\ddot{u}}_{-a} \end{aligned} \quad (\text{III.33})$$

For comparison, the above equation may be put in the form

$$\Delta(\text{L.H.S.}) = \left([{}^1K_{a\beta}^{(1)} + {}^1K_{a\beta}^{(2)} + {}^1K_{a\beta}^{(3)}] \underline{\ddot{u}}_{-B} + [{}^1M_{a\beta}] \underline{\ddot{u}}_{-B} \right) \underline{\ddot{u}}_{-a} \quad (\text{III.34})$$

where

$${}^1K_{a\beta}^{(1)} = \int_{0V} \frac{\partial \psi_{ia}}{\partial {}^0X_j} {}^0D_{ijkl} \frac{\partial \psi_{k\beta}}{\partial {}^0X_l} d {}^0V \quad (\text{III.35})$$

is the usual small displacement, or the incremental stiffness matrix;

$${}^1K_{a\beta}^{(2)} = \int_{0V} {}^1S_{ij} \frac{\partial \psi_{m\beta}}{\partial {}^0X_i} \frac{\partial \psi_{m\alpha}}{\partial {}^0X_j} d {}^0V \quad (\text{III.36})$$

is the initial stress, or the geometric, or the tangent stiffness matrix;

$$\begin{aligned} {}^1K_{a\beta}^{(3)} &= \int_{0V} {}^0D_{ijkl} \left(\frac{\partial \psi_{ia}}{\partial {}^0X_j} \frac{\partial^1 u_n}{\partial {}^0X_k} \frac{\partial \psi_{n\beta}}{\partial {}^0X_l} + \frac{\partial \psi_{k\beta}}{\partial {}^0X_l} \frac{\partial^1 u_m}{\partial {}^0X_i} \frac{\partial \psi_{m\alpha}}{\partial {}^0X_j} \right. \\ &\quad \left. + \frac{\partial^1 u_m}{\partial {}^0X_i} \frac{\partial \psi_{m\alpha}}{\partial {}^0X_j} \frac{\partial^1 u_n}{\partial {}^0X_k} \frac{\partial \psi_{n\beta}}{\partial {}^0X_l} \right) d {}^0V \end{aligned} \quad (\text{III.37})$$

is the initial displacement, or the initial rotation stiffness matrix; and

$${}^1M_{\alpha\beta} = \int_{0V} {}^0\rho (\psi_{i\alpha} \psi_{i\beta}) d^0V \quad (\text{III.38})$$

is the consistent mass matrix of the element.

Now, let us consider the right hand side of eqn. (III.25)

$$\text{R.H.S.} = \int_{0V} {}^0\rho {}^2\bar{b}_i \cdot \delta^2\bar{u}_i d^0V + \int_{0\Lambda} d^0\bar{\Lambda} \cdot {}^2\bar{S} \cdot {}^2\bar{F}^T \cdot \delta^2\bar{u}$$

Substituting expressions for the displacement assumption, the deformation gradient tensor, and considering the following relation

$$d^0\bar{\Lambda} \cdot {}^2\bar{S} = {}^2\bar{S}_n d^0\Lambda \quad (\text{III.39})$$

we obtain

$$\text{R.H.S.} = \left(\int_{0V} {}^0\rho {}^2b_i \psi_{i\alpha} d^0V + \int_{0\Lambda} \left[{}^2S_{n_i} (\psi_{i\alpha} + \frac{\partial^1 u_j}{\partial^0 X_i} \psi_{j\alpha}) \right] d^0\Lambda \right) \delta^2 \underline{u}_\alpha$$

increments of the above equation yield

$$\begin{aligned} \Delta(\text{R.H.S.}) &= \left(\int_{0V} \Delta({}^0\rho {}^2b_i) \psi_{i\alpha} d^0V + \int_{0\Lambda} \left[\Delta({}^2S_{n_i} (\psi_{i\alpha} + \frac{\partial^1 u_j}{\partial^0 X_i} \psi_{j\alpha})) \right] d^0\Lambda \right. \\ &\quad \left. + \int_{0\Lambda} \left[{}^2S_{n_i} \left(\frac{\partial^2 u_j}{\partial^0 X_i} \psi_{j\alpha} \right) \right] d^0\Lambda \right) \delta^2 \underline{u}_\alpha \\ &= \left(\int_{0V} \Delta({}^0\rho {}^2b_i) \psi_{i\alpha} d^0V + \int_{0\Lambda} \left[\Delta({}^1S_{n_i} (\psi_{i\alpha} + \frac{\partial^1 u_j}{\partial^0 X_i} \psi_{j\alpha})) \right] d^0\Lambda \right. \\ &\quad \left. + \int_{0\Lambda} \left[{}^2S_{n_i} \frac{\partial \psi_{j\beta}}{\partial^0 X_i} \psi_{j\alpha} \right] d^0\Lambda \left[\begin{matrix} 2 \\ 1-\beta \end{matrix} \right] \right) \delta^2 \underline{u}_\alpha \end{aligned}$$

or

$$\Delta(\text{R.H.S.}) = (\Delta_0^1 \underline{R}_\alpha + [{}^1K_{\alpha\beta}^{(4)}] [{}^2 \underline{u}_\beta]) \delta^2 \underline{u}_\alpha \quad (\text{III.40})$$

where

$$\Delta_0^1 \underline{R}_\alpha = \left\{ \int_{0V} \Delta({}^0\rho {}^2b_i) \psi_{i\alpha} d^0V + \int_{0\Lambda} \left[\Delta({}^1S_{n_i} (\psi_{i\alpha} + \frac{\partial^1 u_j}{\partial^0 X_i} \psi_{j\alpha})) \right] d^0\Lambda \right\} \quad (\text{III.41})$$

is the increment of the load vector, and

$${}^1_0K_{\alpha\beta}^{(4)} = \int_{0A} \left({}^2_0S_{n_i} \frac{\partial \psi_{j\beta}}{\partial X_i} \psi_{j\alpha} \right) d^0A \quad (\text{III.42})$$

is the initial load, or the load-correction matrix.

The incremental virtual work principle is obtained by collecting the results of eqns. (III.34-III.38, III.40-III.42)

$$\left([{}^1_0K_{\alpha\beta}^{(1)} + {}^1_0K_{\alpha\beta}^{(2)} + {}^1_0K_{\alpha\beta}^{(3)}] \{^2_{1-\beta}u\} + [{}^1_0M_{\alpha\beta}] \{^2_{1-\beta}\bar{u}\} \right) \delta^2_{1-\alpha}u = \left(\Delta^1_{0-\alpha}R + [{}^1_0K_{\alpha\beta}^{(4)}] \{^2_{1-\beta}u\} \right) \delta^2_{1-\alpha}u$$

or

$$\left([{}^1_0K_{\alpha\beta}^{(1)} + {}^1_0K_{\alpha\beta}^{(2)} + {}^1_0K_{\alpha\beta}^{(3)} - {}^1_0K_{\alpha\beta}^{(4)}] \{^2_{1-\beta}u\} + [{}^1_0M_{\alpha\beta}] \{^2_{1-\beta}\bar{u}\} - \Delta^1_{0-\alpha}R \right) \delta^2_{1-\alpha}u = 0$$

Considering arbitrary virtual displacement vector $\delta^2_{1-\alpha}u$, the above equation is satisfied if, and only if,

$$\left([{}^1_0K_{\alpha\beta}^{(1)} + {}^1_0K_{\alpha\beta}^{(2)} + {}^1_0K_{\alpha\beta}^{(3)} - {}^1_0K_{\alpha\beta}^{(4)}] \{^2_{1-\beta}u\} + [{}^1_0M_{\alpha\beta}] \{^2_{1-\beta}\bar{u}\} - \Delta^1_{0-\alpha}R \right) = 0$$

or

$$\Delta^1_{0-\alpha}R = [{}^1_0K_{\alpha\beta}^{(1)} + {}^1_0K_{\alpha\beta}^{(2)} + {}^1_0K_{\alpha\beta}^{(3)} - {}^1_0K_{\alpha\beta}^{(4)}] \{^2_{1-\beta}u\} + [{}^1_0M_{\alpha\beta}] \{^2_{1-\beta}\bar{u}\} \quad (\text{III.43})$$

which represents the incremental equilibrium equations in the Lagrangian formulation.

The formulation in the form of eqns. (III.43) is computationally expensive.

Therefore, for numerical convenience one can rearrange the final form of the incremental equilibrium equation as follows:

* For linear increment (first increment)

$$\Delta^0_{0-\alpha}R = [{}^0_0K_{\alpha\beta}^{(1)}] \{\Delta^0_{0-\beta}u\} + [{}^0_0M_{\alpha\beta}] \{\Delta^0_{0-\beta}\bar{u}\} \quad (\text{III.44})$$

where

$${}^0_0K_{\alpha\beta}^{(1)} = \int_{0V} \frac{\partial \psi_{i\alpha}}{\partial X_j} D_{ijkl} \frac{\partial \psi_{k\beta}}{\partial X_l} d^0V \quad (\text{III.45})$$

* For nonlinear increments

$$\Delta^1_{0-\alpha}R = [{}^1_0K_{\alpha\beta}^{(1)} + {}^1_0K_{\alpha\beta}^{(2)} - {}^1_0K_{\alpha\beta}^{(4)}] \{^2_{1-\beta}u\} + [{}^1_0M_{\alpha\beta}] \{^2_{1-\beta}\bar{u}\} \quad (\text{III.46})$$

where

$$\Delta {}^1R_a, {}^1K_{a\beta}^{(2)}, {}^1K_{a\beta}^{(4)} \text{ and } {}^1M_{a\beta}$$

are defined above, and

$${}^1K_{a\beta}^{(T)} = {}^1K_{a\beta}^{(1)} + {}^2K_{a\beta}^{(3)} = \int_{0V} \frac{\partial \phi_{ia}}{\partial {}^0X_j} {}^0D_{ijkl} \frac{\partial \phi_{k\beta}}{\partial {}^0X_l} d^0V \tag{III.47}$$

where

$$\frac{\partial \phi_{ia}}{\partial {}^0X_j} = \left(\frac{\partial \psi_{ia}}{\partial {}^0X_j} + \frac{\partial {}^1u_m}{\partial {}^0X_l} \frac{\partial \psi_{ma}}{\partial {}^0X_j} \right) \tag{III.48}$$

The reason for writing the stiffness matrix ${}^1K_{a\beta}^{(T)}$ in the above form is that both terms

$$\left(\frac{\partial \psi_{ia}}{\partial {}^0X_j} + \frac{\partial {}^1u_m}{\partial {}^0X_l} \frac{\partial \psi_{ma}}{\partial {}^0X_j} \right) \text{ and } \left(\frac{\partial \psi_{k\beta}}{\partial {}^0X_l} + \frac{\partial {}^1u_n}{\partial {}^0X_k} \frac{\partial \psi_{n\beta}}{\partial {}^0X_l} \right)$$

in eqn. (III.33) have the same form. Therefore, the former term can be calculated at each numerical integration point and used to calculate the contribution of that point to the elements of the stiffness matrix ${}^1K_{a\beta}^{(T)}$. This arrangement results in a significant reduction of computation time.

The formulation developed here differs from similar ones in the literature [14,23, 31, 44, 45, 52, 53, 68] in the definition of the load increment, eqn. (III.41), and the development of the load-correction matrix, eqn. (III.42). Once again, Bathe [5,14,15], Bathe et al. [17-21], Ramm [22], Wunderlich [23], and Nagarajan et al [68], among others discarded the transpose of the deformation gradient tensor, ${}^2_0\bar{F}^T$, from the surface traction term. As it is shown above, this term is obtained through the consistent transformation of the virtual work principle without any reference to the type of loading. The importance of including the load-correction matrix in the analysis was pointed out by Oden et al. [39,41] and Gadala et al. [48,49]. Bathe et al. [17] presented a similar argument for the case of deformation-dependent loading, however, their expression is not identical to the expression developed here. In reference [68], Nagarajan et al. follow a similar approach as given by Oden [4] and Larsen et al. [44] for the same type of loading. Hibbit et al. [52] introduced a rather intuitive argument

in setting $\Delta \bar{F} = \Delta_{\text{load}} \bar{F} + \Delta_{\text{geom}} \bar{F}$, where \bar{F} is the surface traction or the body force vector. Based on the above assumption Hibbit et al. developed a load-correction matrix which will have zero value in some loading cases. Frey et al. [27] and Cescotto et al. [25,26] introduce an additional initial stress stiffness matrix and a symmetric initial load matrix. It should be noticed that in the usual isoparametric finite element formulation, where the interpolation functions are independent of the nodal displacements these two matrices will vanish. The formulation developed here coincides with the procedures given by Oden et al. [39,41] and Cadala et al. [48,49], however, the forms of the individual stiffness matrices are different.

III.1.3 UPDATED LAGRANGIAN (RELATIVE) FORMULATION

As discussed above, in the updated Lagrangian formulation the reference configuration coincides with the updated or the present configuration C_1 , see Figure (II.1), which means that in the updated Lagrangian formulation we refer the current and the past configuration to the present configuration. To derive the incremental equilibrium equations, we start with eqn. (III.26) and by following a similar procedure to the development of the Lagrangian formulation, we have

$$\text{L.H.S.} = \int_{V_1} {}^2\bar{S} : \delta {}^2E d^1V - \int_{V_1} {}^1\rho {}^2\bar{a} \cdot \delta {}^2u d^1V$$

Substituting for the displacement assumption eqns. (III.19) and the increment of the strain tensor eqn. (III.22), and by following the method of developing eqn. (III.34) and introducing the assumption

$$\Delta {}^1S_{ij} = {}^1D_{ijkl} \Delta {}^1E_{kl} \quad (III.49)$$

we obtain

$$\Delta(\text{L.H.S.}) = ({}^1K_{\alpha\beta}^{(1)} + {}^1K_{\alpha\beta}^{(2)} + {}^1K_{\alpha\beta}^{(3)}) \{ {}^2u_{-\beta} \} + [{}^1M_{\alpha\beta}] \{ {}^2u_{-\beta} \} \delta {}^2u_{-\beta} \quad (III.50)$$

where

$${}^1K_{\alpha\beta}^{(1)} = \int_{1V} \frac{\partial \psi_{i\alpha}}{\partial {}^1x_j} {}^1D_{ijkl} \frac{\partial \psi_{k\beta}}{\partial {}^1x_l} d^1V \quad (III.51)$$

is the usual small displacement, or the incremental stiffness matrix:

$${}^1K_{\alpha\beta}^{(2)} = \int_{1V} {}^2S_{ij} \frac{\partial \psi_{m\beta}}{\partial {}^1x_l} \frac{\partial \psi_{ma}}{\partial {}^1x_j} d^1V \quad (III.52)$$

is the initial stress, or the geometric, or the tangent stiffness matrix:

$$\begin{aligned} {}^1K_{\alpha\beta}^{(3)} = \int_{1V} {}^1D_{ijkl} & \left(\frac{\partial \psi_{i\alpha}}{\partial {}^1x_j} \frac{\partial {}^1u_n}{\partial {}^1x_k} \frac{\partial \psi_{n\beta}}{\partial {}^1x_l} + \frac{\partial \psi_{k\beta}}{\partial {}^1x_l} \frac{\partial {}^1u_m}{\partial {}^1x_i} \frac{\partial \psi_{ma}}{\partial {}^1x_j} \right. \\ & \left. + \frac{\partial {}^1u_m}{\partial {}^1x_i} \frac{\partial \psi_{ma}}{\partial {}^1x_j} \frac{\partial {}^1u_n}{\partial {}^1x_k} \frac{\partial \psi_{n\beta}}{\partial {}^1x_l} \right) d^1V \end{aligned} \quad (III.53)$$

is the initial displacement, or the initial rotation stiffness matrix, and

$${}^1M_{\alpha\beta} = \int_{1V} {}^1\rho (\psi_{i\alpha} \psi_{i\beta}) d^1V \quad (III.54)$$

is the consistent mass matrix of the element.

Considering the R.H.S. of eqn. (III.26), substituting for the deformation gradient tensor eqn. (III.24), we obtain

$$\text{R.H.S.} = \left(\int_{1V} {}^1\rho ({}^2b_i \psi_{i\alpha}) d^1V + \int_{1A} \left[{}^2S_{n_i} \left(\psi_{i\alpha} + \frac{\partial {}^2u_j}{\partial {}^1X_l} \psi_{j\alpha} \right) \right] d^1A \right) \delta^2u_{-\alpha} \quad (III.55)$$

where in deriving the above equation we employed the following relation

$$d^1\bar{A} \cdot {}^2\bar{S} = {}^2\bar{S}_n d^1A$$

Increments of eqn (III.55) give

$$\begin{aligned} \text{R.H.S.} = & \left(\int_{1V} \Delta({}^1\rho {}^2b_i) \psi_{i\alpha} d^1V + \int_{1A} \left[(\Delta {}^2S_{n_i}) \left(\psi_{i\alpha} + \frac{\partial {}^2u_j}{\partial {}^1X_l} \psi_{j\alpha} \right) \right] d^1A \right. \\ & \left. + \int_{1A} \left[({}^2S_{n_i}) \left(\frac{\partial (\Delta {}^2u_j)}{\partial {}^1X_l} \psi_{j\alpha} \right) \right] d^1V \right) \delta^2u_{-\alpha} \end{aligned}$$

substituting the assumptions

$$\Delta_1^2 S_{n_i} = \Delta_1(S_{n_j} + \Delta_1^1 S_{n_i}) = \Delta_1^1 S_{n_i} + O[\Delta_1(\Delta_1^1 S_{n_i})]$$

and

$$\Delta_1^2 u_j = \Delta_1(\Delta_1^1 u_j) = 0$$

into the above equation, we obtain

$$\begin{aligned} \Delta(\text{R.H.S.}) &= \left(\int_{1_V} \Delta_1^1 \rho^2 b_i \psi_{ia} d^1V + \int_{1_A} (\Delta_1^1 S_{n_i}) \left(\psi_{ia} + \frac{\partial_1^2 u_j}{\partial_1^1 x_i} \psi_{ja} \right) d^1A \right) \delta^2 u_a \\ &= \left(\int_{1_V} \Delta_1^1 \rho^2 b_i \psi_{ia} d^1V + \int_{1_A} (\Delta_1^1 S_{n_i} \psi_{ia}) d^1A \right. \\ &\quad \left. + \left[\int_{1_A} (\Delta_1^1 S_{n_i} \frac{\partial \psi_{j\beta}}{\partial_1^1 x_i} \psi_{ja}) d^1A \right]_{1_{\underline{\beta}}}^2 \right) \delta^2 u_a \end{aligned} \quad (\text{III.56})$$

or

$$\Delta(\text{R.H.S.}) = \left(\Delta_1^1 R_a + [{}^1 K_{a\beta}^{(4)}]_{1_{\underline{\beta}}}^2 \right) \delta^2 u_a \quad (\text{III.57})$$

where

$$\Delta_1^1 R_a = \left\{ \int_{1_V} \Delta_1^1 \rho^2 b_i \psi_{ia} d^1V + \int_{1_A} (\Delta_1^1 S_{n_i} \psi_{ia}) d^1A \right\} \quad (\text{III.58})$$

is the increment of the load vector, and

$${}^1 K_{a\beta}^{(4)} = \int_{1_A} (\Delta_1^1 S_{n_i} \frac{\partial \psi_{j\beta}}{\partial_1^1 x_i} \psi_{ja}) d^1A \quad (\text{III.59})$$

is the initial load, or the load-correction matrix.

Collecting the results of eqns. (III.50-III.54, III.57-III.59), and by following the method of obtaining eqn. (III.43), the final incremental equilibrium equations in the updated Lagrangian may take the form

$$\Delta_1^1 R_a = [{}^1 K_{a\beta}^{(1)} + {}^1 K_{a\beta}^{(2)} + {}^1 K_{a\beta}^{(3)} - {}^1 K_{a\beta}^{(4)}]_{1_{\underline{\beta}}}^2 \delta^2 u_a + [{}^1 M_{a\beta}]_{1_{\underline{\beta}}}^2 \delta^2 u_a \quad (\text{III.60})$$

where all individual terms are defined above.

As was done in the Lagrangian formulation, the final form of the incremental equilibrium equations can be rearranged to make the updated Lagrangian formulation suitable for numerical applications. Therefore, the incremental equilibrium equations may be put in the form

* For linear increment (first increment)

$$\Delta {}^0R_{\alpha} = [{}^0K_{\alpha\beta}^{(1)}] \{\Delta {}^0u_{\beta}\} + [{}^0M_{\alpha\beta}] \{\Delta {}^0\ddot{u}_{\beta}\} \quad (III.61)$$

where

$${}^0K_{\alpha\beta}^{(1)} = \int_{0V} \frac{\partial \psi_{ia}}{\partial {}^0x_j} {}^0D_{ijkl} \frac{\partial \psi_{k\beta}}{\partial {}^0x_l} d {}^0V \quad (III.62)$$

* For nonlinear increments

$$\Delta {}^1R_{\alpha} = [{}^1K_{\alpha\beta}^{(T)} + {}^1K_{\alpha\beta}^{(2)} - {}^1K_{\alpha\beta}^{(4)}] \{\Delta {}^1u_{\beta}\} + [{}^1M_{\alpha\beta}] \{\Delta {}^1\ddot{u}_{\beta}\} \quad (III.63)$$

where

$$\Delta {}^1R_{\alpha}, \quad {}^1K_{\alpha\beta}^{(2)}, \quad {}^1K_{\alpha\beta}^{(4)} \quad \text{and} \quad {}^1M_{\alpha\beta}$$

are defined before, and

$${}^1K_{\alpha\beta}^{(T)} = \int_{1V} \frac{\partial \phi_{ia}}{\partial {}^1x_j} {}^1D_{ijkl} \frac{\partial \phi_{k\beta}}{\partial {}^1x_l} d {}^1V \quad (III.64)$$

It can be noticed from the two eqns. (III.41) and (III.58) that, the dependence of the load increment vector on the deformation gradient tensor exists only in the Lagrangian formulation and not in the updated Lagrangian formulation, which can be visualized from the nature of the reference configuration in each case. For the same reason, it would be expected that the load-correction matrix in the updated Lagrangian formulation is dependent on $\Delta {}^1\bar{S}_n$, the increment of the surface traction vector from configuration C_1 to C_2 , where in the Lagrangian formulation it depends on ${}^0\bar{S}_n$.

The updated Lagrangian formulation presented here differs from similar formulation in the literature [17-21, 23, 25-26, 31] in the definition of the load increment vector eqn. (III.58), the development of the load-correction matrix eqn. (III.59), and the number of the stiffness matrices contributing* to the total stiffness matrix of the element. Bathe et al. [17-21] and Ishizaki et al. [31] introduce the same load increment for the Lagrangian and the updated Lagrangian formulation. Concerning the load-correction matrix, Bathe et al. [17] develop an expression for the case of deformation-dependent loading

based on the same argument as in their Lagrangian formulations. In reference [23] Wunderlich introduces kinematic assumptions which eliminate the initial displacement stiffness matrix in the updated Lagrangian. Cescotto et al. [25,26] assume that only small displacement increments will be used in the updated Lagrangian hence, it is shown that the displacement field is a linear function of the nodal parameters. By such means, both their additional initial stress matrix and the symmetric load-correction matrix vanish. The formulation presented here coincides with the procedures given by Gadala et al. [46-49]. Finally, it should be noticed that the constitutive equations, eqn. (III.49) are different from eqn. (III.32) in the Lagrangian formulation, this will be discussed in the following sub-section.

III.1.4 CONSTITUTIVE EQUATIONS.

(i) Elastic Material

Elastic material are relatively easy to deal with in practical analysis. The constitutive equations may be written in the present configuration as follows:

$${}^1\bar{\sigma} = {}_1\bar{D} : {}^1\bar{\epsilon} \quad (III.65)$$

where ${}^1\bar{\sigma}$ and ${}^1\bar{\epsilon}$ are the Cauchy stress and Euler strain tensors, ${}_1\bar{D} = {}_1D_{ijkl} \bar{e}_i \bar{e}_j \bar{e}_k \bar{e}_l$ is the tensor of appropriate elastic constants of the material under consideration. In this case, however, the analysis still includes geometric nonlinearity and, therefore, it is necessary to employ incremental formulation. Equation (III.65) may be written in its incremental form as follows

$$\Delta {}^1\bar{\sigma} = {}_1\bar{D} : \Delta {}^1\bar{\epsilon} \quad (III.66)$$

where $\Delta {}^1\bar{\sigma}$ and $\Delta {}^1\bar{\epsilon}$ are the increments of the Cauchy stress and the Euler strain tensors respectively. In the updated Lagrangian formulation the constitutive equations may be written in the form

$$\Delta_1^1 \bar{\bar{S}} = {}_1 \bar{\bar{D}} : \Delta_1^1 \bar{\bar{E}} \quad (\text{III.67})$$

where $\Delta_1^1 \bar{\bar{S}}$ and $\Delta_1^1 \bar{\bar{E}}$ are the increments of the second Piola-Kirchhoff stress tensor and the Green-Lagrange strain tensor, respectively. In the Lagrangian formulation a similar form may be introduced

$$\Delta_0^1 \bar{\bar{S}} = {}_0 \bar{\bar{D}} : \Delta_0^1 \bar{\bar{E}} \quad (\text{III.68})$$

where all the terms are defined as in the updated Lagrangian formulation but referred to the initial (undeformed) configuration.

It should be noticed that ${}_0 \bar{\bar{D}}$ and ${}_1 \bar{\bar{D}}$ are both constant tensors and defined in terms of elastic moduli and Poisson's ratio of the material. However, specifying ${}_1 \bar{\bar{D}}$ is equivalent to using a material tensor ${}_0 \bar{\bar{D}}$ which is deformation-dependent. This comes mainly from the transformation of the constitutive equations, eqn. (III.67), to the initial configuration, namely the following transformation exists between the two material tensors

$${}_1 \bar{\bar{D}} = \frac{1}{|{}_0 \bar{\bar{F}}|} {}_0 \bar{\bar{D}}_{mnpq} ({}_0 \bar{\bar{F}} \cdot \bar{\bar{e}}_m) ({}_0 \bar{\bar{F}} \cdot \bar{\bar{e}}_n) ({}_0 \bar{\bar{F}} \cdot \bar{\bar{e}}_p) ({}_0 \bar{\bar{F}} \cdot \bar{\bar{e}}_q) \quad (\text{III.69})$$

the components of ${}_1 \bar{\bar{D}}$ are

$${}_1 \bar{\bar{D}}_{ijkl} = \left| \frac{\partial^0 \bar{\bar{X}}}{\partial^1 \bar{\bar{x}}} \right| \frac{\partial^1 \bar{x}_i}{\partial^0 \bar{X}_m} \frac{\partial^1 \bar{x}_j}{\partial^0 \bar{X}_n} {}_0 \bar{\bar{D}}_{mnpq} \frac{\partial^0 \bar{X}_k}{\partial^1 \bar{x}_p} \frac{\partial^0 \bar{X}_l}{\partial^1 \bar{x}_q} \quad (\text{III.70})$$

The inverse transformation is

$${}_0 \bar{\bar{D}} = |{}_0 \bar{\bar{F}}| {}_1 \bar{\bar{D}}_{mnpq} ({}_0 \bar{\bar{F}}^{-1} \cdot \bar{\bar{e}}_m) ({}_0 \bar{\bar{F}}^{-1} \cdot \bar{\bar{e}}_n) ({}_0 \bar{\bar{F}}^{-1} \cdot \bar{\bar{e}}_p) ({}_0 \bar{\bar{F}}^{-1} \cdot \bar{\bar{e}}_q) \quad (\text{III.71})$$

the components of ${}_0 \bar{\bar{D}}$ are

$${}_0 \bar{\bar{D}}_{ijkl} = \left| \frac{\partial^1 \bar{\bar{x}}}{\partial^0 \bar{\bar{X}}} \right| \frac{\partial^0 \bar{X}_i}{\partial^1 \bar{x}_m} \frac{\partial^0 \bar{X}_j}{\partial^1 \bar{x}_n} {}_1 \bar{\bar{D}}_{mnpq} \frac{\partial^0 \bar{X}_k}{\partial^1 \bar{x}_p} \frac{\partial^0 \bar{X}_l}{\partial^1 \bar{x}_q} \quad (\text{III.72})$$

Another possibility in deriving the constitutive equations is to characterize the material behaviour using stress rate defined with respect to the present configuration C_1 [5,17,18,29,79,116,117]. The stress rate used must be frame-indifferent (invariant with

respect to rigid body rotation). The most common stress rate used is the Jaumann rate which is defined in configuration C_1 as

$$\left(\frac{\delta {}^1\sigma_{ij}}{\delta t} \right)^J = \left(\frac{d {}^1\sigma_{ij}}{dt} \right) - {}^1\sigma_{ik} {}^1w_{kj} - {}^1\sigma_{kj} {}^1w_{ki} \quad (\text{III.73})$$

where $(\delta {}^1\sigma_{ij}/\delta t)^J$ is the Jaumann stress rate, ${}^1\sigma_{ik}$ are the components of the Cauchy stress tensor, and

$${}^1w_{kj} = \frac{1}{2} \left(\frac{\partial {}^1v_j}{\partial {}^1x_k} - \frac{\partial {}^1v_k}{\partial {}^1x_j} \right) \quad (\text{III.74})$$

are the components of the spin tensor

$${}^1w = \frac{1}{2} \left(\frac{\partial {}^1\bar{v}}{\partial {}^1\bar{x}} - \frac{{}^1\bar{v} \partial}{\partial {}^1\bar{x}} \right)$$

Considering a unit increment of time, the Jaumann stress increment is

$$(\delta {}^1\sigma_{ij})^J = \Delta {}^1\sigma_{ij} - \frac{1}{2} {}^1\sigma_{ik} \left(\frac{\partial {}^1u_j}{\partial {}^1x_k} - \frac{\partial {}^1u_k}{\partial {}^1x_j} \right) - \frac{1}{2} {}^1\sigma_{kj} \left(\frac{\partial {}^1u_i}{\partial {}^1x_k} - \frac{\partial {}^1u_k}{\partial {}^1x_i} \right) \quad (\text{III.75})$$

where

$$(\delta {}^1\sigma_{ij})^J = {}^1D_{ijkl} \Delta {}^1e_{kl} \quad (\text{III.76})$$

It should be noticed that in eqn. (III.75) $\Delta {}^1\sigma_{ij}$ is the increment of the Cauchy stress tensor measured and referred to the current configuration C_2 . If this stress increment is transformed back to the updated Lagrangian configuration C_1 it becomes the increment of the second Piola-Kirchhoff stress tensor from configuration C_1 to C_2 while referred to configuration C_1 . Also, ${}^1\sigma_{ij}$ is the Cauchy stress tensor referred to configuration C_1 which is equivalent to the second Piola-Kirchhoff stress tensor measured and referred to the configuration C_1 , ${}^1S_{ij}$. Therefore, eqn. (III.75) may be written as

$$\Delta {}^1S_{ij} = {}^1D_{ijkl} \Delta {}^1e_{kl} + \frac{1}{2} {}^1\sigma_{ik} \left(\frac{\partial {}^1u_j}{\partial {}^1x_k} - \frac{\partial {}^1u_k}{\partial {}^1x_j} \right) + \frac{1}{2} {}^1\sigma_{kj} \left(\frac{\partial {}^1u_i}{\partial {}^1x_k} - \frac{\partial {}^1u_k}{\partial {}^1x_i} \right) \quad (\text{III.77})$$

Owing to the same argument of using Jaumann stress rate, any possible frame-indifferent stress rate may be used to derive the constitutive equations. For example consider the use of the convected stress rate which is given as

$$\left(\frac{\delta^1 \sigma_{ij}}{\delta t} \right)^C = \left(\frac{\delta^1 \sigma_{ij}}{\delta t} \right)^J + {}^1D_{ik} {}^1\sigma_{kj} + {}^1\sigma_{ik} {}^1D_{kj} \quad (\text{III.78})$$

where $(\delta^1 \sigma_{ij}/\delta t)^C$ is the convected stress rate, $(\delta^1 \sigma_{ij}/\delta t)^J$ is the Jaumann stress rate, and

$${}^1D_{ik} = \frac{1}{2} \left(\frac{\partial^1 v_k}{\partial^1 x_i} + \frac{\partial^1 v_i}{\partial^1 x_k} \right) \quad (\text{III.79})$$

are the components of the rate of deformation tensor.

$${}^1\bar{D} = \frac{1}{2} \left(\frac{\partial^1 \bar{v}}{\partial^1 \bar{x}} + \frac{\partial^1 \bar{v}}{\partial^1 \bar{x}} \right)$$

Considering a unit-increment of time, the stress increment is

$$\Delta {}^1S_{ij} = \Delta {}^1S_{ij}^J + \frac{1}{2} {}^1\sigma_{kj} \left(\frac{\partial^2 u_k}{\partial^1 x_i} + \frac{\partial^2 u_i}{\partial^1 x_k} \right) + \frac{1}{2} {}^1\sigma_{ij} \left(\frac{\partial^2 u_j}{\partial^1 x_k} + \frac{\partial^2 u_k}{\partial^1 x_j} \right) \quad (\text{III.80})$$

Hibbit et al. [52] and Marcal [53] utilize the Jaumann stress rate and the Truesdell stress increment to develop their form for the constitutive equations as given by

$$\Delta {}^1S_{ij} = \left[\frac{\partial^1 \bar{x}}{\partial^0 \bar{X}} \right] \frac{\partial^0 X_i}{\partial^1 X_m} \frac{\partial^1 X_j}{\partial^1 X_n} \frac{\partial^1 X_r}{\partial^1 X_k} \left\{ {}^1D_{mnkl} \frac{\partial^0 X_s}{\partial^1 X_l} + {}^1\sigma_{mn} \frac{\partial^0 X_s}{\partial^1 X_k} - {}^1\sigma_{mk} \frac{\partial^0 X_s}{\partial^1 X_n} - {}^1\sigma_{nk} \frac{\partial^0 X_s}{\partial^1 X_m} \right\} \Delta {}^1E_{rs} \quad (\text{III.81})$$

Since the above form is complicated, Hibbit et al. [52] and Marcal [53] proposed the use of the current configuration as a reference for the development of the stiffness matrices. When such procedure was carried out, it yielded a more complicated initial stress stiffness matrix.

It is worth mentioning that there are some other stress rates which may be used to derive acceptable constitutive equations such as: Hill's rate, Truesdell's rate, Oldroyd's rate, and some other rates. Hill's stress rate has been used in the rate-type theory of formulation [97-99, 104-108] while the Truesdell stress rate is rarely used in the finite element analysis [118].

(ii) **Elasto-Plastic Material**

Dealing with the elasto-plastic behaviour of the material is quite difficult because the constitutive equations in this case are governed by three concepts: a yield criterion, a flow rule, and a strain-hardening rule. The yield criterion determines whether the material is behaving elastically or plastically; the flow rule relates plastic strain increments to the current stresses and stress increments subsequent to yielding; and finally, the hardening rule specifies how the yield condition is modified during the plastic flow. The most widely used practical approach to elasto-plastic analysis is to employ a generalized infinitesimal constitutive equations in which we may assume a linear decomposition of strain increments into their elastic and plastic parts. However, Lee [102] and Lee et al. [101,103] show that the linear decomposition of strain increments is, in general, not true. In Lagrangian formulation, the incremental constitutive equations may take the form of eqn. (III.68) given above, where the components of the tensor ${}^4_0\bar{D}$, ${}^4_0D_{ijkl}$ are now derived from the elastic constants, the second Piola-Kirchhoff stress tensor, and the work hardening characteristics of the material. In the updated Lagrangian formulation, a similar form to that given in eqn. (III.67), can be used but the components ${}^4_1D_{ijkl}$ in this case depend on the current state of the stress (Cauchy stress tensor) besides the elastic constants and the work hardening characteristics. The constitutive equations in the updated Lagrangian formulation could be more appealing than in the Lagrangian formulation since the true stress components are used to define the material tensor. For this reason, the transformation of the two material tensors, ${}^4_1\bar{D}$ and ${}^4_0\bar{D}$, one into the other, may not exist since in the elasto-plastic analysis, the one-to-one mapping of the two Lagrangian formulations may not exist. Presently, a great deal of research is being performed to improve the constitutive equations in the case of elasto-plastic material behaviour, see for example reference [142].

Another possibility is to characterize the material behaviour using stress rates which are frame-indifferent. Once again, the most commonly used stress rate is the Jaumann rate given by eqn. (III.75) [5,17,18,29,116,117].

III.2 APPLICATIONS

So far, the incremental equilibrium equations for the Lagrangian and the updated Lagrangian formulation have been developed. It should be observed that the final equations for each formulation possesses two types of nonlinearity: the geometric nonlinearity arising from the generalized strain-displacement relations given by eqns. (III.21, III.22), and the material nonlinearity arising from the nonlinear material response such as inelastic, elastoplastic, and creep behaviour of the material. To demonstrate the applicability of the presented formulations for static and dynamic analysis, the Lagrangian and the updated Lagrangian formulation have been incorporated into a special purpose finite element programme which can be used for geometric and/or material nonlinearity analysis. Two example problems have been solved using this programme, these are large displacement static analysis of a cantilever beam under uniformly distributed load, and a dynamic analysis of pipe-whip. In the following, we are going to discuss the finite element idealizations, numerical integration, and computer implementation for the two example problems.

III.2.1 LARGE DISPLACEMENT STATIC ANALYSIS OF A CANTILEVER

III.2.1.1 Analysis Using the Isoparametric Plane Stress Element

Figure (III.1) shows a cantilever beam subjected to uniformly distributed loading. The dimensions and the properties of the cantilever have been chosen to enable comparison of the results obtained using the presented formulations with the available analytical and numerical solutions in the literature. For the finite element analysis, the cantilever is

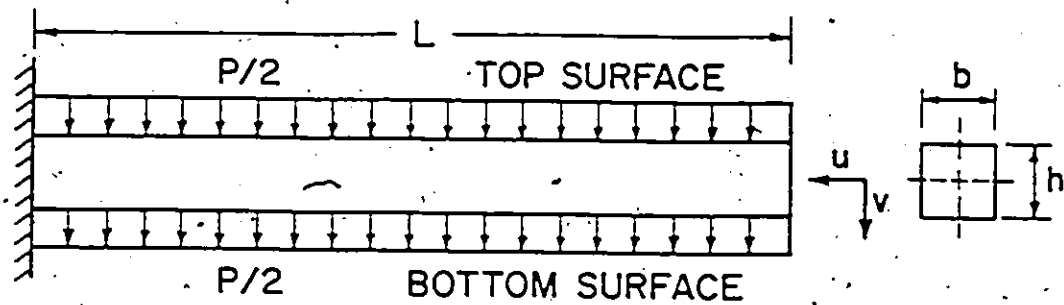
idealized as an assemblage of five 8-node isoparametric plane stress elements as shown in Figure (III.2). It should be noted that in the isoparametric formulation the elements can have curved boundaries without any difficulties. Even if the element boundaries are initially straight, they become curved and distorted after deformation which is relatively easy to take into account in the isoparametric formulation, especially when the updated Lagrangian formulation is used in the analysis. This is an important advantage over the generalized coordinate finite element formulation. The material of the cantilever is assumed to be isotropic linear elastic material. This problem provides a good example for the analysis of geometric nonlinearity [15,17-19,68,94,114] since the cantilever stiffens with increasing displacements.

For the calculations of the element stiffness matrices and the load increment vectors in both formulations, consider a typical two-dimensional element in the configuration at time 0 and time t , as shown in Figure (III.3). In the isoparametric formulation, the coordinates and the displacements are interpolated in the same way [5-9]. Therefore, the coordinates and the components of the displacement vector of a point in the element can be expressed as follows:

$${}^t x_i(r,s) = \sum_{K=1}^8 h_K {}^t x_i^K \quad (III.81)$$

$${}^t u_i(r,s) = \sum_{K=1}^8 h_K {}^t u_i^K, \quad i = 1, 2 \quad (III.82)$$

where ${}^t x_i$ are the coordinates of the point referred to the global axes x_1 and x_2 , $h_K(r,s)$ are the interpolation functions [5-9], r and s are the coordinates of the point with respect to the natural axes, ${}^t x_i^K$ are the coordinates of nodal point K and, finally, ${}^t u_i$ and ${}^t u_i^K$ are the components of the displacement vector of the point and nodal point K respectively. The shape functions ψ_{ia} and the global shape function derivatives $\partial \psi_{ia} / \partial {}^t x_i$ are given in Appendix B.



$$\begin{aligned}
 L &= 10 \text{ IN.} & E &= 1.2 \times 10^4 \text{ LB/IN}^2 \\
 h &= 1 \text{ IN.} & \nu &= 0.2 \\
 b &= 1 \text{ IN.}
 \end{aligned}$$

Figure (III.1) Cantilever under uniformly distributed load

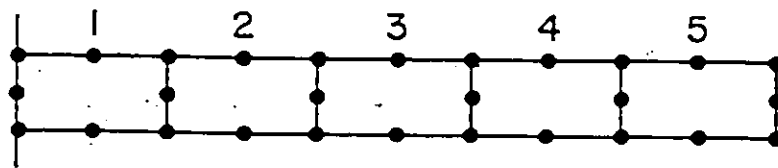


Figure (III.2) Finite element mesh for the cantilever.

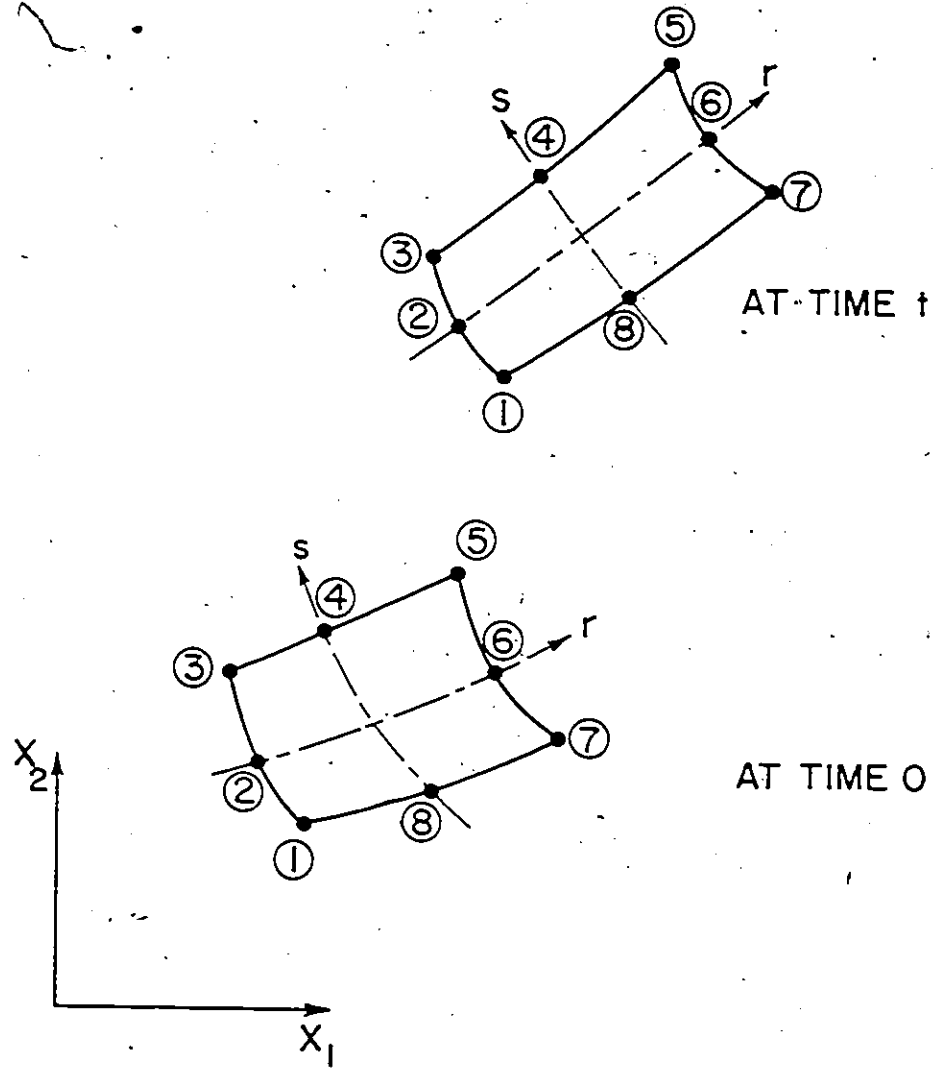


Figure (H1.3) Two-dimensional element undergoing large deformation.

(i) Lagrangian Formulation

Considering the shape functions and the shape function derivatives at time 0, and the constitutive equations, eqn. (III.68), the element stiffness matrices, eqns. (III.44-III.48), and the increment of the load vector, eqn. (III.41), are calculated using numerical integration. The Gauss-Legendre integration procedure of order 3x3 is employed. To evaluate the components of the material tensor (often called Hookean tensor), it is necessary to establish the relationship between this tensor and the matrix relating the stresses and the strains, see Appendix C. The material tensor components ${}_0D_{ijkl}$ are evaluated in the same way as in the small deformation analysis.

For the numerical integration, it should be noticed that the shape functions and the shape function derivatives are functions of the natural coordinates, r and s . Therefore, the volume integration extends over the natural coordinate volume and the volume differential d^tV needs also be expressed in terms of the natural coordinates. In general, we have

$$d^tV = \det {}^tJ \, dr \, ds \quad (\text{III.84})$$

where $\det {}^tJ$ is the determinant of the Jacobian matrix at time t . To carry out the integration over the surface area in eqns. (III.41, III.42), let us first consider the representation of the Jacobian matrix in the three-dimensional case [7] as

$${}^tJ = \begin{bmatrix} \frac{\partial {}^tx_1}{\partial r} & \frac{\partial {}^tx_2}{\partial r} & \frac{\partial {}^tx_3}{\partial r} \\ \frac{\partial {}^tx_1}{\partial s} & \frac{\partial {}^tx_2}{\partial s} & \frac{\partial {}^tx_3}{\partial s} \\ \frac{\partial {}^tx_1}{\partial t} & \frac{\partial {}^tx_2}{\partial t} & \frac{\partial {}^tx_3}{\partial t} \end{bmatrix} = \begin{bmatrix} t_{r_1} & t_{r_2} & t_{r_3} \\ t_{s_1} & t_{s_2} & t_{s_3} \\ t_{t_1} & t_{t_2} & t_{t_3} \end{bmatrix} = \begin{bmatrix} t_r^- \\ t_s^- \\ t_t^- \end{bmatrix} \quad (\text{III.85})$$

and

$$\det {}^tJ = t_r^- \times t_s^- \cdot t_t^- \quad (\text{III.86})$$

for two-dimensional analysis tJ takes the form

$${}^tJ = \begin{bmatrix} {}^t r_1 & {}^t r_2 & 0 \\ {}^t s_1 & {}^t s_2 & 0 \\ 0 & 0 & 1 \end{bmatrix} = \begin{bmatrix} {}^t \bar{r} \\ {}^t \bar{s} \\ {}^t \bar{t} \end{bmatrix} \quad (III.87)$$

Referring to Figure (III.4), the elementary parallelogram on the face $s=1$ has sides ${}^t \bar{r} dr$ and ${}^t \bar{t} dt$ and hence the vectorial surface area $d^t \bar{A} = {}^t \bar{t} \times {}^t \bar{r} dr dt$. The special programming associated with the vector product can be avoided if the Jacobian inverse is interpreted as follows [7]:

$${}^t J^{-1} = \frac{1}{\det {}^t J} \begin{bmatrix} {}^t \bar{s} \times {}^t \bar{t} & {}^t \bar{t} \times {}^t \bar{r} & {}^t \bar{r} \times {}^t \bar{s} \end{bmatrix} \quad (III.88)$$

Thus the components of the differential surface area vector $d^t \bar{A}$ can easily be extracted from the Jacobian inverse. Considering this differential surface area vector in the initial configuration C_0 with the relation given above in eqn. (III.39), namely, $d^0 \bar{A} = {}^0 \bar{S}_n d^0 A$, the components of the vector ${}^0 \bar{S}_n d^0 A$ is calculated at each integration point on the surface and then used in the integration of eqn. (III.42). The increment of the load vector, eqn. (III.41), is calculated using the components of the surface traction $\Delta {}^0 \bar{S}_n$, together with $d^0 A = |{}^0 \bar{t} \times {}^0 \bar{r}| dr ds$

Solution Technique

For the solution of the incremental equilibrium equations, there are two different methods: direct solution methods and iterative solution methods. However, in finite element applications the direct solution methods are currently most effective. The more efficient direct solution methods are based on the applications of the Gaussian elimination technique. The effectiveness of the equation solver is largely a result of the specific storage scheme used and the specific implementation of the Gaussian elimination technique. In this analysis, the

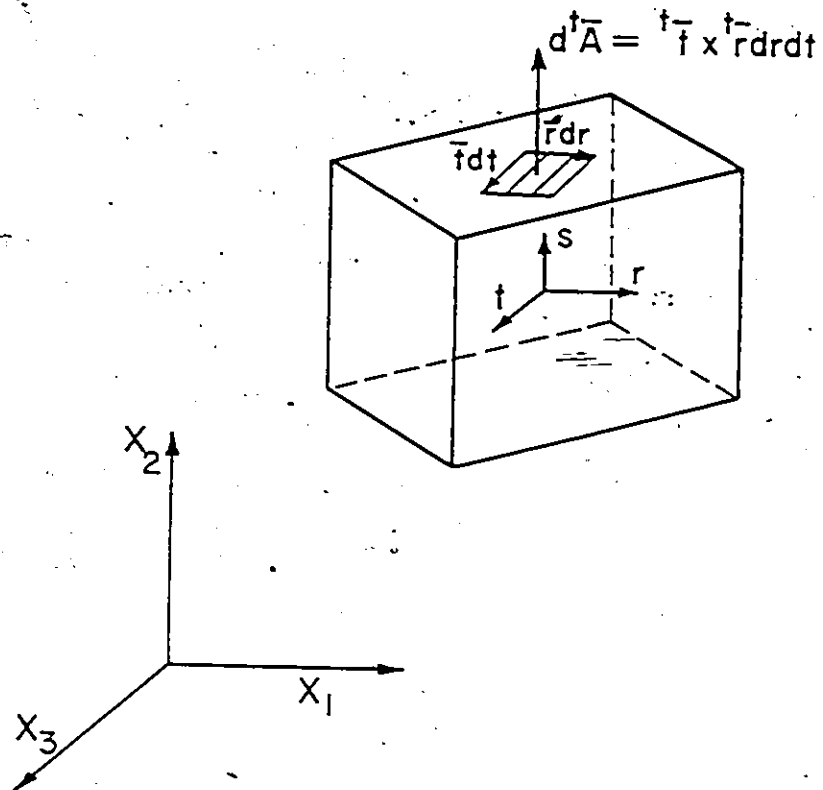


Figure (III.4) A three-dimensional element showing an infinitesimal surface area as a vector normal to the face.

Frontal solution technique [7,9] has been employed. The main idea of Frontal technique is to assemble the equations, eliminate the variables and store them on back-up disc storage at the same time. Therefore, the Frontal technique is designed to minimize the core storage requirements and the number of arithmetic operations.

Numerical Results

In the Lagrangian formulation, it is found that by integrating the first term of the second integral in the load increment, eqn. (III.41), gives the increment of the vertical load, or the conservative load (load retains its vertical direction). Figure (III.5) shows the numerical and the analytical solutions for the vertical load. The analytical solution is given by Holden [94]. The numerical solutions include the results obtained from the developed programme with and without the load-correction matrix, ${}^0_1K_{\alpha\beta}^{(4)}$, the result obtained from the ADINA programme by Bathe et al. [15,17-19], and the result obtained by Nagarajan and Popov [68]. When the second term of the second integral in the load increment is included in the integration, it is found that it becomes the increment of the follower load, or nonconservative load (load remains perpendicular to the top and the bottom surfaces of the cantilever). Figure (III.6) depicts the results obtained and the result presented by Bathe et al. [17] for the follower load. In this specific example the top and the bottom surface nodal points of the cantilever are used in Bathe et al.'s analysis [17] to define the direction of the follower load increment. Therefore, instead of following the deformation of the structure to specify the normal direction to the deformed surfaces, the second term of the second integral in the load increment can be included, and then the load increment will be the follower load increment. Table (III.1) gives the required number of equal load increments for the present Lagrangian formulation with and without the load-correction matrix, ${}^0_1K_{\alpha\beta}^{(4)}$, for the formulation

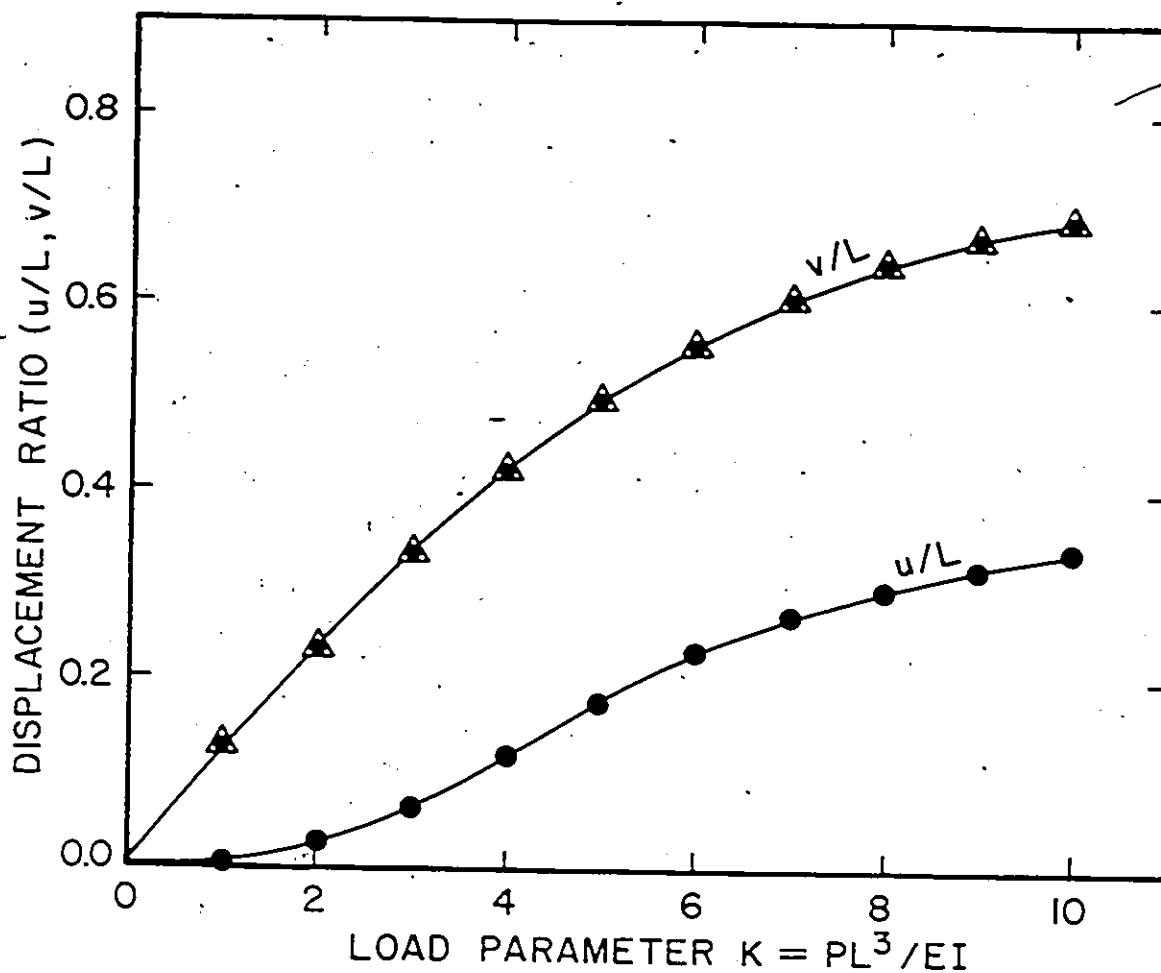


Figure (III.5) Large displacement analysis of a cantilever using Lagrangian formulation.

- Present without ${}^1K_{off}^{(4)}$, 100 equal increments
- Present with ${}^1K_{off}^{(4)}$, 61 equal increments
- Δ Bathe et al., 100 equal increments
- Δ Nagarajan and Popov, 100 equal increments
- Analytical solution [Holden], vertical load

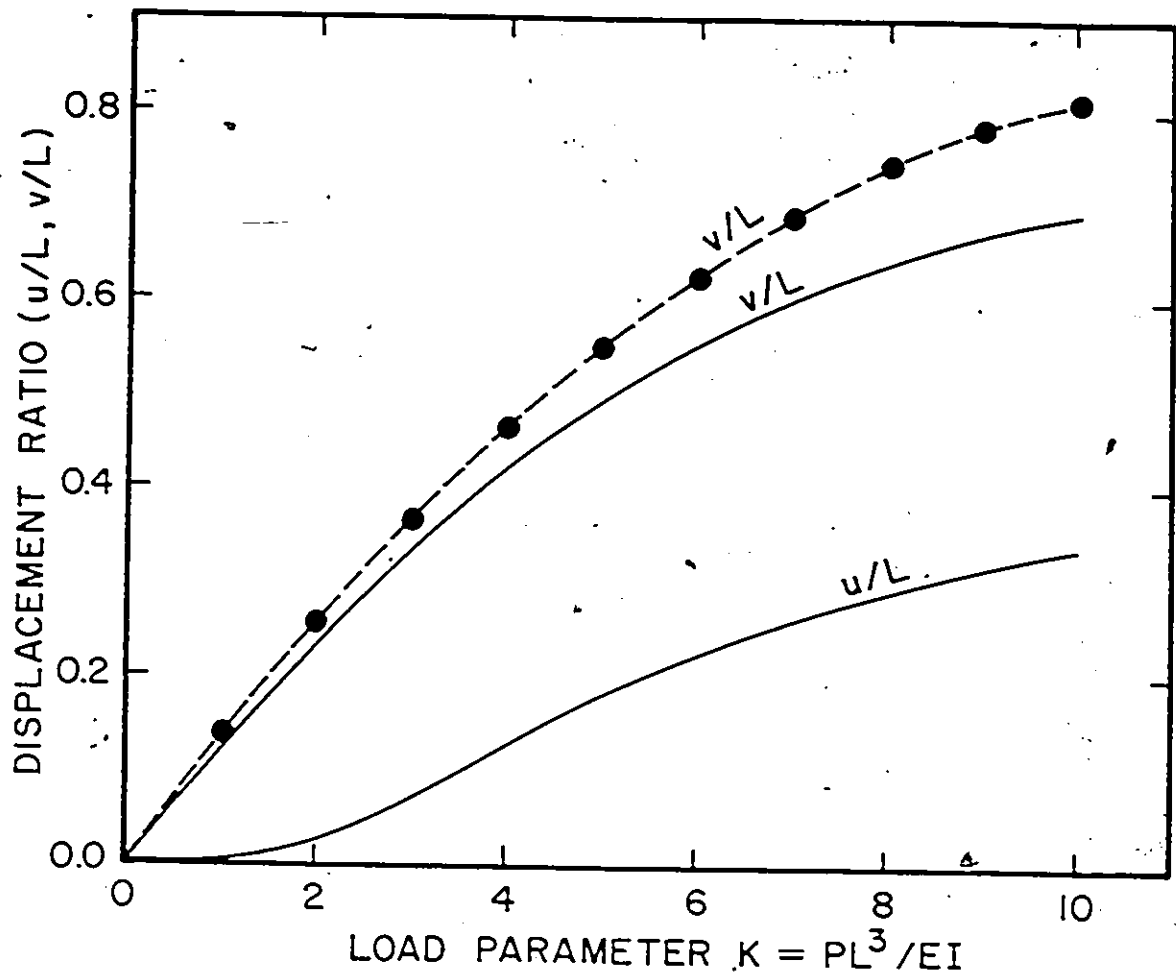


Figure III.6) Large displacement analysis of a cantilever using Lagrangian formulation.

- Present without ${}^1K_{\alpha\beta}^{(4)}$, 100 equal increments
- Present with ${}^1K_{\alpha\beta}^{(4)}$, 61 equal increments
- Bathe et al., 100 equal increments
- Nagarajan and Popov, 100 equal increments
- Analytical solution [Holden], vertical load.

of Bathe et al. [15;17-19], and for the formulation of Nagarajan and Popov [68] to obtain identical solutions to the analytical solution given by Holden [94]. All these solutions have been obtained without equilibrium checks.

Table (III.1): Number of equal load increments required to obtain identical solutions for different Lagrangian formulations.

Load Case	Present Formulation		Bathe et al.	Nagarajan and Popov
	without ${}^1K_{\alpha\beta}^{(4)}$	with ${}^1K_{\alpha\beta}^{(4)}$		
Vertical load	100	61	100	100
Follower load	100	61	100	100

It is seen from Table (III.1) that the present Lagrangian formulation needs the same number of equal load increments as of Bathe et al. However, by including the load-correction matrix ${}^1K_{\alpha\beta}^{(4)}$ in the analysis, a total reduction of 39 increments is achieved. The same problem was also solved for the case when the total vertical load is applied in five equal increments in order to show the effect of the load increment size on the solution. Figure (III.7) shows the calculated results and the comparison with that of Bathe et al. [19]. In this case the solutions obtained by using the present and the Bathe et al.'s formulation are significantly different from the exact solution because the incremental solution using either formulation is not obtained accurately. The results also show that the two solutions are different because in the present formulation the second order incremental term in the increment of the strain tensor, eqn. (III.21), was omitted whereas, in Bathe's formulation this term cannot be eliminated because it leads to the development of the initial stress stiffness matrix.

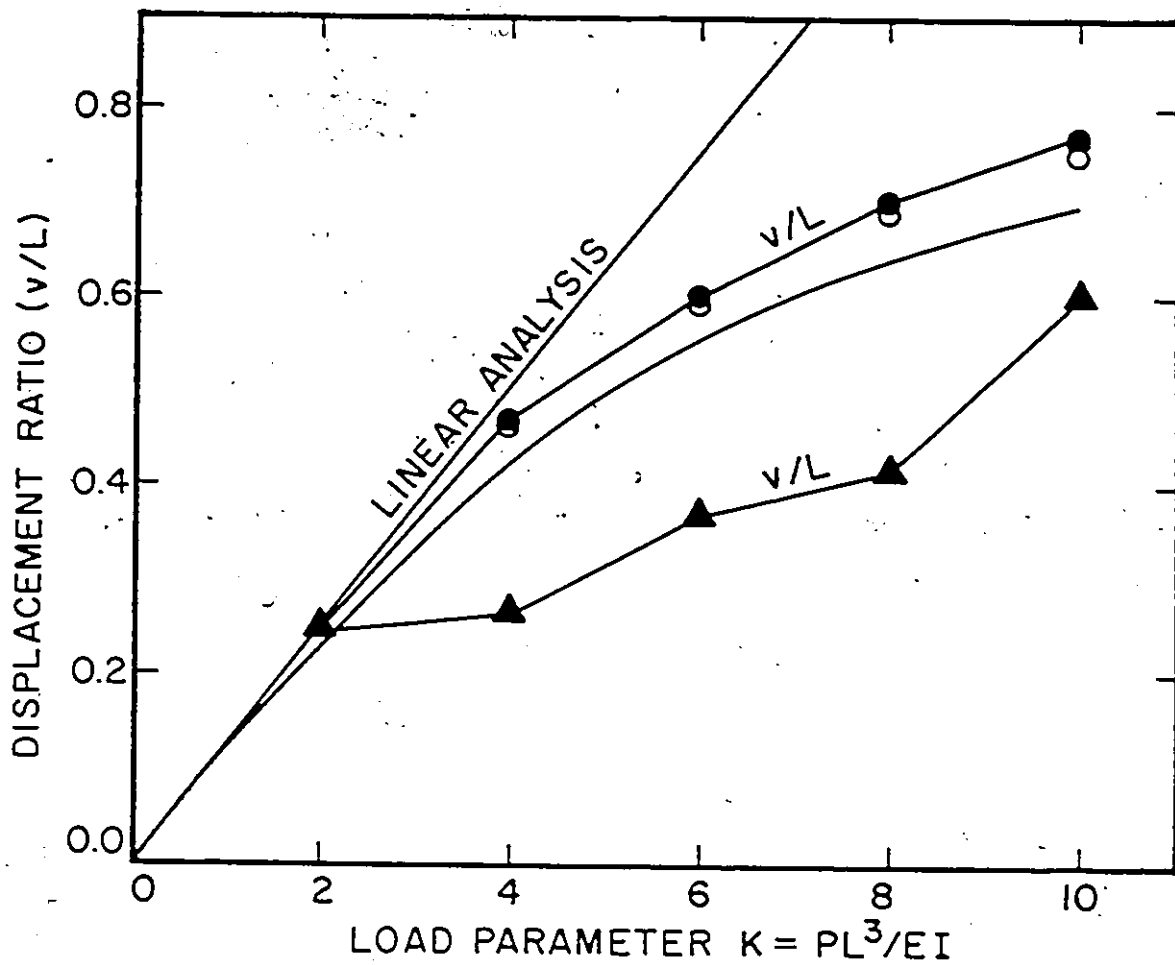


Figure (III.7) Large displacement analysis of a cantilever using Lagrangian formulation.

- Present without ${}_0^1K_{\alpha\beta}^{(4)}$, 5 equal increments
- Present with ${}_0^1K_{\alpha\beta}^{(4)}$, 5 equal increments
- ▲ Bathe et al., 5 equal increments
- Analytical solution [Holden], vertical load.

(ii) Updated Lagrangian Formulation

In the updated Lagrangian formulation, the shape functions and the shape function derivatives are evaluated at time t (configuration C_1). Once the tensor components ${}^0D_{ijkl}$ are defined in the constitutive equations, the components of the tensor ${}^1D_{ijkl}$ can be calculated at each integration point using eqn. (III.70). The components of the second Piola-Kirchhoff stress tensor ${}^1S_{ij}$ defined and measured per unit area in the present configuration C_1 , which is equivalent to the components of the Cauchy stress tensor ${}^1\sigma_{ij}$ can be obtained using the following transformation formula at each integration point.

$${}^1S_{ij} = \left| \frac{\partial {}^0\bar{X}}{\partial {}^1\bar{x}} \right| \frac{\partial {}^1x_i}{\partial {}^0X_k} {}^0S_{kl} \frac{\partial {}^1x_j}{\partial {}^0X_l} \quad (III.89)$$

$${}^2S_{ij} = {}^1S_{ij} + \Delta {}^2S_{ij} \quad (III.90)$$

and

$${}^2S_{ij} = \left| \frac{\partial {}^1\bar{x}}{\partial {}^2\bar{x}} \right| \frac{\partial {}^2x_i}{\partial {}^1x_k} {}^1S_{kl} \frac{\partial {}^2x_j}{\partial {}^1x_l} \quad (III.91)$$

Having defined the shape functions ψ_{ia} , the shape function derivatives $\partial\psi_{ia}/\partial{}^1x_j$, the Jacobian matrix 1J and its inverse ${}^1J^{-1}$, the components of the material tensor ${}^1D_{ijkl}$, and the components of the second Piola-Kirchhoff stress tensor ${}^1S_{ij}$, the element stiffness matrices are calculated using the same numerical procedure discussed in the Lagrangian formulation.

Numerical Results

Figure (III.8) shows the obtained results using the present updated Lagrangian formulation in case of the vertical load. The total load was applied in 100, 10, and 5 equal increments. It is apparent from Figure (III.8) that as the displacements are getting larger the predicted solutions deviate significantly from the numerical solution obtained by using the

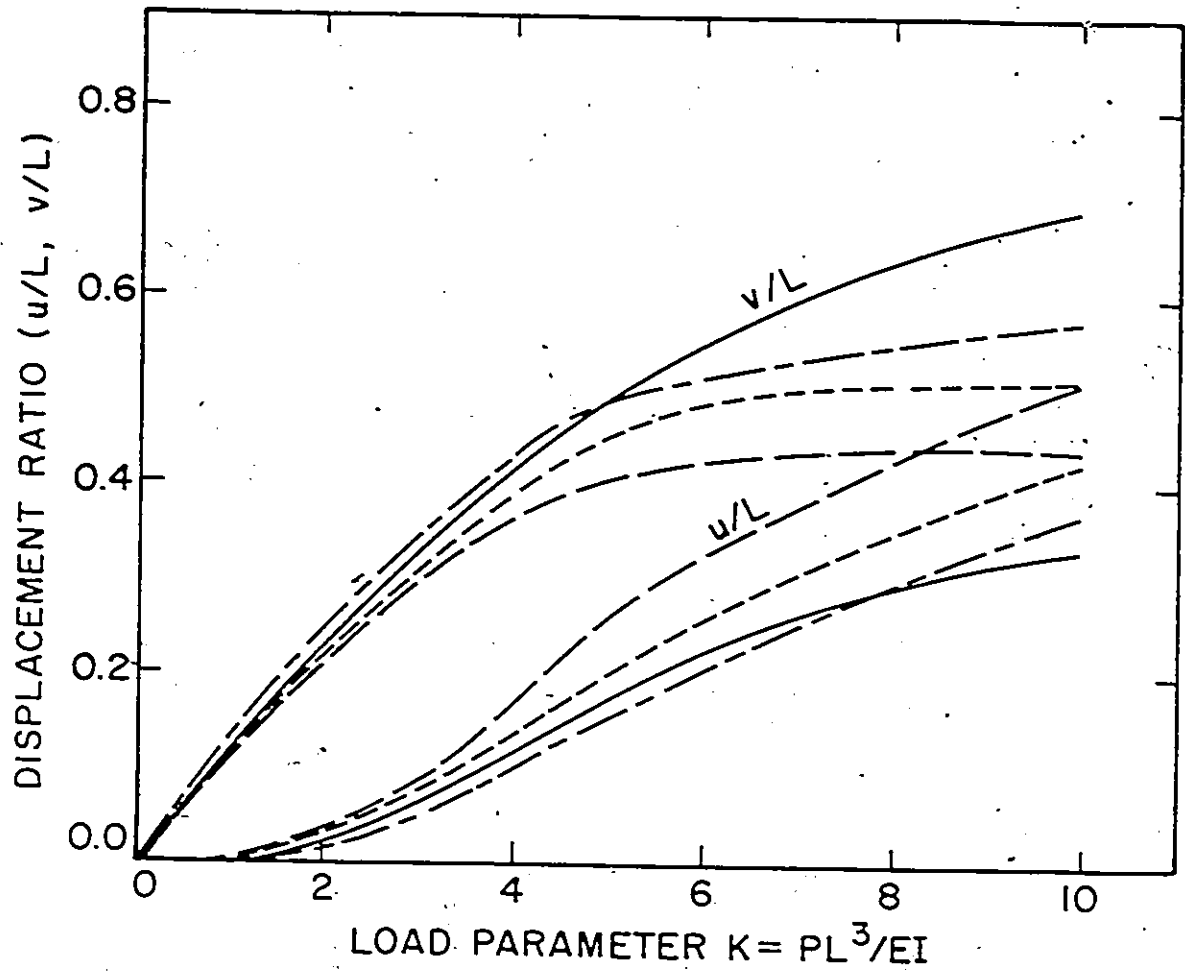


Figure (III.8) Large displacement analysis of a cantilever using updated Lagrangian formulation.

- — Present with ${}^1K_{u\beta}^{(3)}$, 100 equal increments
- Present with ${}^1K_{u\beta}^{(3)}$, 10 equal increments
- Present with ${}^1K_{u\beta}^{(3)}$, 5 equal increments
- Present Lagrangian, 100 equal increments
- Analytical solution [Holden], vertical load.

Lagrangian formulation. However, the invertible transformation between the two Lagrangian formulations should exist, specifically for the elastic response of the material where the one-to-one mapping exists. In considering the transformation of the increment of the second Piola-Kirchhoff stress tensor between the two Lagrangian formulations, one can start with the increment of the second Piola-Kirchhoff stress tensor in the updated Lagrangian formulation given by eqn. (III.67), and then substitute for the strain tensor increment from eqn. (III.22), which gives

$$\begin{aligned} \Delta_1^1 S_{ij} &= \frac{1}{2} {}_1 D_{ijkl} \left[\left(\frac{\partial \psi_{ka}}{\partial^1 x_l} + \frac{\partial \psi_{la}}{\partial^1 x_k} + \frac{\partial^1 u_r}{\partial^1 x_k} \frac{\partial \psi_{ra}}{\partial^1 x_l} + \frac{\partial^1 u_r}{\partial^1 x_l} \frac{\partial \psi_{ra}}{\partial^1 x_k} \right) \right]_{1^2 u_a} \\ &= {}_1 D_{ijkl} \left[\left(\frac{\partial \psi_{ka}}{\partial^1 x_l} + \frac{\partial^1 u_r}{\partial^1 x_k} \frac{\partial \psi_{ra}}{\partial^1 x_l} \right) \right]_{1^2 u_a} \end{aligned} \quad (\text{III.92})$$

where the symmetry of the material tensor ${}_1 \bar{D}_{ijkl} = D_{ijkl} \bar{e}_i \bar{e}_j \bar{e}_k \bar{e}_l$ is utilized in the above equation. Substituting for the material tensor from eqn. (III.70), we obtain:

$$\begin{aligned} \Delta_1^1 S_{ij} &= \left[\frac{\partial^0 \bar{X}}{\partial^1 \bar{X}} \right] \frac{\partial^1 x_i}{\partial^0 X_m} \frac{\partial^1 x_j}{\partial^0 X_n} {}_0 D_{mnpq} \frac{\partial^1 x_k}{\partial^0 X_p} \frac{\partial^1 x_l}{\partial^0 X_q} \left[\left(\frac{\partial \psi_{ka}}{\partial^1 x_l} + \frac{\partial^1 u_r}{\partial^1 x_k} \frac{\partial \psi_{ra}}{\partial^1 x_l} \right) \right]_{1^2 u_a} \\ &= \left[\frac{\partial^0 \bar{X}}{\partial^1 \bar{X}} \right] \frac{\partial^1 x_i}{\partial^0 X_m} \frac{\partial^1 x_j}{\partial^0 X_n} {}_0 D_{mnpq} \left[\left(\frac{\partial \psi_{pa}}{\partial^0 X_q} + \frac{\partial^1 u_k}{\partial^0 X_p} \frac{\partial \psi_{ka}}{\partial^0 X_q} + \frac{\partial^1 u_r}{\partial^0 X_p} \frac{\partial \psi_{ra}}{\partial^0 X_q} \right) \right]_{1^2 u_a} \\ &= \left[\frac{\partial^0 \bar{X}}{\partial^1 \bar{X}} \right] \frac{\partial^1 x_i}{\partial^0 X_m} \frac{\partial^1 x_j}{\partial^0 X_n} {}_0 D_{mnpq} \left(\Delta_0^1 E_{pq} + \frac{\partial^1 u_r}{\partial^0 X_p} \frac{\partial \psi_{ra}}{\partial^0 X_q} \right)_{1^2 u_a} \\ &= \left[\frac{\partial^0 \bar{X}}{\partial^1 \bar{X}} \right] \frac{\partial^1 x_i}{\partial^0 X_m} \frac{\partial^1 x_j}{\partial^0 X_n} \left[\Delta_0^1 S_{mn} + {}_0 D_{mnpq} \frac{\partial^1 u_r}{\partial^0 X_p} \frac{\partial \psi_{ra}}{\partial^0 X_q} \right]_{1^2 u_a} \end{aligned} \quad (\text{III.93})$$

The first bracket represents the transformation formula for the increment of the second Piola-Kirchhoff stress tensor between the two configurations C_1 and C_0 . This expression implies that the second term does not conform to the reversibility of the transformation of the stress tensor increments, therefore, this term and the corresponding stiffness matrix ${}^1K_{\alpha\beta}^{(3)}$ have been omitted in the updated Lagrangian formulation. In the literature, this term has been discarded owing to certain assumptions imposed on the kinematic relations, or to restrictions on the displacement field. Some analysts used various stress rates to describe the material behaviour within the increment to overcome this difficulty.

Figures (III.9, III.10) show the calculated results for the vertical and the follower loads respectively. The increments of the vertical and the follower load were calculated through the integration of eqn. (III.58). For the vertical load increment, the increment of the surface traction, Δ_1^1S , is kept vertical, whereas for the follower load increment, the increment of the surface traction is kept normal to the loaded surfaces of the cantilever. The normal direction to the loaded surfaces is defined by means of using the top and the bottom nodal points of the cantilever. Table (III.2) indicates the required number of equal load increments to apply the total load for the present updated Lagrangian formulation with and without the load-correction-matrix, ${}^1K_{\alpha\beta}^{(4)}$, and that of Bathe et al. [15,17-19] to obtain identical solutions to the analytical one given by Holden [94]. All these solutions were obtained without using equilibrium checks in the analysis.

Table (III.2). Number of equal load increments required to obtain identical solutions for different updated Lagrangian formulations

Load Case	Present Formulation		Bathe et al.
	without ${}^1K_{\alpha\beta}^{(4)}$	with ${}^1K_{\alpha\beta}^{(4)}$	
Vertical load	100	80	100
Follower load	100	80	100

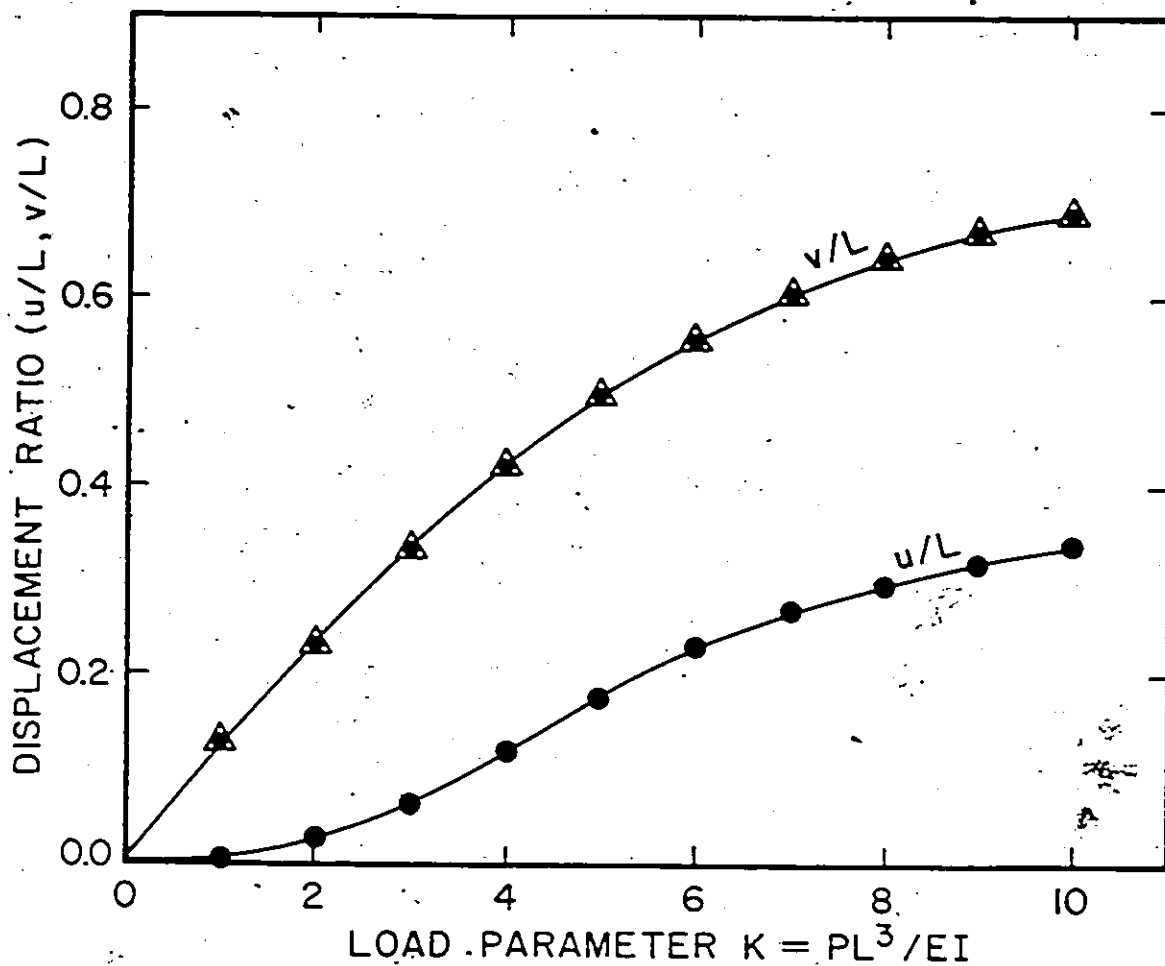
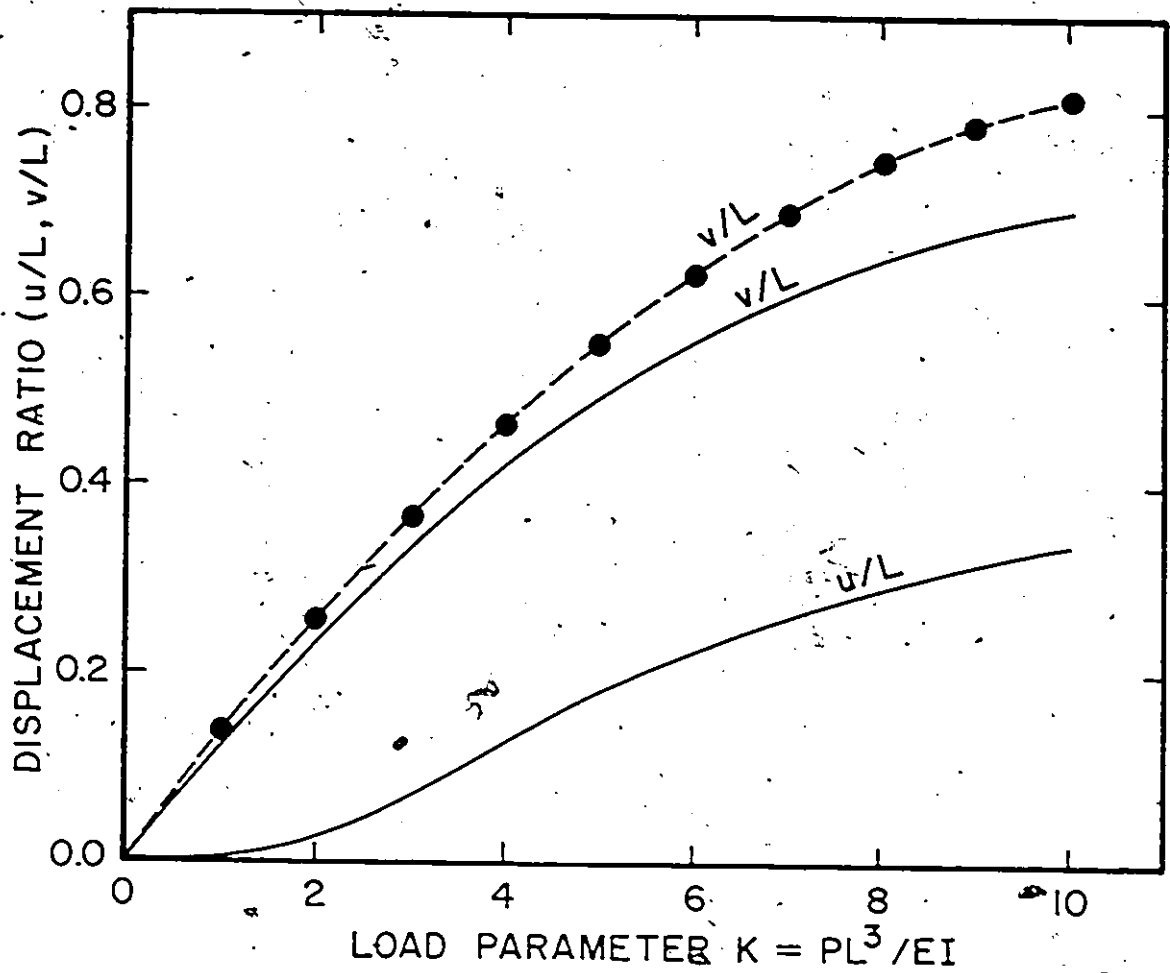


Figure (III.9) Large displacement analysis of a cantilever using updated Lagrangian formulation.

- Present without ${}^1K_{up}^{(4)}$, 100 equal increments
- Present with ${}^1K_{up}^{(4)}$, 80 equal increments
- Present without ${}^1K_{up}^{(4)}$, 100 equal increments using Jaumann stress rate
- Δ Bathe et al., 100 equal increments
- Analytical solution [Holden], vertical load



Figure(III.10) Large displacement analysis of a cantilever using updated

Lagrangian formulation.

- Present without ${}^1K_{\alpha\beta}^{(4)}$; 100 equal increments.
- Present with ${}^1K_{\alpha\beta}^{(4)}$; 80 equal increments.
- Bathe et al., 100 equal increments.
- Analytical solution [Holler], vertical load.

Owing to the argument of omitting the initial displacement effect from the increment of the Green-Lagrange strain tensor, proper transformation should make it possible to transform the two Lagrangian formulations from one into the other. Therefore, it is expected that the updated Lagrangian formulation needs the same number of equal load increments as the Lagrangian formulation to obtain identical results, in spite of the use of different numerical procedures. Table (III.2) shows that by including the ${}^1K_{\alpha\beta}$, the load-correction matrix, in the analysis, a total reduction of 20 increments is achieved. Once again, to show the effect of the size of the load increment on the predicted solution the same problem was solved for the case when the total vertical load was applied in five equal increments. Figure (III.11) shows the solution obtained and the comparison with the solution obtained by Bathe et al. [19]. Owing to the same argument in the Lagrangian formulation the two predicted solutions differ from the analytical one because the incremental solution by either formulation was not obtained accurately.

(III.2.1.2) Analysis Using the Isoparametric Beam Element

The same problem is analyzed using the isoparametric 3-node beam element. The cantilever beam in this case is modelled as a 3-node beam element with six degrees of freedom at each node. Figure (III.12) shows a typical beam element in the original configuration and the configuration at time t [5]. The basic kinematic assumption in the formulation of the element is that plane sections originally normal to the axis of the element remain plane but not necessarily normal to the deformed axis. Therefore, we can express the Cartesian coordinates and the components of the displacement vector of a point in the element as follows:

$${}^t x_i(r,s,t) = \sum_{K=1}^3 h_K {}^t x_i^K + \frac{s}{2} \sum_{K=1}^3 a_K h_K {}^t v_{s1}^K + \frac{t}{2} \sum_{K=1}^3 b_K h_K {}^t v_{t1}^K \quad (III.94)$$

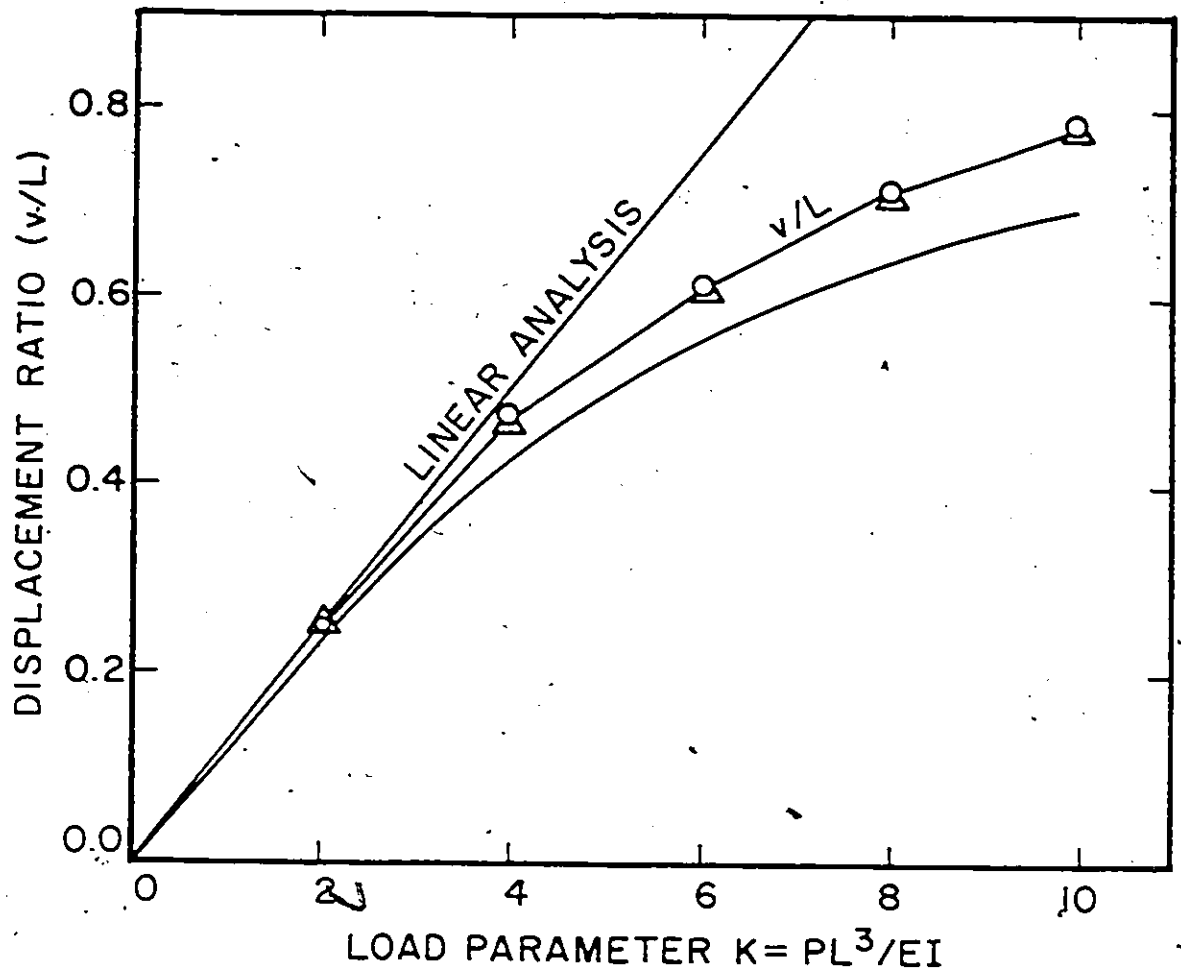


Figure (III.11) Large displacement analysis of a cantilever using updated Lagrangian formulation.

- Present without $1K_{0B}^{(4)}$, 5 equal increments
- △ Present with $1K_{0B}^{(4)}$, 5 equal increments
- Bathe, 5 equal increments
- Analytical solution [Hollen], vertical load.

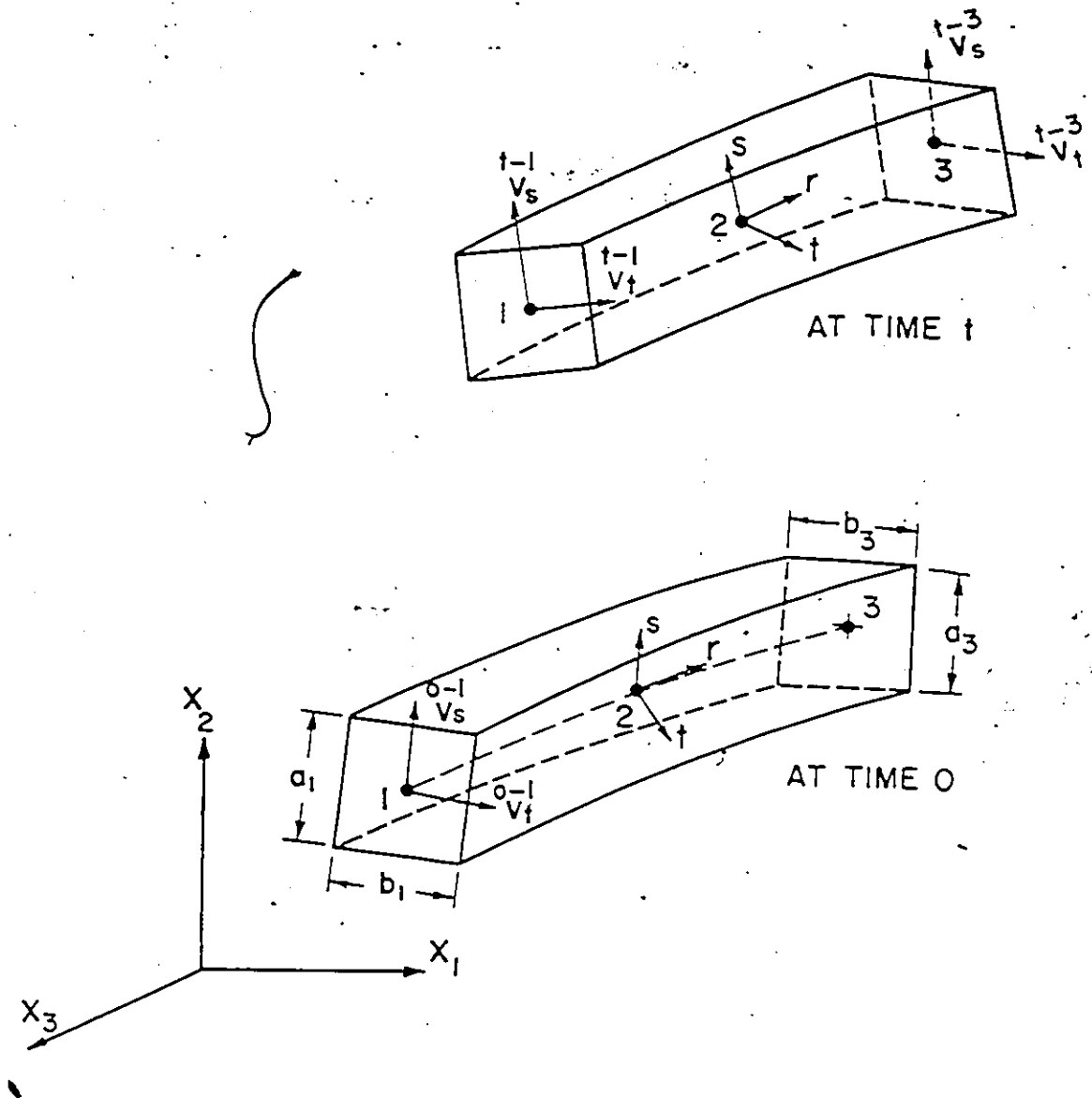


Figure (III.12) Beam element undergoing large displacements and rotations.

$${}^t u_i(r,s,t) = \sum_{K=1}^3 h_K {}^t u_i^K + \frac{s}{2} \sum_{K=1}^3 a_K h_K V_{si}^K + \frac{t}{2} \sum_{K=1}^3 b_K h_K V_{ti}^K \quad (\text{III.95})$$

where

$$V_{ti}^K = {}^t V_{ti}^K - {}^0 V_{ti}^K, \quad V_{si}^K = {}^t V_{si}^K - {}^0 V_{si}^K \quad (\text{III.96})$$

and

$r, s,$ and t are the coordinates of the point referred to the natural coordinate system,

${}^t x_i$ are the Cartesian coordinates of the point referred to the global axes x_1, x_2 and x_3 ,

$h_k(r)$ are the interpolation functions,

${}^t x_i^k$ are the Cartesian coordinates of nodal point k referred to the global axes x_1, x_2 and x_3 ,

a_K, b_K are the cross-section dimensions at nodal point K ,

${}^t V_{si}^K, {}^t V_{ti}^K$ are the components of unit vectors in s and t directions at nodal point K ,

${}^t u_i$ are the components of the displacement vector of the point,

${}^t u_i^K$ are the components of the displacement vector of nodal point K .

Finally, the vector \bar{V}_s^K and \bar{V}_t^K can be expressed in terms of the rotations about the global Cartesian axes as follows:

$$\bar{V}_s^K = {}^t \bar{\theta}_K \times {}^0 \bar{V}_s^K, \quad \bar{V}_t^K = {}^t \bar{\theta}_K \times {}^0 \bar{V}_t^K \quad (\text{III.97})$$

where ${}^t \bar{\theta}_K$ is a vector listing the nodal point rotations at nodal point K . Equation (III.97) holds provided that the angles of rotation are small. However, having calculated the angles in the finite element solution the unit vectors can be evaluated accurately using

$${}^{t+\Delta t} \bar{V}_s^K = {}^t \bar{V}_s^K + \int_0^{\Delta t} d {}^t \bar{\theta}_K \times {}^t \bar{V}_s^K \quad (\text{III.98})$$

$${}^{t+\Delta t}\bar{V}_t^K = {}^t\bar{V}_t^K + \int_{\bar{\theta}_K} d\bar{\theta}_K x {}^t\bar{V}_t^K \quad (\text{III.99})$$

The integration in eqns. (III.98, III.99) can be carried out numerically using, for example, Euler forward-integration procedure, see for example [141]. It should be noted that the unit lengths of the vector ${}^t\bar{V}_s^K$ and ${}^t\bar{V}_t^K$ must be preserved.

The shape functions, the shape function derivatives, and the Jacobian matrix are derived in Appendix D. The constitutive equations are established through the relation existing between the Hookean tensor components ${}_0D_{ijkl}$ and the matrix components C_{ij} relates the stresses to the strains (see Appendix C). In similar numerical procedures and in the interpretation of the Jacobian matrix that enables us to carry out the integration over the surface area subjected to the surface traction, the stiffness matrices and the increments of the load vector in the Lagrangian and the updated Lagrangian formulation are calculated. The Gauss-Legendre integration procedure of order 3x2x2 is employed.

(i) Lagrangian formulation

Figure (III.13) depicts the results calculated for the vertical load and the comparison of these results with the analytical solution given by Holden [94]. It is found that the present Lagrangian formulation needs 11 equal load increments without equilibrium checks to apply the total vertical load in order to obtain a numerical solution which is comparable to the analytical solution. However, including the load-correction matrix ${}_0^1K_{\alpha\beta}^{(4)}$ in the analysis, the required number of equal load increments has decreased from 11 to 7. The first increment is kept sufficiently small so that the solution does not drift away from the analytical solution. Figure (III.15) shows the result for the follower load. Once again, to calculate the follower load increment, the second term of the second integral in eqn. (III.41) is

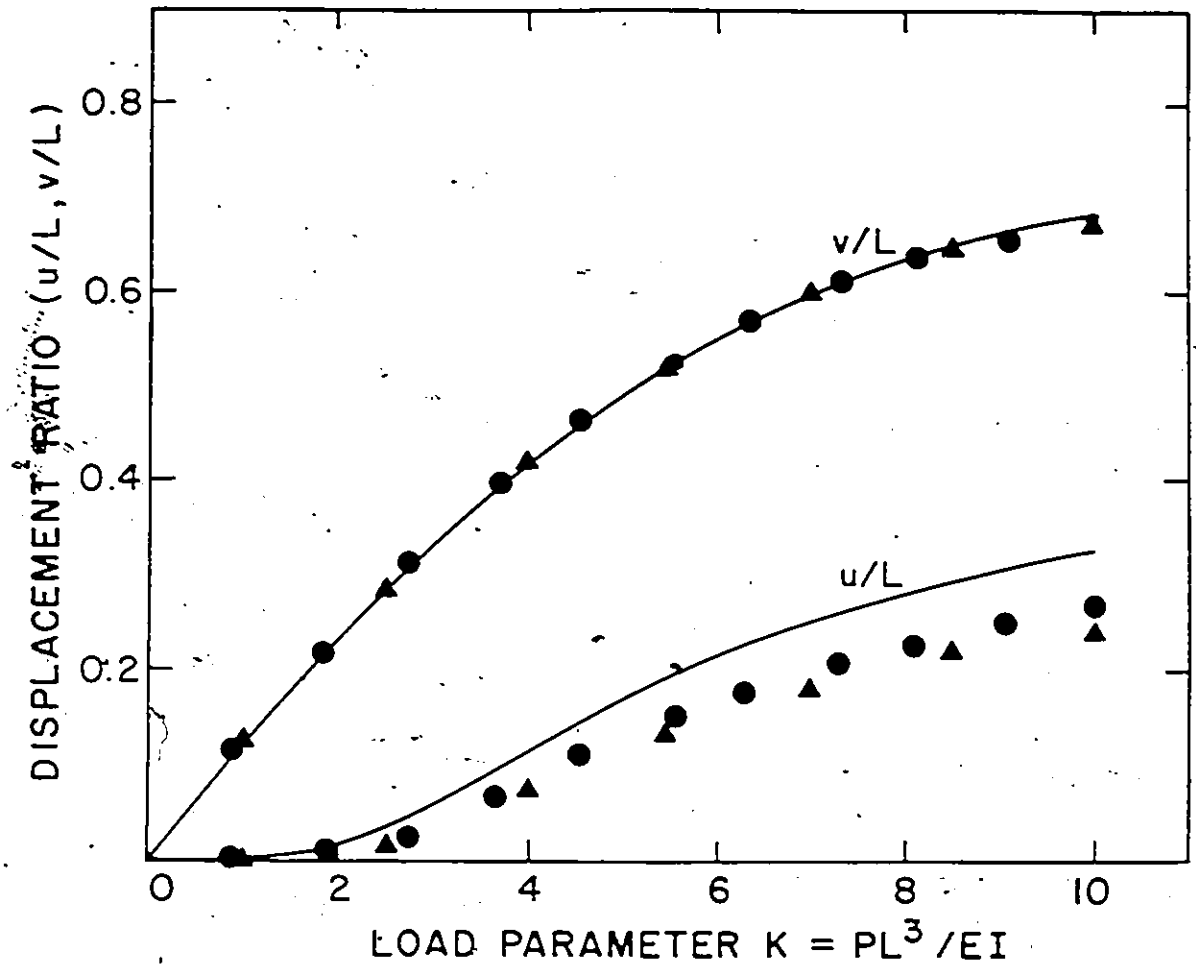


Figure (III.13) Large displacement analysis of a cantilever using Lagrangian formulation.

- Present without ${}_0^1K_{\alpha\beta}^{(4)}$, 11 equal increments.
- △ Present with ${}_0^1K_{\alpha\beta}^{(4)}$, 7 equal increments except the first.
- Analytical solution [Holden], vertical load.

included in the integration over the surface areas subjected to the traction force. It can be seen that as the displacements are getting larger in the case of the follower load, the predicted solution deviates from the solution presented earlier in Figure (III.6) and also from the solution by Bathe et al. [17], where in both analyses the isoparametric 8-node plane stress element has been used. This is so because in this case, the total load has been applied in 11 equal increments whereas, by using the isoparametric 8-node plane stress element the analysis needs 100 equal increments. This means that in the latter case the follower load increments trace the deformation of the cantilever more accurately than in the case of the analysis using the isoparametric 3-node beam element.

(ii) Updated Lagrangian Formulation

The calculated results using the present updated Lagrangian formulation for the vertical load are shown in Figure (III.14). All these results were obtained without employing equilibrium checks in the analysis. It is apparent that the predicted solution with the ${}^1K_{\alpha\beta}^{(3)}$, the initial displacement stiffness matrix, deviates significantly as the cantilever deforms. Once again, owing to the same argument of the reversible transformation of the one-to-one mapping between the two Lagrangian formulations, the effects of the initial displacement have been omitted in the updated Lagrangian formulation. Therefore, it is expected that both Lagrangian formulations need the same number of equal load increments to obtain comparable solutions, but this is not so judging from the results of Figure (III.15), because in updating the dimensions of the beam element, the integration in eqns. (III.98, III.99) are carried out numerically using Euler forward-integration technique. The integration was obtained by forward-integration over a sufficient number of subincrements to get the maximum accuracy. This method of updating the dimensions introduces some errors

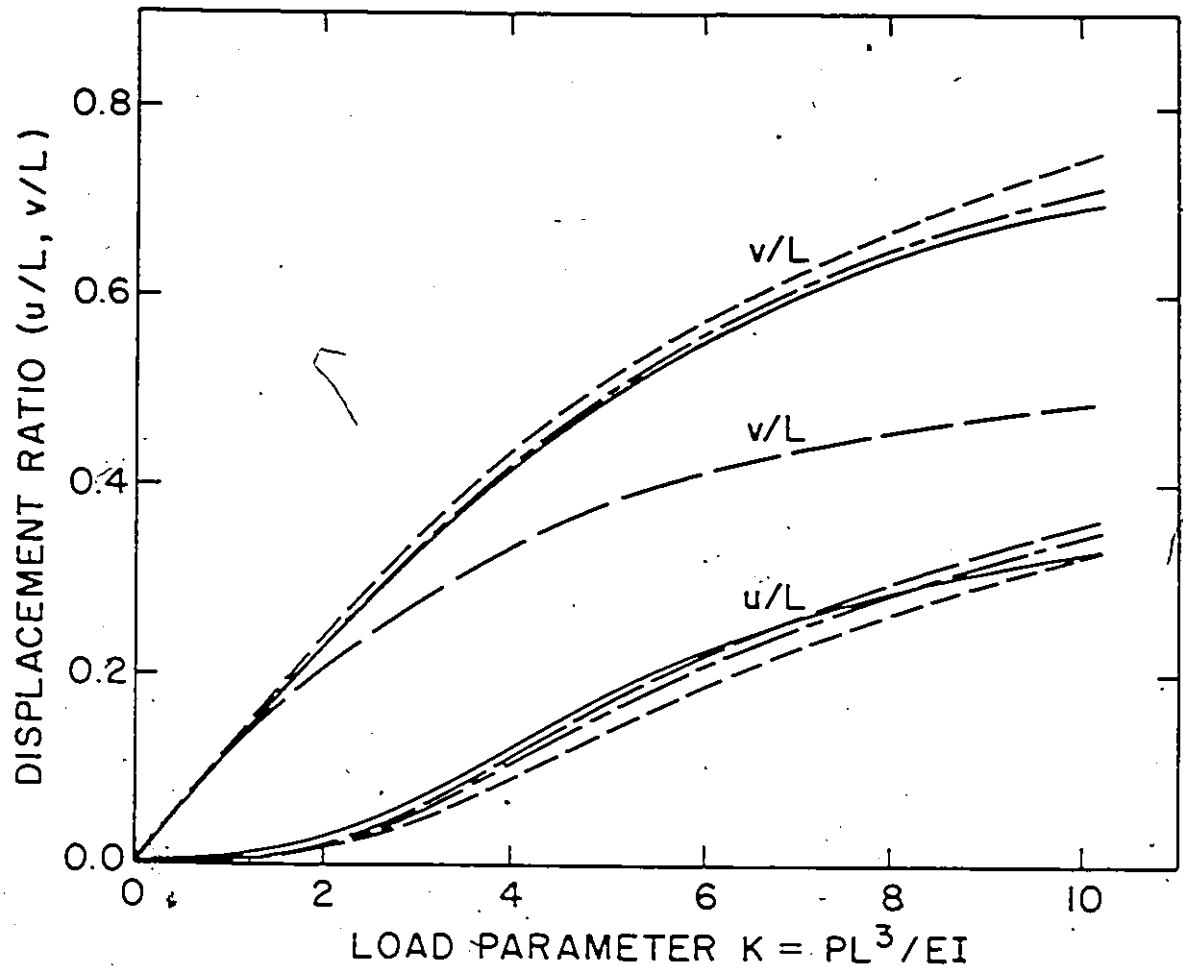


Figure (III.14) Large displacement analysis of a cantilever using updated Lagrangian formulation

- Present without ${}^1K_{up}^{(3)}$ and ${}^1K_{up}^{(4)}$, 11 equal increments
- - Present without ${}^1K_{up}^{(3)}$ and ${}^1K_{up}^{(4)}$, 21 equal increments
- - Present without ${}^1K_{up}^{(3)}$ with ${}^1K_{up}^{(4)}$, 17 equal increments.
- Present with ${}^1K_{up}^{(3)}$ without ${}^1K_{up}^{(4)}$, 21 equal increments.
- Analytical solution (Holden), vertical load.

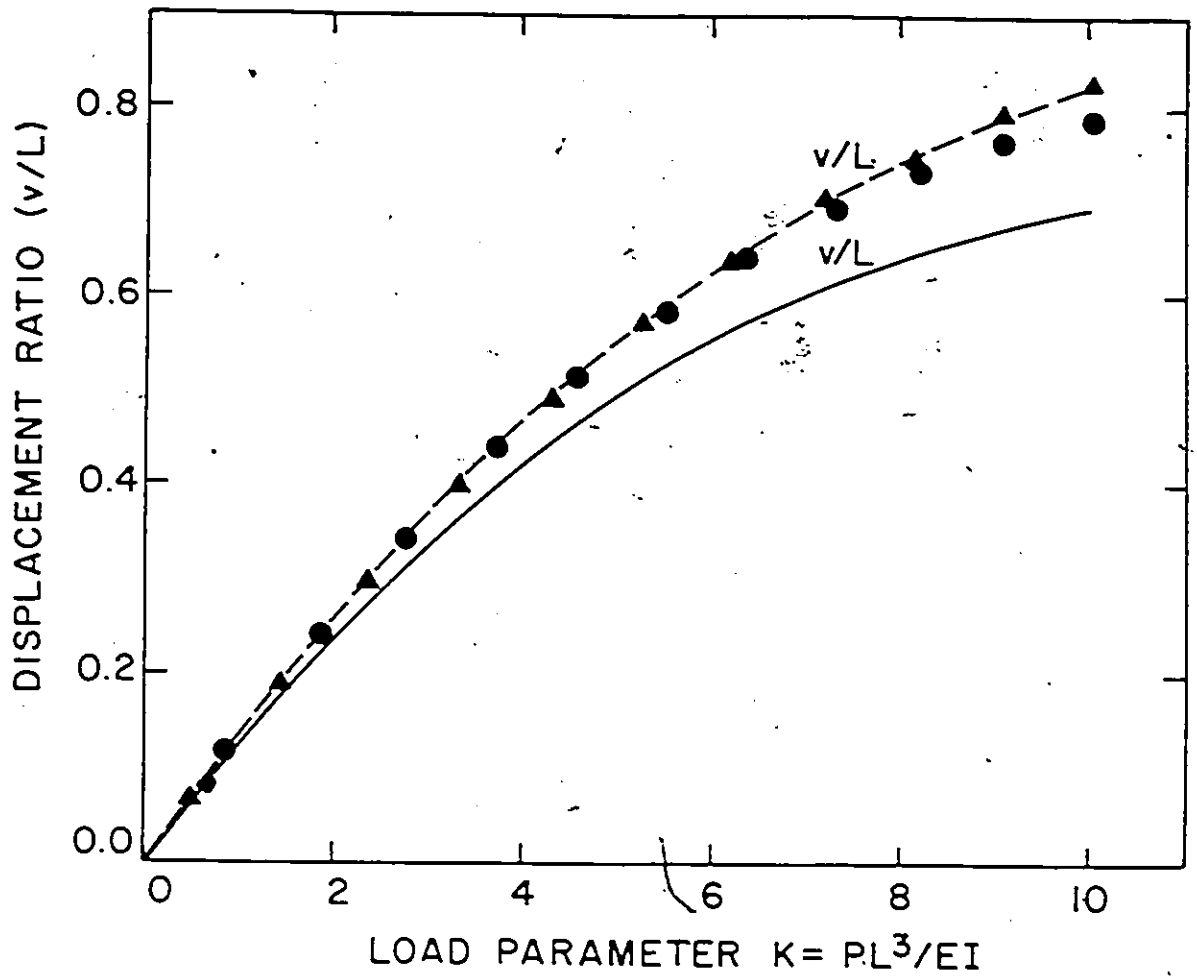


Figure (III.15) Large displacement analysis of a cantilever.

- o Present Lagrangian without K_{upd}^4 , follower load, 11 equal increments.
- Δ Present updated Lagrangian without K_{upd}^4 , follower load, 21 equal increments
- Bathe, follower load.
- Analytical solution [Holden], vertical load.

in the solution, therefore, it was found that the analysis using the updated Lagrangian formulation needs 21 equal load increments to get a comparable solution to that obtained using 11 increments in the Lagrangian formulation. Figure (III.15) shows the results for the follower load. Referring to Figure (III.12), the rotation about X_3 axis, θ_3 , is used to define the direction of the increment of the follower load.

III.2.2 DYNAMIC ANALYSIS OF A PIPE-WHIP PROBLEM

In the design of the nuclear reactor piping system an important problem is the analysis of pipes that are subjected to high impact forces and impinging on the restraints. The purpose of installing the restraints is to prevent the large displacement in case of a pipe-break.

Figure (III.16) illustrates the pipe-whip problem. Once again, the dimensions and the properties of the pipe and the restraint have been chosen to enable comparison of the calculated results with the available results in the literature [14,15,113-115]. The behaviour of the system is highly nonlinear because the materials of the pipe and the restraint are assumed to be linearly elastic-perfectly plastic, see Fig. (III.16), and because the restraint introduces instantaneously large stiffness into the system. For the finite element modelling the pipe cantilever beam was modelled as an assemblage of two 3-node isoparametric pipe beam elements with six degrees of freedom at each node. The gap and the restraint was modelled using a truss element with initial gap as shown in Figure (III.17). The mass of the restraint is assumed to be negligible with respect to the mass of the pipe. The material density of the pipe is assumed $\rho = 0.287 \text{ lb/in}^3$.

Figure (III.18) shows the geometry of the isoparametric 3-node pipe beam element. To describe the behaviour of the element, the same assumption employed in the isoparametric 3-node beam element is used, namely that plane sections normal to the axis of the pipe

element remain plane but not necessarily normal to the deformed axis. Using the same notation as in the beam element, the Cartesian coordinates and the components of the displacement vector of a point in the pipe element can be written as follows:

$${}^t x_i(r,s,t) = \sum_{K=1}^3 h_K {}^t x_i^K + s \sum_{K=1}^3 r_0 h_K {}^t V_{si}^K + t \sum_{K=1}^3 r_0 h_K {}^t V_{ti}^K \quad (\text{III.100})$$

$${}^t u_i(r,s,t) = \sum_{K=1}^3 h_K {}^t u_i^K + s \sum_{K=1}^3 r_0 h_K V_{si}^K + t \sum_{K=1}^3 r_0 h_K V_{ti}^K \quad (\text{III.101})$$

where all the variables are defined in the beam element, and r_0 is the outer radius of the pipe element.

It should be noted that the cross-section of the pipe element is hollow, meaning that eqns. (III.100, III.101) are only applicable for the values of s and t that satisfy the equation

$$\left(1 - \frac{T}{r_0}\right)^2 \leq (s^2 + t^2) < 1 \quad (\text{III.102})$$

where T is the wall thickness of the pipe. This fact is properly taken into consideration in the numerical integration.

In a similar treatment to that given in Appendix D, the shape functions ψ_{i0} and the shape function derivatives $\partial\psi_{i0}/\partial x_j$ have been constructed. It should be noted that the shape function derivatives, similar to eqn. (D.10), are established referring to the global axes by utilizing the Jacobian transformation. In the pipe beam element, however, the stress strain matrix $[C]$ referred to the local axes η_1, η_2 , and η_3 is known, see Figure (III.18). Therefore, the global shape function derivatives are transformed to the local axes, see Appendix-E. Since the element stiffness matrices are evaluated using numerical integration, the transformation from the global to the local axes are performed during the numerical integration at each integration point. The stress-strain matrix used in the analysis corresponds to plane stress condition in the $\eta_1 - \eta_3$ plane, see Figure (III.18):

$$\{\Delta S\} = [C_{ij}] \{\Delta E\} \quad (\text{III.103})$$

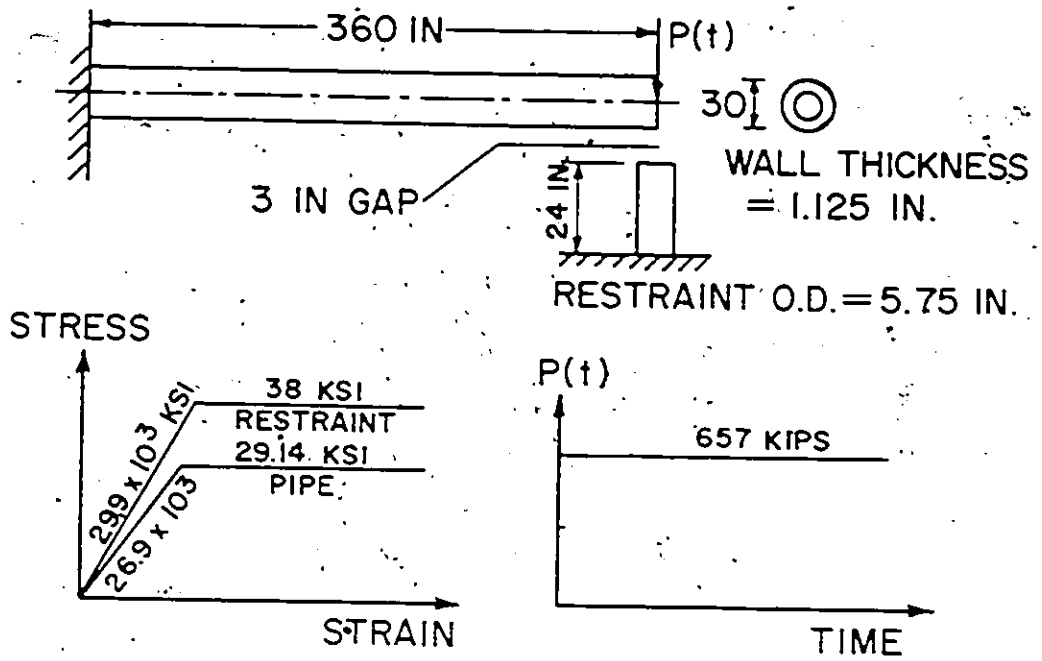


Fig. (III.16) Pipe-whip problem

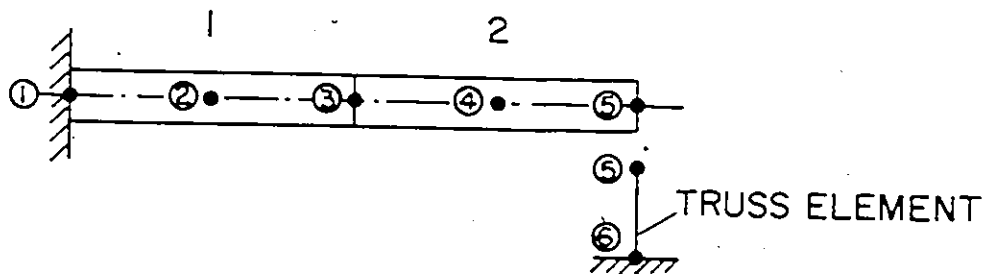


Fig. (III.17) Finite element modelling of the pipe-whip problem.

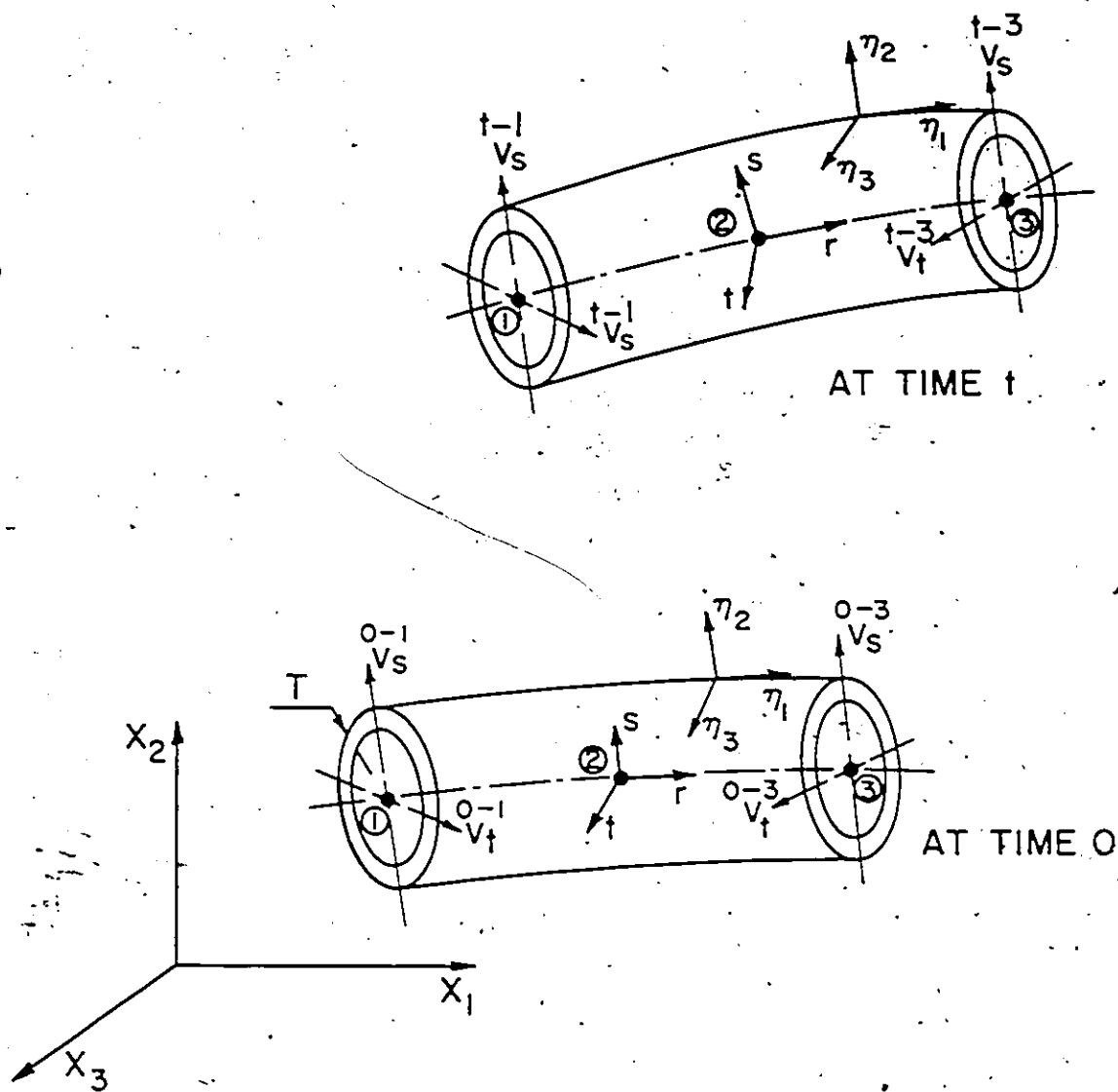


Fig. (III.18) Pipe beam element undergoing large displacements and rotations.

$$\begin{bmatrix} \Delta S_{11} \\ \Delta S_{22} \\ \Delta S_{33} \\ \Delta S_{12} \\ \Delta S_{23} \\ \Delta S_{31} \end{bmatrix} = \frac{E}{1-\nu^2} \begin{bmatrix} 1 & 0 & \nu & 0 & 0 & 0 \\ 0 & 0 & 0 & 0 & 0 & 0 \\ & & 1 & 0 & 0 & 0 \\ & & & \frac{1-\nu}{2} & 0 & 0 \\ \text{symm} & & & & 0 & 0 \\ & & & & & \frac{1-\nu}{2} \end{bmatrix} \begin{bmatrix} \Delta E_{11} \\ \Delta E_{22} \\ \Delta E_{33} \\ \Delta Y_{12} \\ \Delta Y_{23} \\ \Delta Y_{31} \end{bmatrix} \quad (\text{III.104})$$

where E is the Elastic Modulus and ν is the Poisson's ratio of the material.

Once again, to calculate the stiffness matrices and the mass matrix of the element, numerical integration technique is used in the developed programme. Considering the assumed displacement distribution and the restriction given by eqn. (III 102), the Gauss-Legendre procedure is employed with the following order: 3-integration points along the axis of element, one-integration point through the wall-thickness, and 6-integration points around the circumference. From numerical point of view, it is recommended not to use less than 6-integration points around the circumference

The material of the pipe is assumed isotropic, linearly elastic up to the yield limit, and perfectly-plastic thereafter. In this analysis, the von Mises yield criterion and the associated flow rule have been employed. In a similar procedure to that given in Appendix C, the compliance matrix $[C]_{pp}$ or the stress-strain relation valid beyond the proportional limit has been calculated. In the Lagrangian formulation the yield criteria and the compliance matrix $[C]_{cp}$ are dependent on the second Piola-Kirchhoff stress tensor, ${}^0\bar{\bar{S}}$ whereas, in the updated Lagrangian they depend on the Cauchy stress tensor ${}^1\bar{\bar{\sigma}}$. In this case, the strain hardening modulus H is set to zero.

Solution of the (Dynamic) Incremental Equilibrium Equations

For the solution of the incremental equilibrium equations eqns. (III.44) or (III.46) in the Lagrangian formulation, and eqns. (III.61) or (III.63), in the updated Lagrangian formulation, there are two techniques: direct integration and mode superposition techniques. In the direct integration technique these equations are integrated using a numerical step-by-step procedure which means that, instead of satisfying these equations at any time t , it is aimed to satisfy them only at a discrete time interval. The direct integration technique is based on the idea that the variations of displacements, velocities, and accelerations in each time interval Δt are assumed. There are four methods commonly used for direct integration of the incremental equations of motion [5,15,113-115,139,140]: the central difference method, the Houbolt method, the Wilson θ -method, and the Newmark method. In choosing between these methods, the stability, the accuracy, and the initial conditions required for each method are considered. On the other hand, in the mode superposition technique, the incremental equilibrium equations are transformed from the finite element basis to the normal basis by using the modal matrix which consists of the mode shapes of the structure. By such means, the above equations are reduced to a set of uncoupled second order differential equations, each of which represents a single degree of freedom system, and which can be solved separately. However, in the solution of the nonlinear transient dynamic problems, the natural frequencies and mode shapes of the structure are continuously changing. Therefore, it might be too expensive to use the mode superposition technique in the analysis. In general, the use of the mode superposition in nonlinear dynamic analysis can be effective when the solution can be obtained without updating the total stiffness matrix of the structure too frequently. According to the given discussion it is preferable to employ the direct integration technique in the nonlinear dynamic analysis. The most effective direct integration methods presently used are the Newmark method and the Wilson θ -method [5,14,15,17-19,31,115,139,140]. The

Newmark method with time step $\Delta t = 0.0002$ second is used in the developed computer programme.

In the Newmark method, the direct integration scheme is based on the following assumptions for the velocity and the displacement and vector in each time interval Δt

$${}^{t+\Delta t}\underline{\dot{u}} = {}^t\underline{\dot{u}} + [(1-\delta) {}^t\underline{\ddot{u}} + \delta {}^{t+\Delta t}\underline{\ddot{u}}] \Delta t \quad (105)$$

$${}^{t+\Delta t}\underline{u} = {}^t\underline{u} + {}^t\underline{\dot{u}} \Delta t + [(1/2 - \alpha) {}^t\underline{\ddot{u}} + \alpha {}^{t+\Delta t}\underline{\ddot{u}}] (\Delta t)^2 \quad (106)$$

where α and δ are parameters that can be determined to obtain integration accuracy and stability. Newmark [139] originally proposed the constant-average-acceleration method as an unconditionally stable scheme, in which $\delta = 1/2$ and $\alpha = 1/4$. The complete algorithm using the Newmark scheme is given in Table (III.3).

It is clear that by employing Newmark method, the incremental equilibrium equations which include the dynamic term become incremental static equilibrium equations at discrete time interval Δt apart which include the effect of the inertia. Therefore, it appears that all solution techniques used in static analysis can also be used effectively in this case. In our programme the Frontal solution technique [7,9] is employed. In the solution, however, the resulting incremental equilibrium equations are not satisfied exactly. Therefore, there is an out-of-balance nodal force vector. In order to minimize this out-of-balance force vector and to prevent the solution from drifting away from the exact solution, equilibrium checks are employed with modified Newton-Raphson method within each increment, see Table (III.3), Step C. It is worth mentioning at this point that the equilibrium check is more important in dynamic analysis than in static analysis. Namely, any error that is introduced in the dynamic step-by-step solution will accumulate and cannot be later compensated for, as in the solution of many static geometrically nonlinear analyses.

Table (III.3) Step-by-Step Solution using Newmark method

A. Initial Calculations

1. Form the stiffness matrix $[{}^0_0\mathbf{K}]$, and the mass matrix $[{}^0_0\mathbf{M}]$.
2. Initialize ${}^0\mathbf{u}$, ${}^0\dot{\mathbf{u}}$, then compute ${}^0\ddot{\mathbf{u}}$.
3. Select time step size Δt , using $\alpha = 0.25$ and $\delta = 0.5$, calculate integration constants:

$$a_0 = \frac{1}{\alpha(\Delta t)^2}; \quad a_1 = \frac{\delta}{\alpha \Delta t}; \quad a_2 = \frac{\delta}{\alpha \Delta t}; \quad a_3 = \frac{1}{2\alpha} - 1;$$

$$a_4 = \frac{\delta}{\alpha} - 1; \quad a_5 = \frac{\Delta t}{2} \left(\frac{\delta}{\alpha} - 2 \right); \quad a_6 = \Delta t(1 - \delta); \quad a_7 = \delta \Delta t$$

B. In Each Time Step

1. Calculate new stiffness matrix $[{}^t_0\mathbf{K}]$, if it is required
2. Form the effective stiffness matrix:

$$[{}^t_0\mathbf{K}]_{\text{eff}} = [{}^t_0\mathbf{K}] + a_0 [{}^t_0\mathbf{M}]$$

3. Calculate the effective load vector at time $t + \Delta t$:

$$\{{}^{t+\Delta t}{}_0\mathbf{R}\}_{\text{eff}} = \{{}^{t+\Delta t}{}_0\mathbf{R}\} + [{}^t_0\mathbf{M}][a_0 \{{}^t\mathbf{u}\} + a_2 \{{}^t\dot{\mathbf{u}}\} + a_3 \{{}^t\ddot{\mathbf{u}}\}]$$

4. Solve for the displacement vector at time $t + \Delta t$:

$$[{}^t_0\mathbf{K}]_{\text{eff}} \{{}^{t+\Delta t}\mathbf{u}\} = \{{}^{t+\Delta t}{}_0\mathbf{R}\}_{\text{eff}}$$

5. Calculate the acceleration and the velocity vector at time $t + \Delta t$:

$$\{{}^{t+\Delta t}\ddot{\mathbf{u}}\} = a_0 (\{{}^{t+\Delta t}\mathbf{u}\} - \{{}^t\mathbf{u}\}) - a_2 \{{}^t\dot{\mathbf{u}}\} - a_3 \{{}^t\ddot{\mathbf{u}}\}$$

$$\{{}^{t+\Delta t}\dot{\mathbf{u}}\} = \{{}^t\dot{\mathbf{u}}\} + a_6 \{{}^t\ddot{\mathbf{u}}\} + a_7 \{{}^{t+\Delta t}\ddot{\mathbf{u}}\}$$

6. If equilibrium check is required put $i = 0$, GO TO C.

GO TO B

C. Equilibrium Check

1. $i = i + 1$.
2. Calculate the $(i-1)$ effective out-of-balance nodal force vector:

$$\{ {}^{t+\Delta t}R \}^{i-1} = \{ {}^{t+\Delta t}R \} - [{}^t_0M] \{ {}^{t+\Delta t}u \}^{i-1} - \{ {}^{t+\Delta t}F \}^{i-1}$$

3. Solve for i'th correction to the displacement vector:

$$[{}^t_0K]_{\text{eff}} \{ \Delta {}^{t+\Delta t}u \}^i = \{ {}^{t+\Delta t}R \}^{i-1}$$

4. Check if the convergence factor $\| \{ \Delta {}^{t+\Delta t}u \}^i \|_2 / \| \{ {}^{t+\Delta t}u \}^i \|_2 < 10^{-4}$

If convergent GO TO B

If not convergent, then check if the number of the equilibrium iterations (i) within the time increment exceeds the limit number.

Yes: restart using new total stiffness matrix and/or a smaller time-step size.

No: calculate new displacement vector, and then calculate the corresponding change in the velocity and the acceleration vector

$$\{ {}^{t+\Delta t}u \}^i = \{ {}^{t+\Delta t}u \}^{i-1} + \{ \Delta {}^{t+\Delta t}u \}^i$$

$$\{ {}^{t+\Delta t}\dot{u} \}^i = \{ {}^{t+\Delta t}\dot{u} \}^{i-1} + A_7 \times A_0 \times \{ \Delta {}^{t+\Delta t}u \}^i$$

$$\{ {}^{t+\Delta t}\ddot{u} \}^i = \{ {}^{t+\Delta t}\ddot{u} \}^{i-1} + A_0 \times \{ \Delta {}^{t+\Delta t}u \}^i$$

Calculate the increment of stresses, and then the total stresses

GO TO C

where

${}^t_0K, {}^t_0M$ are the total stiffness and mass matrix of the structure

${}^{t+\Delta t}R$ is the total applied load vector

${}^{t+\Delta t}u, {}^{t+\Delta t}\dot{u}, {}^{t+\Delta t}\ddot{u}$ are the total displacement, velocity, and acceleration vector of the structure respectively

$\Delta {}^{t+\Delta t}u$ are the total incremental displacement vector due to the out-of-balance load

and

$\mathbf{F}_{0-a}^{t+\Delta t}$ is the total internal force vector, and is formed from the local internal force vector of each element, which is defined in the Lagrangian formulation as:

$$\mathbf{F}_{0-a}^{t+\Delta t} = \int_{0V} \mathbf{S}_{ij}^{t+\Delta t} \left(\frac{\partial \psi_{ia}}{\partial X_j^0} + \frac{\partial^{t+\Delta t} u_k}{\partial X_i^0} \frac{\partial \psi_{ka}}{\partial X_j^0} \right) d^0V$$

and in the updated Lagrangian formulation as:

$$\mathbf{F}_{t-a}^{t+\Delta t} = \int_{tV} \mathbf{S}_{ij}^{t+\Delta t} \frac{\partial \psi_{ia}}{\partial X_j^t} d^tV$$

Finally, $\|\{\Delta^{t+\Delta t} u\}\|_2$ is the Euclidean norm of the vector $\{\Delta^{t+\Delta t} u\}$ and is defined as

$$\|\{\Delta^{t+\Delta t} u\}\|_2 = \{\Sigma (\Delta^{t+\Delta t} u)^2\}^{1/2}$$

The pipe-whip problem has been analyzed using the developed programme and the results are given in the following.

(i) Lagrangian Formulation

Figure (III.19) shows the response of the pipe with respect to the time elapsed using the Lagrangian formulation and the result obtained by Bathe [15], Ma and Bathe [113] using the ADINA programme. The two responses are comparable, however, there is a small difference which becomes larger with the time. The main reason for this difference is that in the analysis of Bathe, Ma and Bathe, the pipe is modelled as an assemblage of six 8-node isoparametric plane stress elements. The thickness of the plane stress elements was chosen to give the same value of the second moment of the cross-section about the centroidal x axis as that of the actual pipe-section. This modelling imposes some additional constraint on the system. Figures (III.20-III.23) give the response of the pipe at various instants of time. It would be expected in the static analysis that the first yielding will occur at the root of the cantilever but this is not the case in the dynamic analysis where the yielding started close to the loaded end, see Figure (III.21).

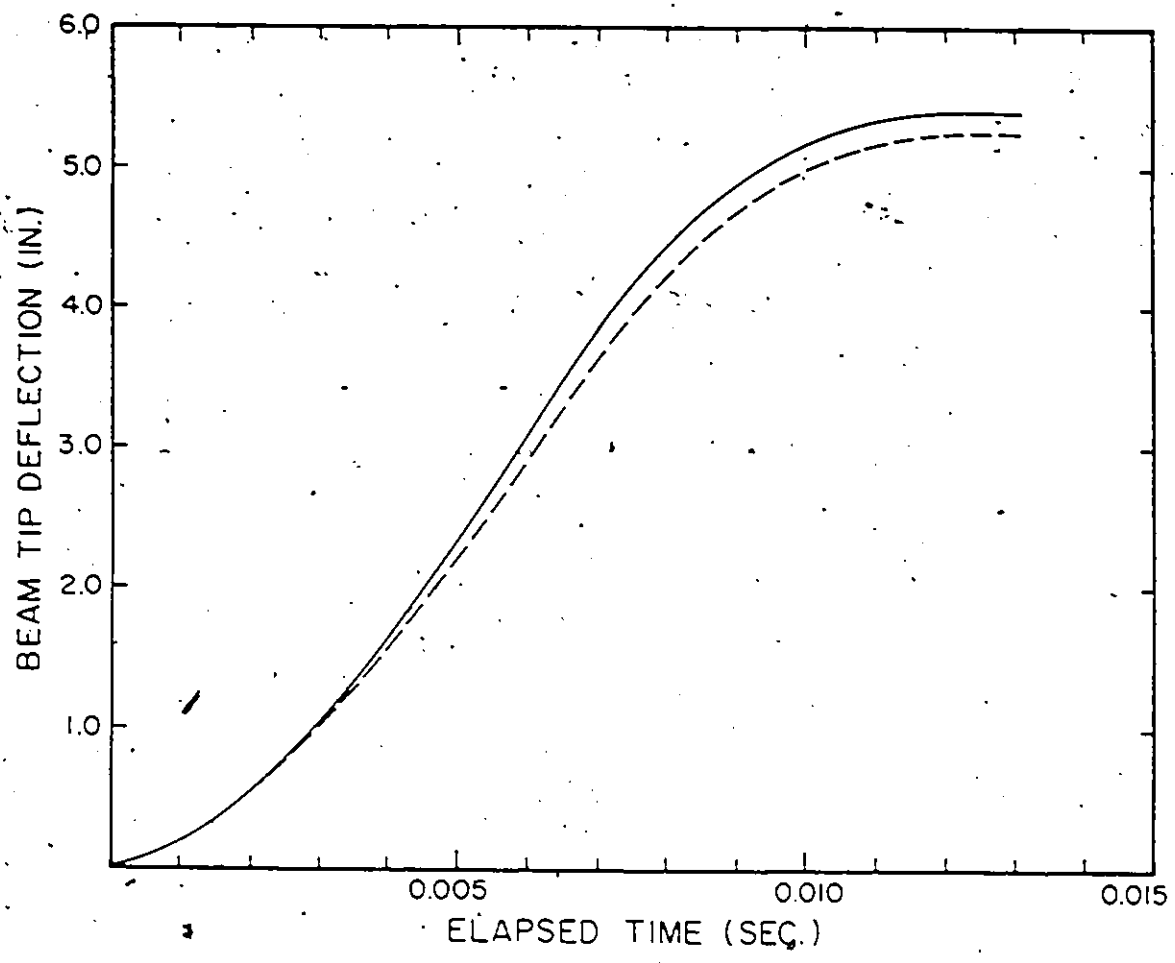


Fig. (III.19) Predicted displacement response in the pipe-whip analysis.
 — Present Lagrangian without $\frac{1}{2} K_{\alpha\beta}^4$, 5 increments.
 --- Bathe [15], and Ma-and Bathe [113]

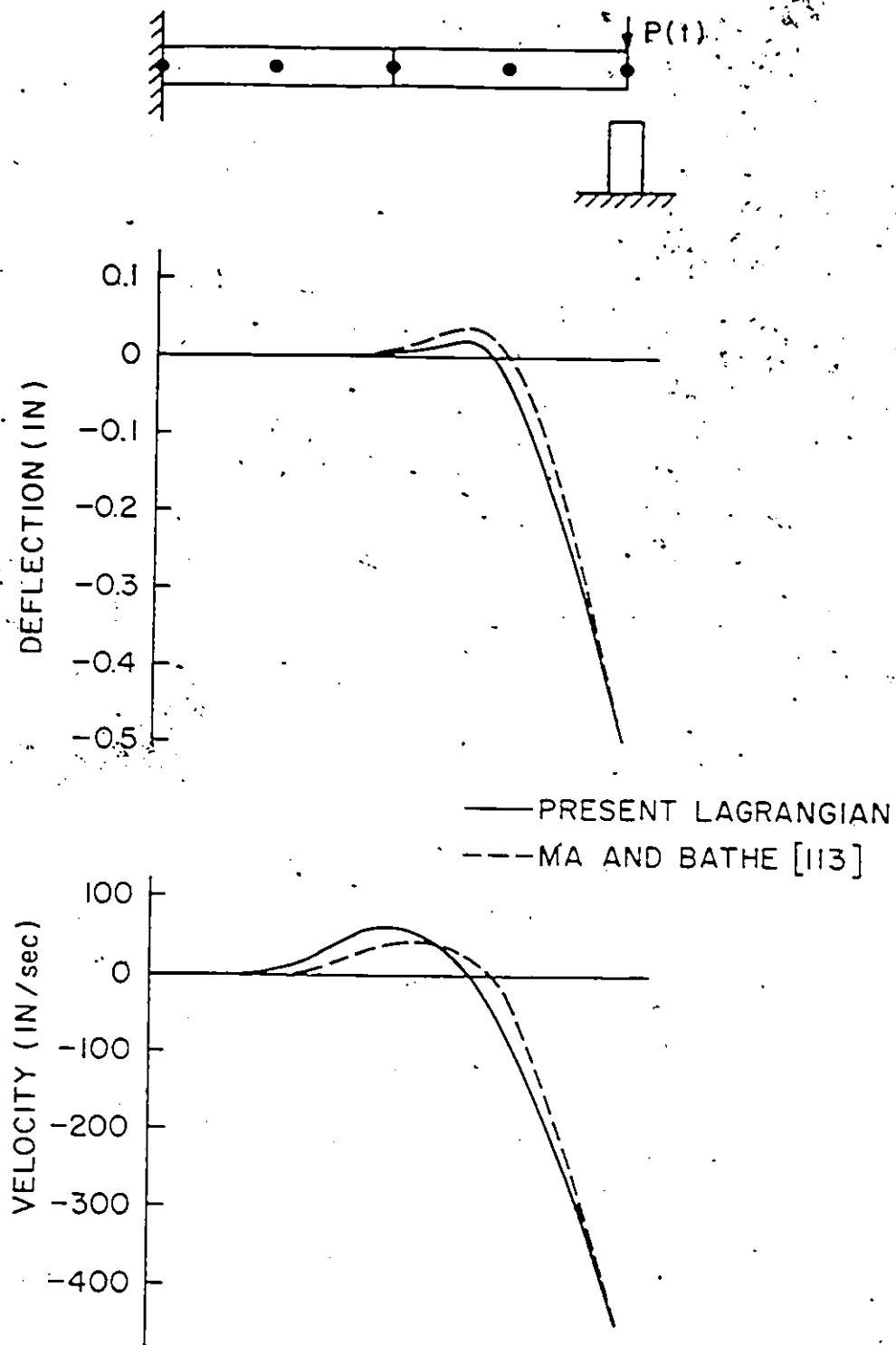


Fig. (III.20) Beam response at neutral axis at $t = 0.002$ second.

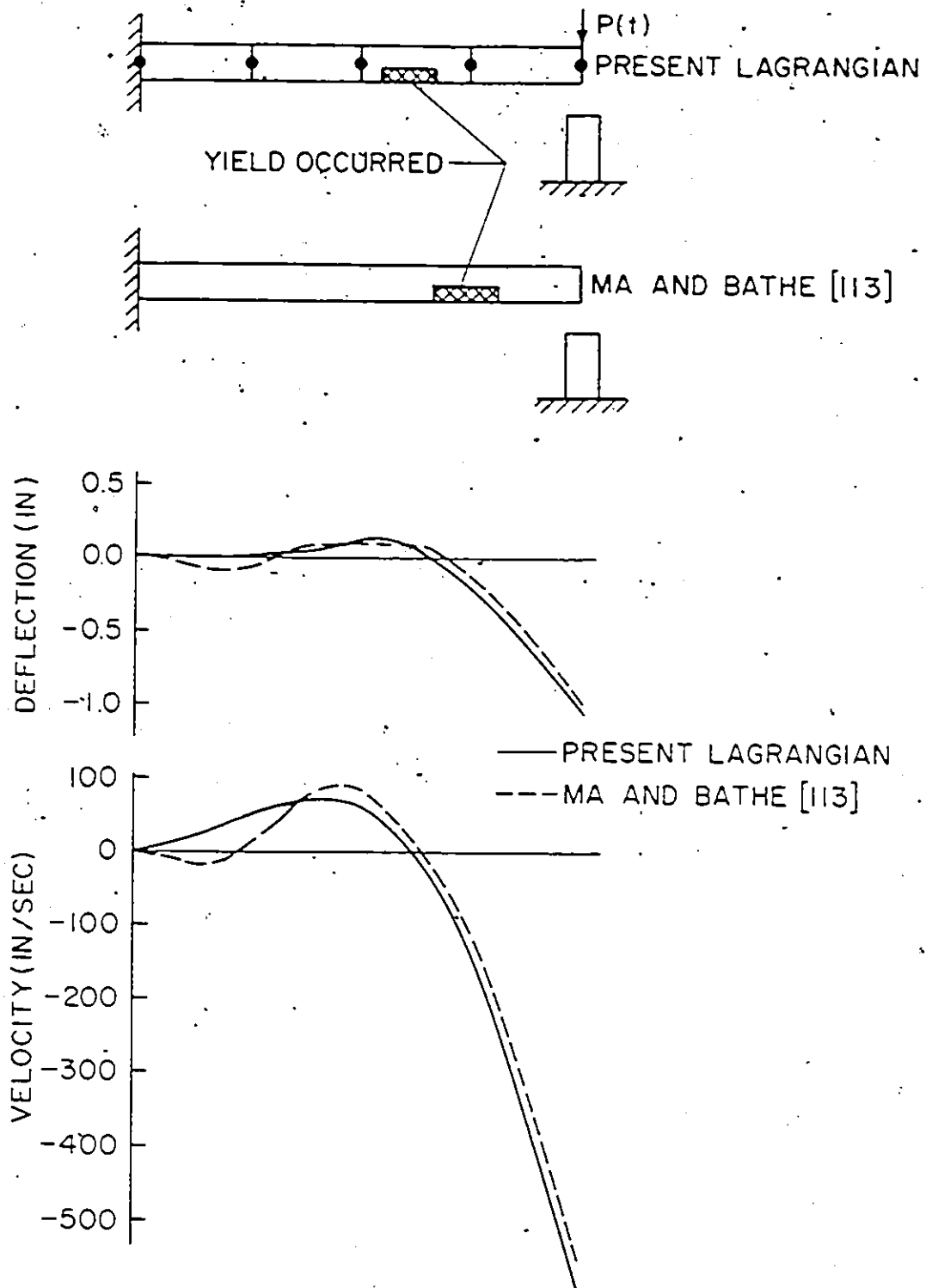


Fig. (III 21) Beam response at neutral axis at $t = 0.003$ second

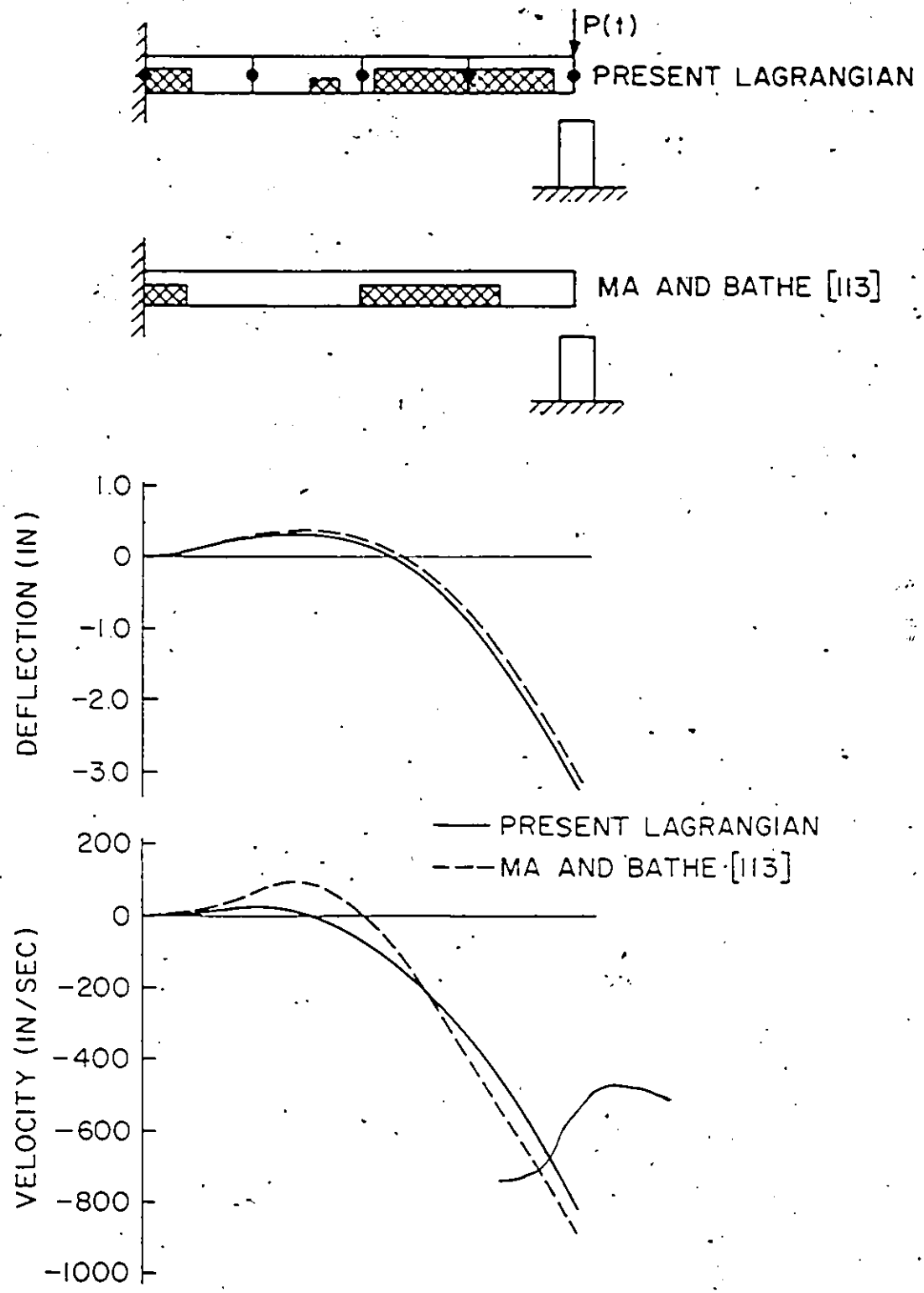


Fig (H 22) Beam response at neutral axis at $t = 0.006$ second.

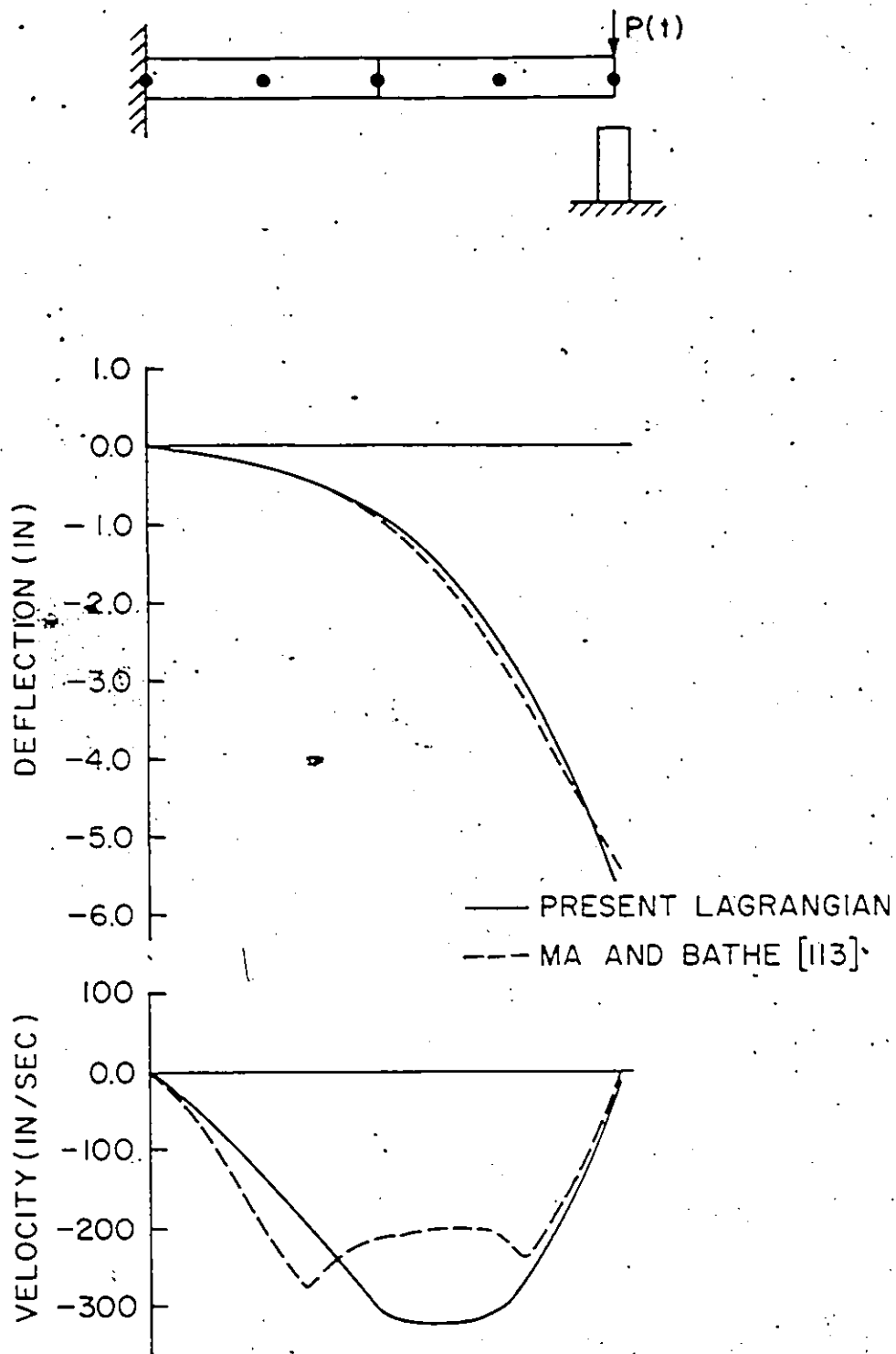


Fig. (III.23) Beam response at neutral axis at $t = 0.012$ second.

The effect of including the load-correction matrix ${}_0^1K_{\alpha\beta}^{(4)}$ is shown in Figure (III.24). The solution needs 4 time increments instead of 5 increments needed in the solution without the use of the load-correction matrix in order to obtain comparable results. In the above two solutions, only one equilibrium check was needed in order to obtain the maximum deflection of the cantilever pipe.

(ii) Updated Lagrangian Formulation

Figure (III.24) depicts the obtained results using the updated Lagrangian formulation with, and without the load-correction matrix ${}_1^1K_{\alpha\beta}^{(4)}$. In the solution without the load-correction matrix, two equilibrium checks were needed, while with the load-correction matrix only one was required in order to obtain the maximum deflection of the cantilever pipe. One possible reason for the small difference resulting between the responses obtained by using the Lagrangian and the updated Lagrangian formulation is that in the updating of the dimensions of the pipe element, the integration in eqns. (III.98, III.99) were carried out numerically [141]. Another possible reason for that small difference is the constitutive equations. As discussed in the sub-section III.1.4 in the elasto-plastic analysis, the constitutive equations in the updated Lagrangian formulation could be more appropriate. For this reason, the two predicted responses using the Lagrangian and the updated Lagrangian formulation can exhibit some difference [18,19]. However, if the analysis contains moderate deformation, which is the case in the present analysis, the responses predicted using the two formulations are expected to be only slightly different.

III.3 DISCUSSION

In this chapter, the Lagrangian and the updated Lagrangian formulation have been developed. The formulations are based on the principles of continuum mechanics and

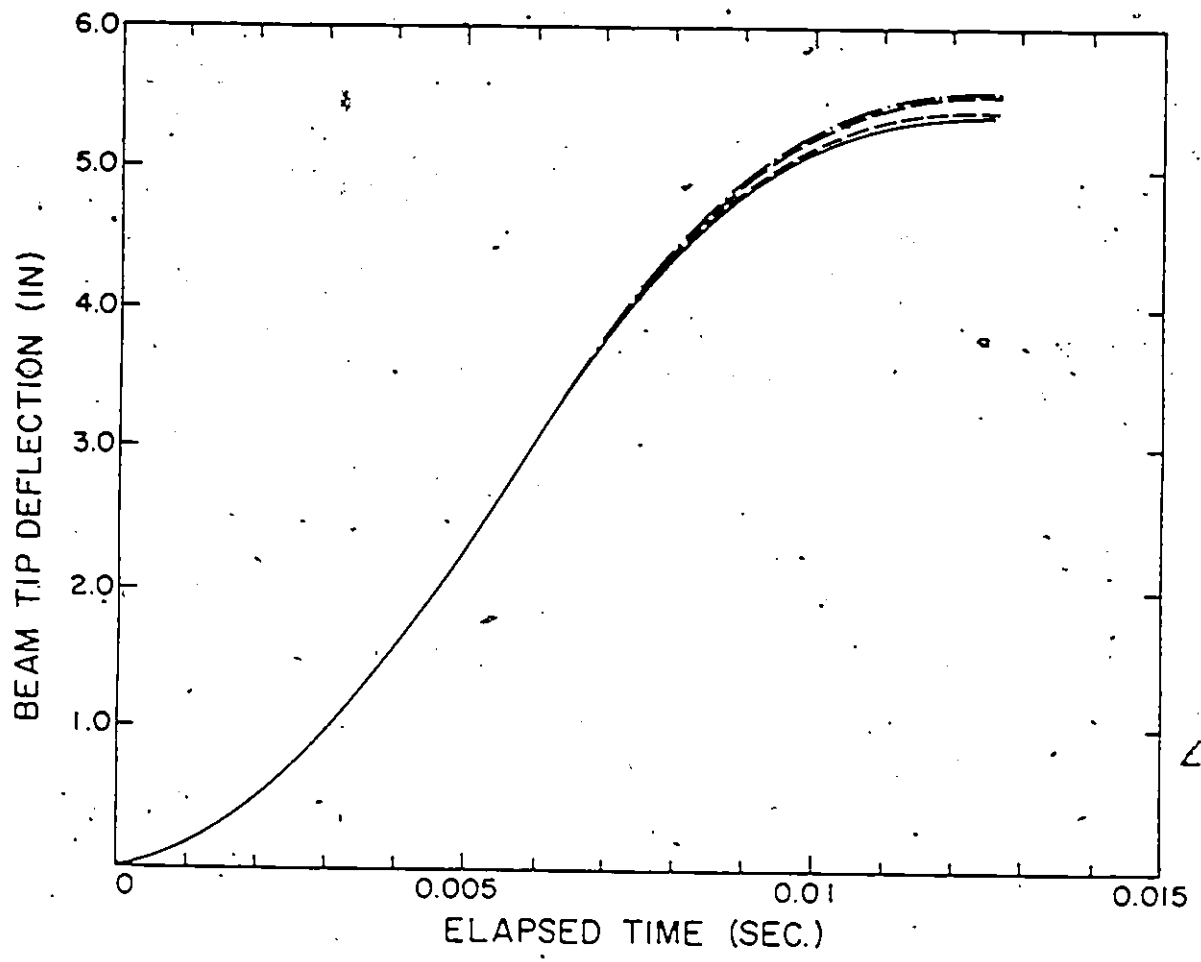


Fig (III 24)

- Predicted displacement response in the pipe whip analysis
- Present Lagrangian without ${}^1K_{up}^{(4)}$, 5 increments
 - - Present Lagrangian with ${}^1K_{up}^{(4)}$, 4 increments
 - - - Present updated Lagrangian without ${}^1K_{up}^{(4)}$, 5 increments
 - · - Present updated Lagrangian with ${}^1K_{up}^{(4)}$, 4 increments

include all nonlinear effects (both geometric and material). To show the applicability and effectiveness of the developed formulations, two example problems have been solved. The results obtained compare well with the existing analytical and numerical solutions. It should be noted that if the constitutive equations are defined appropriately, both formulations give the same numerical results.

A natural question to ask is how to choose between the two formulations in a specific class of nonlinear problems. The choice between the two formulations is decided on the basis of their numerical effectiveness. Furthermore, in applications such as in metal-forming problems, in contact problems and in crack-propagation problems, the updated Lagrangian formulation should be employed owing to its effectiveness in handling the continuous updating of the boundary conditions and the distortion of the finite element mesh.

CHAPTER IV

EULERIAN FORMULATION AND APPLICATION

Once again, the key difference between the Eulerian formulation and other formulations is that we are concerned with the determination of the deformation of a continuous medium moving through a fixed region in space instead of determining the deformation of the material-element by tracing its motion in space. In the Eulerian formulation the independent variables are the current position x of the body-point X and the time t where x itself depends on the Lagrangian position X of the body-point X and the time t when material time derivatives are to be calculated. As it is seen here and also in references [51,79,80,85], this fact complicates material time derivatives as well as other relations in the Eulerian formulation. In what follows, the basic equations and the general simplifying assumptions will be discussed and we will develop consistent Eulerian formulation by means of the virtual work principle expressed in the current configuration. The specific approximations which make the Eulerian formulation suitable for numerical applications are discussed. Differences between the present formulation and similar formulations in the literature [51,85] are examined. Finally, procedures of the stress and deformation analysis of metal-extrusion process using the Eulerian fixed finite element mesh technique based on the derived formulation are presented.

IV.1 FORMULATION OF THE INCREMENTAL EQUILIBRIUM EQUATIONS

IV.1.1 ASSUMPTIONS AND BASIC EQUATIONS

IV.1.1.1 General Assumptions

In the Eulerian formulation, it is intended to determine the deformation of a continuous medium moving through a fixed region R of the three-dimensional space as shown in Figure (IV.1). A fixed rectangular frame with Cartesian coordinate system in three-dimensional space is established to describe the motion of the body. The Cartesian coordinates of a point Q in the space (not a body-point) are x_1 , x_2 , and x_3 , and for this reason x_i are called spatial coordinates. In the analysis, it is convenient to locate the position of the body-point X . For this purpose, we should adopt a reference configuration in which the position vector of the body-point X is ${}^0\bar{X}$. Once again, in order to develop the incremental equilibrium equations in the Eulerian formulation, complete nonlinear kinematic relations within a linear increment is used. The second order incremental variables will be neglected. Only perfect mechanical systems which take no account of thermodynamical effects will be considered.

IV.1.1.2 Nomenclature

In the development of the Eulerian formulation, we are going to use the same notations employed in the Lagrangian and the updated Lagrangian formulation.

IV.1.1.3 Kinematics of the Motion

On the basis of the assumptions discussed above, the position vector of the body point X in the current configuration, see Figure (II.1), is

$${}^2\bar{X} = {}^0\bar{X} + {}^2\bar{u} \quad (IV.1)$$

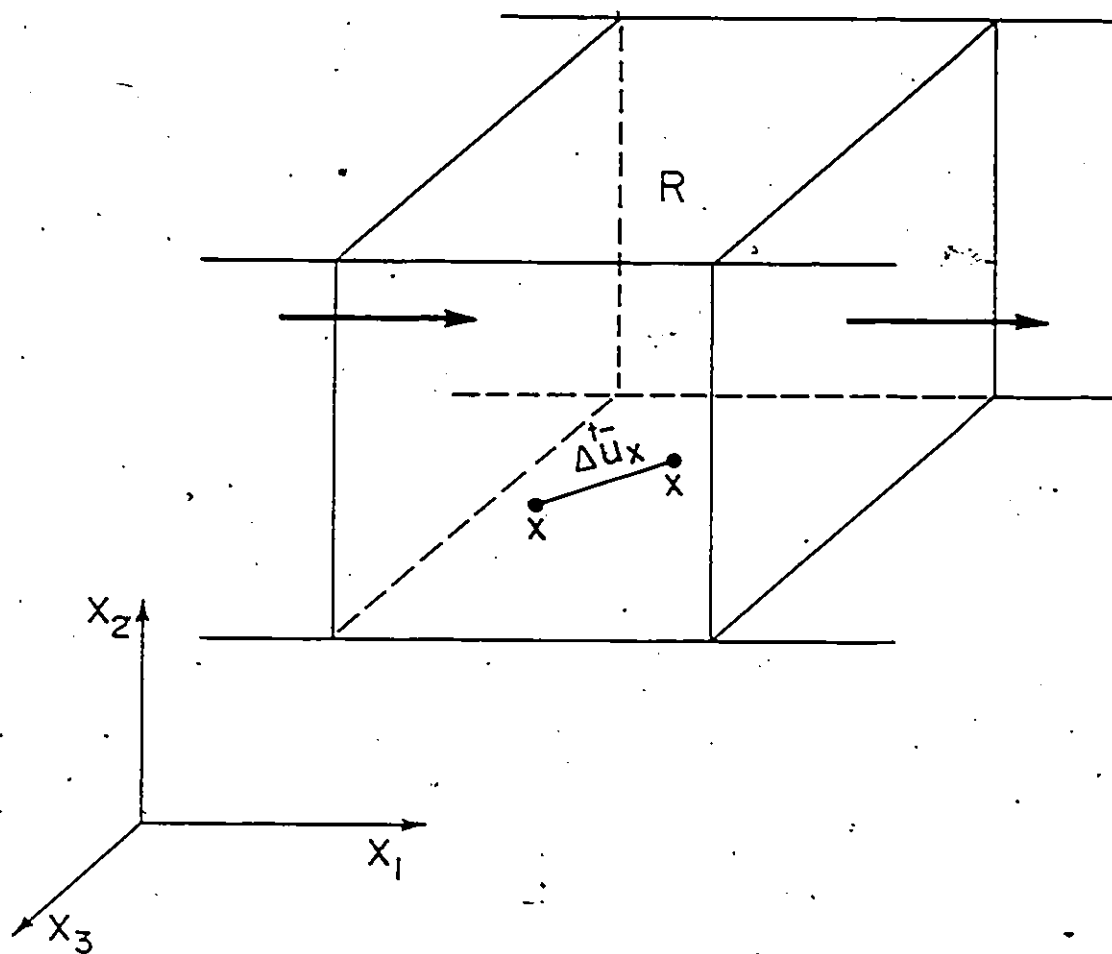


Figure (IV.1) Continuous medium moving through a fixed region R in space.

Spatial Velocity and Spatial Acceleration

The velocity of the body-point X is defined as the material time derivative of the position vector ${}^2\bar{x}$, so that

$${}^2\bar{v} = \frac{d {}^2\bar{x}}{d t} = \frac{d({}^0\bar{X} + {}^2\bar{u})}{d t} = \frac{d {}^2\bar{u}}{d t} \quad (\text{IV.2})$$

Considering the spatial description of the velocity field as a function of the current position ${}^2\bar{x}$ and the time t as

$${}^2\bar{v} = {}^2\bar{v}({}^2\bar{x}, t) \quad (\text{IV.3})$$

where

$${}^2\bar{x} = {}^2\bar{x}({}^0\bar{X}, t) \quad (\text{IV.4})$$

therefore

$${}^2\bar{v} = {}^2\bar{v}({}^2\bar{x}({}^0\bar{X}, t), t) \quad (\text{IV.5})$$

The acceleration field as the material time derivative of the velocity field is given by

$$\begin{aligned} {}^2\bar{a} &= \left. \frac{d {}^2\bar{v}}{d t} \right|_{{}^0\bar{X} = \text{const.}} = \left. \frac{d {}^2\bar{v}({}^2\bar{x}({}^0\bar{X}, t), t)}{d t} \right|_{{}^0\bar{X} = \text{const.}} \\ &= \left. \frac{d {}^2\bar{v}}{d t} \right|_{{}^2\bar{x} = \text{const.}} + \left. \frac{d {}^2\bar{x}}{d t} \right|_{{}^0\bar{X} = \text{const.}} \cdot \frac{\partial {}^2\bar{v}}{\partial {}^2\bar{x}} \\ &= \frac{\partial {}^2\bar{v}}{\partial t} + {}^2\bar{v} \cdot \frac{\partial {}^2\bar{v}}{\partial {}^2\bar{x}} \end{aligned}$$

or

$${}^2\bar{a} = \frac{\partial {}^2\bar{v}}{\partial t} + {}^2\bar{v} \cdot \frac{\partial {}^2\bar{v}}{\partial {}^2\bar{x}} \quad (\text{IV.6})$$

The first term in the above equation represents the local rate of change of the velocity, whereas, the second one gives the convected rate of change of the velocity.

Strain Measure

In the spatial formulation, the deformation is always referred to the current configuration. Therefore, the finite deformation strain measure in this case is the Eulerian or Almansi strain tensor, which is defined by

$${}^2\bar{\epsilon} = \frac{1}{2} \left(\bar{1} - ({}^2\bar{F}^{-1})^T \cdot {}^2\bar{F}^{-1} \right) \quad (IV.7)$$

where $\bar{1}$ is the identity tensor and ${}^2\bar{F}$ is the deformation gradient tensor which is defined by

$${}^2\bar{F} = \frac{\partial {}^2\bar{x}}{\partial {}^0X} \quad (IV.8)$$

upon the substitution of the current position of the body-point X, eqn. (IV.1), into the above equation, and the resulting expression into eqn. (IV.7), the strain tensor becomes

$${}^2\bar{\epsilon} = \frac{1}{2} \left(\frac{\partial {}^2\bar{u}}{\partial {}^2\bar{x}} + \frac{{}^2\bar{u}}{\partial {}^2\bar{x}} \frac{\partial}{{}^2\bar{x}} - \frac{\partial {}^2\bar{u}}{\partial {}^2\bar{x}} \cdot \frac{{}^2\bar{u}}{\partial {}^2\bar{x}} \right) \quad (IV.9)$$

and the increment of the Eulerian strain tensor may be given by

$$\Delta {}^2\bar{\epsilon} = \frac{1}{2} \left| \frac{\partial \Delta {}^2\bar{u}}{\partial {}^2\bar{x}} + \frac{\Delta {}^2\bar{u}}{\partial {}^2\bar{x}} \frac{\partial}{{}^2\bar{x}} - \left(\frac{\partial {}^2\bar{u}}{\partial {}^2\bar{x}} \cdot \frac{\Delta {}^2\bar{u}}{\partial {}^2\bar{x}} \frac{\partial}{{}^2\bar{x}} + \frac{\partial \Delta {}^2\bar{u}}{\partial {}^2\bar{x}} \cdot \frac{{}^2\bar{u}}{\partial {}^2\bar{x}} \frac{\partial}{{}^2\bar{x}} + \frac{\Delta {}^2\bar{u}}{\partial {}^2\bar{x}} \cdot \frac{\Delta {}^2\bar{u}}{\partial {}^2\bar{x}} \frac{\partial}{{}^2\bar{x}} \right) \right| \quad (IV.10)$$

which for linear increment becomes

$$\Delta {}^2\bar{\epsilon} = \frac{1}{2} \left| \frac{\partial \Delta {}^2\bar{u}}{\partial {}^2\bar{x}} + \frac{\Delta {}^2\bar{u}}{\partial {}^2\bar{x}} \frac{\partial}{{}^2\bar{x}} - \left(\frac{\partial {}^2\bar{u}}{\partial {}^2\bar{x}} \cdot \frac{\Delta {}^2\bar{u}}{\partial {}^2\bar{x}} \frac{\partial}{{}^2\bar{x}} + \frac{\partial \Delta {}^2\bar{u}}{\partial {}^2\bar{x}} \cdot \frac{{}^2\bar{u}}{\partial {}^2\bar{x}} \frac{\partial}{{}^2\bar{x}} \right) \right| \quad (IV.11)$$

IV.1.1.4 Displacement Assumption

In Eulerian formulation, we assume the displacement within any given element in the form

$${}^2u_i = \psi_{ia}({}^2x) {}^2u_{ia} \quad (IV.12)$$

and

$$\Delta {}^2u_i = \psi_{ia}({}^2x) \Delta {}^2u_{ia} \quad (IV.13)$$

For the velocity within the element, we assume also the following form

$${}^2\dot{u}_i = \psi_{ia}({}^2x) {}^2\dot{u}_{ia} \quad (IV.14)$$

and

$$\Delta^2 \underline{u}_i = \psi_{ia}(\underline{x}) \Delta^2 \underline{u}_a \quad (IV.15)$$

where ψ_{ia} are the shape function

\underline{u}_a is the nodal displacement vector.

$\dot{\underline{u}}_a$ is the nodal velocity vector

IV.1.2 EULERIAN FORMULATION

As mentioned above, the development of the Eulerian formulation is based on the virtual work principle referred to the current configuration for a single element, eqn. (II.1).

Starting with the left hand side of equation (II.1),

$$\text{L.H.S.} = \int_{\mathcal{V}} \bar{\sigma} : \delta \bar{\epsilon} d^2V + \int_{\mathcal{V}} \bar{\rho} \bar{a} \cdot \delta \bar{u} d^2V \quad (IV.16)$$

Substituting for the displacement assumption, eqn. (IV.13), the above equation takes the form

$$\text{L.H.S.} = \left(\int_{\mathcal{V}} \bar{\sigma} : \left[\frac{1}{2} \left(\frac{\partial \psi_{ia}}{\partial x_j} + \frac{\partial \psi_{ja}}{\partial x_i} \right) \bar{e}_i \bar{e}_j \right] d^2V + \int_{\mathcal{V}} \bar{\rho} \bar{a} \cdot (\psi_{ia} \bar{e}_i) d^2V \right) \delta \underline{u}_a \quad (IV.17)$$

where \bar{e}_i is the unit base vector in the Cartesian frame of reference. Taking increments of the above equation, yields

$$\begin{aligned} \Delta(\text{L.H.S.}) = & \left(\int_{\mathcal{V}} \Delta \bar{\sigma} : \left[\frac{1}{2} \left(\frac{\partial \psi_{ia}}{\partial x_j} + \frac{\partial \psi_{ja}}{\partial x_i} \right) \bar{e}_i \bar{e}_j \right] d^2V \right. \\ & \left. + \int_{\mathcal{V}} \Delta(\bar{\rho} \bar{a} \cdot (\psi_{ia} \bar{e}_i)) d^2V \right) \delta \underline{u}_a \end{aligned} \quad (IV.18)$$

Following the above procedures for the right hand side of the virtual work principle together with the following relation

$$d^2 \bar{A} : \Delta \bar{\sigma} = \Delta \bar{\sigma}_n d^2 A \quad (IV.19)$$

we obtain

$$\Delta(\text{R.H.S.}) = \left(\int_{\mathcal{V}} \Delta(\bar{\rho} \bar{b}_i) \psi_{ia} d^2V + \int_{\mathcal{A}} \Delta \bar{\sigma}_n \psi_{ia} d^2 A \right) \delta \underline{u}_a \quad (IV.20)$$

The incremental virtual work principle can be obtained by collecting the results of eqns. (IV.18, IV.20) as follows:

$$\begin{aligned} (\Delta \bar{R}_{-a}^2) \delta \bar{u}_{-a}^2 = & \int_{2V} \Delta \bar{\sigma}^2 : \left[\frac{1}{2} \left(\frac{\partial \psi_{ia}}{\partial x_j^2} + \frac{\partial \psi_{ja}}{\partial x_i^2} \right) \bar{e}_i \bar{e}_j \right] d^2V \\ & + \int_{2V} \Delta(\bar{\rho}^2 \bar{a}_{-a}) \cdot (\psi_{ia} \bar{e}_i) d^2V \end{aligned} \delta \bar{u}_{-a}^2$$

where

$$\Delta \bar{R}_{-a}^2 = \left\{ \int_{2V} \Delta(\bar{\rho}^2 \bar{b}_{-a}) \psi_{ia} d^2V + \int_{2A} \Delta \bar{\sigma}_{n_i}^2 \psi_{ia} d^2A \right\} \quad (IV.21)$$

is the increment of the load vector.

On a similar basis of the development of eqn. (III.43), and by considering a virtual displacement vector $\delta \bar{u}_{-a}^2$, we obtain

$$\Delta \bar{R}_{-a}^2 = \int_{2V} \bar{\sigma}^2 : \left[\frac{1}{2} \left(\frac{\partial \psi_{ia}}{\partial x_j^2} + \frac{\partial \psi_{ja}}{\partial x_i^2} \right) \bar{e}_i \bar{e}_j \right] d^2V + \int_{2V} \Delta(\bar{\rho}^2 \bar{a}_{-a}) \cdot (\psi_{ia} \bar{e}_i) d^2V \quad (IV.22)$$

which represents the incremental equilibrium equations.

To complete the formulation, we assume a constitutive equation in the form

$$\Delta \bar{\sigma}^2 = {}_2\bar{D} : \Delta \bar{\epsilon}^2 \quad (IV.23)$$

where ${}_2\bar{D}$ is a fourth-order tensor, $\Delta \bar{\sigma}^2$ and $\Delta \bar{\epsilon}^2$ are the increments of the Cauchy stress and Eulerian strain tensors.

Substitution of the displacement assumption eqn. (IV.13), into the increment of the strain tensor, gives

$$\begin{aligned} \Delta \bar{\epsilon}^2 &= \frac{1}{2} \left[\frac{\partial \Delta \bar{u}_i^2}{\partial x_j^2} + \frac{\partial \Delta \bar{u}_j^2}{\partial x_i^2} - \frac{\partial \bar{u}_k^2}{\partial x_i^2} \frac{\partial \Delta \bar{u}_k^2}{\partial x_j^2} - \frac{\partial \Delta \bar{u}_k^2}{\partial x_i^2} \frac{\partial \bar{u}_k^2}{\partial x_j^2} \right] \bar{e}_i \bar{e}_j \\ &= \frac{1}{2} \left[\left(\frac{\partial \psi_{i\beta}}{\partial x_j^2} + \frac{\partial \psi_{j\beta}}{\partial x_i^2} - \frac{\partial \bar{u}_k^2}{\partial x_i^2} \frac{\partial \psi_{k\beta}}{\partial x_j^2} - \frac{\partial \psi_{k\beta}}{\partial x_i^2} \frac{\partial \bar{u}_k^2}{\partial x_j^2} \right) \Delta \bar{u}_{-\beta}^2 \right] \bar{e}_i \bar{e}_j \end{aligned} \quad (IV.24)$$

then the increment of the stress tensor takes the form

$$\begin{aligned} \Delta^2 \bar{\sigma} &= \Delta^2 \sigma_{ij} \bar{e}_i \bar{e}_j = ({}^2D_{ijkl} \Delta^2 \epsilon_{kl}) \bar{e}_i \bar{e}_j \\ &= \frac{1}{2} \left[{}^2D_{ijkl} \left(\frac{\partial \psi_{k\beta}}{\partial^2 x_l} + \frac{\partial \psi_{l\beta}}{\partial^2 x_k} - \frac{\partial^2 u_m}{\partial^2 x_k} \frac{\partial \psi_{m\beta}}{\partial^2 x_l} - \frac{\partial \psi_{m\beta}}{\partial^2 x_k} \frac{\partial^2 u_m}{\partial^2 x_l} \right) \Delta^2 u_{-\beta} \right] \bar{e}_i \bar{e}_j \end{aligned} \quad (IV.25)$$

utilizing the symmetry of the material tensor ${}^2D_{ijkl}$, the increment of the strain tensor may be put in the form

$$\Delta^2 \bar{\sigma} = \left[{}^2D_{ijkl} \left(\frac{\partial \psi_{k\beta}}{\partial^2 x_l} - \frac{\partial^2 u_m}{\partial^2 x_k} \frac{\partial \psi_{m\beta}}{\partial x_l} \right) \Delta^2 u_{-\beta} \right] \bar{e}_i \bar{e}_j \quad (IV.26)$$

Considering the acceleration expression given by eqn. (IV.6), which upon incrementations yield

$$-\Delta^2 \bar{a}_* = \frac{\partial \Delta^2 \bar{v}}{\partial t} + \Delta^2 \bar{v} \cdot \frac{\partial^2 \bar{v}}{\partial^2 x} + {}^2 \bar{v} \cdot \frac{\partial \Delta^2 \bar{v}}{\partial^2 x} \quad (IV.27)$$

substituting for the velocity from eqns. (IV.14, IV.15) into the above equation, we obtain

$$\Delta^2 \bar{a}_* = \left[\psi_{i\beta} \Delta^2 \ddot{u}_{-\beta} + \left(\psi_{k\beta} \frac{\partial^2 \dot{u}_i}{\partial^2 x_k} + {}^2 \dot{u}_k \frac{\partial \psi_{i\beta}}{\partial^2 x_k} \right) \Delta^2 \ddot{u}_{-\beta} \right] \bar{e}_i \quad (IV.28)$$

To obtain the final incremental equilibrium equations, we substitute eqn. (IV.26) together with eqn. (IV.28) into the incremental form of the virtual work principle, eqn. (IV.21),

$$\begin{aligned} \Delta^2 \bar{R}_a &= \left| \int_{2V} \frac{1}{2} {}^2D_{ijkl} \left(\frac{\partial \psi_{i\alpha}}{\partial^2 x_j} + \frac{\partial \psi_{j\alpha}}{\partial^2 x_i} \right) \left(\frac{\partial \psi_{k\beta}}{\partial^2 x_l} - \frac{\partial^2 u_m}{\partial^2 x_k} \frac{\partial \psi_{m\beta}}{\partial^2 x_l} \right) d^2V \right| \Delta^2 u_{-\beta} \\ &= \left| \int_{2V} {}^2\rho \psi_{i\beta} \psi_{i\alpha} + {}^2\rho \left(\psi_{k\beta} \psi_{i\alpha} \frac{\partial^2 \dot{u}_i}{\partial^2 x_k} + {}^2 \dot{u}_k \psi_{i\alpha} \frac{\partial \psi_{i\beta}}{\partial^2 x_k} \right) d^2V \right| \Delta^2 \ddot{u}_{-\beta} \end{aligned} \quad (IV.29)$$

which may be written as

$$\Delta^2 \bar{R}_a = [{}^2K_{\alpha\beta}^{(1)} - {}^2K_{\alpha\beta}^{(2)}] \{\Delta^2 u_{-\beta}\} + [{}^2M_{\alpha\beta}^{(1)}] \{\Delta^2 \ddot{u}_{-\beta}\} + [{}^2M_{\alpha\beta}^{(2)}] \{\Delta^2 \ddot{u}_{-\beta}\} \quad (IV.30)$$

where $\Delta^2 \bar{R}_a$ is the increment of the load vector given by eqn. (IV.21),

$${}^2K_{\alpha\beta}^{(1)} = \int_{2V} \frac{1}{2} {}^2D_{ijkl} \left(\frac{\partial \psi_{i\alpha}}{\partial^2 x_j} + \frac{\partial \psi_{j\alpha}}{\partial^2 x_i} \right) \left(\frac{\partial \psi_{k\beta}}{\partial^2 x_l} \right) d^2V \quad (IV.31)$$

corresponds to the usual small displacement, or the incremental stiffness matrix,

$${}^2K_{\alpha\beta}^{(2)} = \int_{2V} \frac{1}{2} {}^2D_{ijkl} \left(\frac{\partial \psi_{i\alpha}}{\partial x_j} + \frac{\partial \psi_{j\alpha}}{\partial x_i} \right) \left(\frac{\partial u_m}{\partial x_k} \frac{\partial \psi_{m\beta}}{\partial x_l} \right) d^2V \quad (IV.32)$$

corresponds to the initial displacement, or the initial rotation stiffness matrix,

$${}^2M_{\alpha\beta}^{(1)} = \int_{2V} {}^2\rho (\psi_{i\beta} \psi_{i\alpha}) d^2V \quad (IV.33)$$

is the mass matrix and, finally

$${}^2M_{\alpha\beta}^{(2)} = \int_{2V} {}^2\rho \left(\psi_{k\beta} \psi_{i\alpha} \frac{\partial u_i}{\partial x_k} + u_k \psi_{i\alpha} \frac{\partial \psi_{i\beta}}{\partial x_k} \right) d^2V \quad (IV.34)$$

is the convected mass matrix.

If the lumped mass approximation is introduced for the dynamic term, the final incremental equilibrium equations takes the form

$$\Delta {}^2R_{\alpha} = [{}^2K_{\alpha\beta}^{(1)} - {}^2K_{\alpha\beta}^{(2)}] \{\Delta u_{\beta}\} + [{}^2M_{\alpha\beta}] \{\Delta u_{\beta}\} \quad (IV.35)$$

where all individual terms are defined above, and

$${}^2M_{\alpha\beta} = \frac{1}{N} I_{\alpha\beta} \int_{2V} {}^2\rho d^2V \quad (IV.36)$$

is the lumped mass matrix, where N is the number of nodes per element and $[I]$ is the identity matrix.

It is important to notice that the expression for the load increment, eqn. (IV.21), is independent of the deformation gradient tensor which is contrary to the Lagrangian and the updated Lagrangian formulation. This form of the load vector eliminates the existence of the initial load or the load-correction matrix in the Eulerian formulation. Also, the use of σ and $\Delta\epsilon$ as the conjugate pair of the variables, which are discussed in Chapter II, in the development of the Eulerian formulation eliminates the initial stress or the geometric stiffness matrix.

Once again, little work has been devoted to the development of a consistent Eulerian formulation. The formulation presented here, however, differs from the similar formulations in the literature. Gadala [51] and Gadala et al. [85] introduce a consistent

Eulerian formulation which is based on the energy balance equation and utilization of increments of the variables inside a linear increment. They present an accurate discussion of the treatment of the constitutive equations and the stress and strain increments. However, to obtain an expression for the velocity of the body-point X , they apply the general form of the material time derivative in the spatial formulation. This leads to an expression for the velocity which depends on the deformation gradient tensor. Accordingly, their expression for the total stiffness matrix of the element is dependent on the deformation gradient tensor which makes it computationally difficult. For the same reason, the acceleration expression is very complicated and highly nonlinear. To overcome this difficulty, the lumped mass approximation is introduced for the dynamical term in the energy balance equation. In the formulation developed here, the expressions of the total stiffness matrix given in eqn. (IV.30) and of the velocity vector given in eqn. (IV.2) are independent of the deformation gradient tensor. Accordingly, the acceleration expression in the developed formulation given in equation (IV.6) appears to be less complicated. In reference [85] no applications are given to support their formulation, to demonstrate the numerical procedures, and to discuss the specific approximations which make the finite element analysis using the Eulerian formulation suitable for numerical applications.

IV.1.3 CONSTITUTIVE EQUATIONS

(i) Elastic Material

In Eulerian formulation, we may assume a linear incremental constitutive equations similar to eqn. (II.66), this equation may, as well, be expressed in the current configuration C_2 instead of C_1 , namely

$$\Delta^2 \bar{\sigma} = \frac{4}{2} \bar{D} : \Delta^2 \bar{\epsilon} \quad (IV.37)$$

where all individual terms are defined in Chapter III. However, in the finite element analysis using the Eulerian formulation the mesh is fixed in space. Therefore, eqn. (IV.24) is used to determine the increments of the strain tensor of the body-points momentarily occupying the integration points at the beginning of each incremental step. Then, the constitutive equations, eqn. (IV.37), is used to calculate the increments of the stress tensor at these body-points. This aspect of calculation will be discussed in more detail in Section (IV.3.3).

Another possibility for deriving the constitutive equations is to characterize the material behaviour with a stress rate which is frame-indifferent. Once again, the Jaumann stress rate given above in eqn. (III.75) is the most commonly used stress rate in the finite element analysis [5,17,18,29,79,116,117].

(ii) Elasto-Plastic Material

For the elasto-plastic behaviour of the material, we can assume a constitutive equations similar to that given in eqn. (IV.37). In this case, the components ${}_2D_{ijkl}$ of the material tensor in each integration point depend on the current stress state of the body-point momentarily occupying this point in space; the elastic constant of the material, and the work hardening characteristics of the material. Once again, Jaumann stress rate or any other frame-indifferent stress rate can be used to derive the constitutive equations.

IV.2 FINITE ELEMENT ANALYSIS PROCEDURES USING THE EULERIAN FORMULATION (EULERIAN FIXED MESH TECHNIQUE)

Referring to Figure (IV.1), in the finite element analysis using the Eulerian formulation, it is required to determine the deformation of the body through the fixed region R . It is assumed that the solution has been determined up to the time t so that the field functions are known in the configuration of the body at time t . Consider the body-point X

subjected to the incremental displacement $\Delta \bar{u}_X$ in the time interval Δt . The increments of the strain and the stress tensor can be calculated using eqns. (IV.24, IV.26) respectively. Therefore, the stress at the moved body-point X at time $t + \Delta t$ is given by

$${}^{t+\Delta t}\bar{\sigma} = {}^t\bar{\sigma} + \Delta {}^t\bar{\sigma} \quad (\text{IV.38})$$

As discussed in the section of the constitutive equations, it is necessary to determine the state of the stress of the body-points momentarily occupying the fixed integration points in the beginning of each incremental step. The displacements of the body-points momentarily occupying the nodal points should also be known. Again referring to Figure (IV.1), assume that the body-point X was occupying an integration point at time t . At time $t + \Delta t$ another body-point occupies the same integration point. The state of the new body-point at the fixed integration point is determined through an interpolation of the field functions from the known values at the moved body-points to those which come to the integration points. To achieve this, we utilize an imaginary finite element mesh to interpolate the stresses and the displacements at the beginning of each incremental step.

IV.3 APPLICATION: STRESS AND DEFORMATION ANALYSIS OF METAL- EXTRUSION PROCESS

In metal-forming processes, it is necessary to evaluate the stress and the deformation distribution throughout the work-piece. This permits investigation of the generation of high residual stresses and the initiation of the metal-forming defect such as surface and internal cracks. The residual stresses constitute the stress field after the work-piece has emerged from the process. The criteria governing the initiation and the growth of cracks in the material are commonly based on the stress history in the material.

In many metal-forming processes, as, for example, in extrusion processes, finite strains occur. The components of the elastic strain in these processes are generally limited to

the order of 10^{-3} because the elastic moduli of metals are typically about three orders of magnitude larger than the yield stress. Therefore, plastic strains dominate elastic strains in a work-piece passing through such a process. Elastic strains, however, play an essential role in determining the stress distribution in the work-piece. Therefore, in the solution of such a process using rigid-plastic material model [119,120] can only predict stresses in the region of active plastic strains which, in case of the extrusion, usually represents a small portion of the work-piece. Elastic regions would then be modeled as rigid regions. Furthermore, residual stresses in the processed work-piece cannot be determined using the rigid-plastic material model. According to the given discussion, it is recommended to employ the elasto-plastic material model to be able to predict more accurately the stress history in the work-piece. This is easy to handle in the analysis when the finite element technique is used.

In the analysis of the metal-extrusion process using the updated Lagrangian formulation, it is necessary to have the mesh division of equal size along the longitudinal direction of the billet [97-99,106,121] since each cross-section will be subjected to the same history of deformation followed by unloading. Also, to obtain steady-state extrusion analysis requires a long billet so that a region of uniform residual stresses can develop in the extrudate. Furthermore, difficulties arise from the updating of the boundary conditions on the surface of the die in the analysis using the updated Lagrangian formulation. On the other hand, utilizing the Eulerian formulation in the finite element analysis (Eulerian fixed mesh technique) such difficulties do not exist. In this technique, we have the ability to make localized finite mesh refinements, such as, for example, the mesh used in the present study, Figure (IV.2), to improve the accuracy of the results in regions of high stress variations. In the updated Lagrangian formulation, such a refinement would be needed for a long billet. Furthermore, in the Eulerian fixed mesh technique, there is no such need for a long billet; the size of the finite element mesh can be reduced to include only the reduction die and a short

billet and extrudate since we assume that the work-piece is sufficiently long and the material comes in and goes out through the inlet and the outlet boundaries respectively (see the sub-section IV.3.2).

IV.3.1 Problem Description and Solution Procedures

Figure (IV.2) shows the geometry and the dimensions of the metal-extrusion process of an aluminum billet. The billet material is initially in a stress-free condition and is forced into a symmetric die after sliding between smooth rigid plates. The die is shaped in the form of a fifth-order polynomial curve with zero curvature and slope at both ends. It is assumed that the die produces a 25% thickness reduction over a distance of $1.2a$, where a is the half thickness of the original sheet, see Figure (IV.2). The symmetry of the die about the centre-line of the billet allowed the analysis to be carried out only on half of the billet as shown in Figure (IV.2). This symmetry also determines the boundary conditions on the centre-line of the billet (see the sub-section IV.3.2). The finite element mesh consists of $3 \times 17 = 51$ isoparametric 8-node plane strain elements.

For the calculation of the element stiffness matrices, eqns. (IV.31, IV.32), the shape functions $\psi_{i\alpha}$ and the global shape function derivatives $\partial\psi_{i\alpha}/\partial^2x_j$ given in Appendix B are used. The components of the material tensor ${}_2D_{ijkl}$ is evaluated in the same way as in the Lagrangian and the updated Lagrangian formulation. In the elastic analysis, the usual stress-strain relation for plane strain, i.e., the matrix $[C]$ (see Appendix C) is used whereas, in the elasto-plastic analysis, the compliance matrix $[C]_{cp}^{*}$ is calculated following the same procedures discussed in Appendix C. Equation (C.11) can be expressed in this case as follows:

$$[\Delta^2 \sigma] = \left([C] - \alpha [C] \left\{ \frac{\partial \sigma}{\partial^2 \sigma_{ij}} \right\} (W)^T \right) (\Delta^2 \epsilon) = [C]_{cp}^* (\Delta^2 \epsilon) \quad (IV.39)$$

where all individual terms are defined in Appendix C, and

$$\alpha = 0 \quad \text{for elastic loading and unloading}$$

$\alpha = 1$ for continuation of plastic deformation

In the present analysis, the aluminum material is assumed to be linearly elastic up to the yield point, and isotropic linear strain-hardening with the von Mises yield criterion thereafter. The corresponding stress-strain curve for the aluminum material used is illustrated in Figure (IV.4). The displacement increments applied at the piston boundary were kept small to maintain accuracy; in particular, to insure close following of the stress-strain curve. Finally, the Gauss-Legendre integration procedure with the reduced integration of order 2×2 Gaussian points is employed to calculate the element stiffness matrices.

In the Eulerian fixed mesh finite element analysis, any body-point X may traverse more than one plastic zone and hence deforms plastically after being unloaded. The first yield occurs when the initial yield stress is first exceeded. Unloading of the body-point X is indicated when the assumption of continued plastic deformation would result in a reduction of the effective stress. For the special case under consideration, it was found that only one plastic region arises as shown in Figure (IV.3), and then all body-points change from plastic deformation to elastic deformation due to unloading. This agrees well with the results obtained by Lee et al. [97-99] and Yamada et al. [106] using the updated Lagrangian formulation.

The Eulerian fixed finite element mesh technique has been incorporated into a special purpose programme for two-dimensional metal-extrusion processes. The analysis starts with the part of the billet inside the fixed region being in a stress-free condition. Then, the solution proceeded with the following steps in each increment.

1. Compute the stiffness matrices as discussed above.
2. Implement the boundary conditions (as discussed in the sub-section IV.3.2).

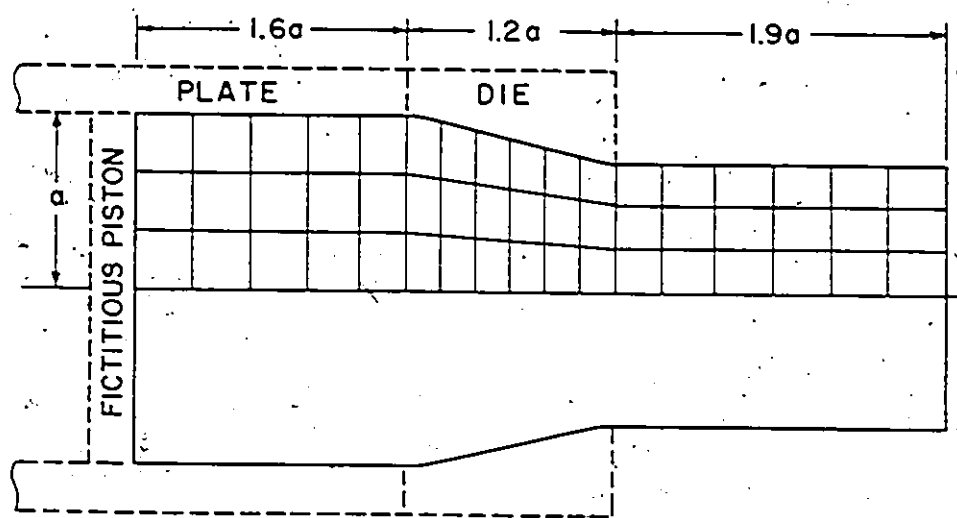


Figure (IV.2) Finite element mesh for the extrusion problem.

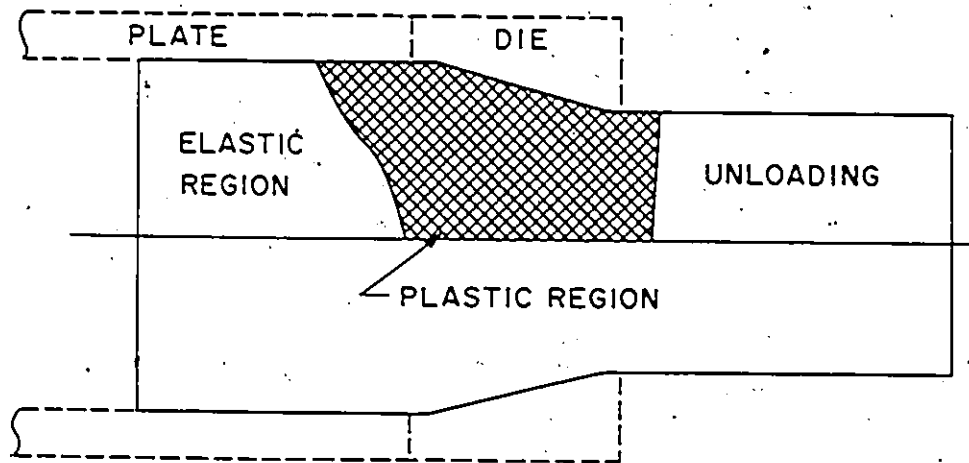


Figure (IV.3) Configuration of the plastic region in the steady-state.

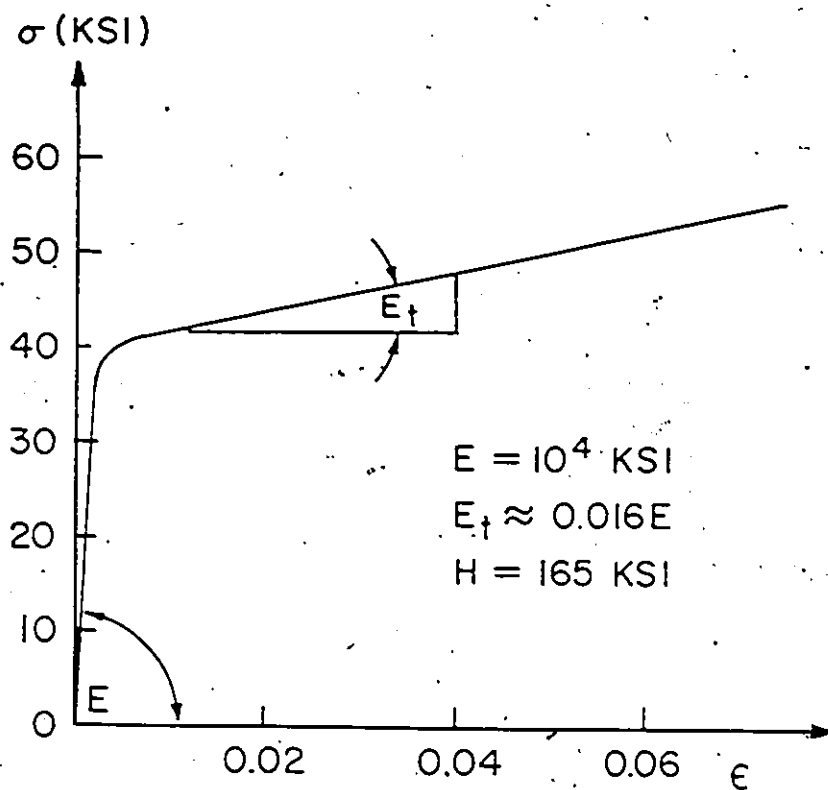


Figure (IV.4) The stress-strain relation for the aluminum which is used in the analysis.

3. Apply a uniform displacement increment for all nodes in contact with the fictitious piston.
4. Solve for the incremental displacements using the Frontal solution technique.
5. Calculate the increment of the strain tensor at each integration point, via eqn. (IV.24), and then calculate the increment of the stress tensor at the same points by using Jaumann stress rate given in eqn. (III.75).
6. The stress tensor of the displaced body-points after the incremental step (see Figure (IV.5)) are calculated using eqn. (IV.38), where the first term on the right-hand side is determined by interpolating the known stress tensors from the previous increment.

The above steps were repeated until steady-state condition was obtained as indicated by the constant state of stress over the entire work-piece, and by constant displacement increments of the extrudate discharged by the process at the outlet boundary for constant incremental displacements imposed by the fictitious piston.

IV.3.2 Boundary Conditions for Fixed Mesh Metal-Extrusion Analysis

Referring to Figure (IV.2), we first consider the boundary conditions imposed by the fictitious piston. It was assumed that we have specially fixed boundary and the material cross this boundary. In each increment, the fictitious piston pushes the billet with a uniform displacement increments parallel to the axis of symmetry with zero lateral nodal forces for all nodes in contact with the piston. New material is being continuously convected to the fixed region with prescribed state of stress. This corresponds to a long billet stressed elastically from zero stress to the state of stress required to derive the process with rigid guide plates which prevent lateral strain. In the numerical computations, the prescribed state of stress was taken as the state of the stress acting on the piston.

Along the axis of symmetry, the normal displacements and the shear forces vanish. The same type of boundary conditions are also applied to the guide plate and the die. However, on the die these boundary conditions are applied to the coordinate axes aligned with the surface of the die and the normal to this surface. Therefore, the stiffness submatrices of the relevant elements and the nodal forces corresponding to the nodal points along the surface of the die are transformed to the local axes. Hence in the solution, all displacement increments are referred to the global axes except the displacement increments of the restrained nodes which will be automatically computed in the local directions. The displacement increments and the reactions in the local directions are then transformed back to the global axes x_1 and x_2 .

The lateral surface of the extrudate is free from surface traction. Therefore, the corresponding nodal forces are zero. Elastic recovery of the extrudate after leaving the die involves an increase in its thickness by less than 1% [97,98,86]. Such bulging could be taken into account in the analysis by adjusting the nodal coordinates on the free surface. However, since the bulging is usually quite small, this procedure may be an unnecessary complication. Therefore, in the present analysis this was assumed to be the case, and the boundary conditions were imposed on a fixed lateral surface. It is found that the lateral incremental displacements of the nodes on the free surface of the extrudate are numerically very small (almost negligible) compared to the longitudinal incremental displacements which assess the assumption employed in the analysis.

For the extrudate discharged from the process, boundary conditions are imposed on a specially fixed cross-section sufficiently removed from the die to generate steady-state of residual stresses. On this cross-section, the shear forces are zero. There will also be no change in elastic strains in the material traversing the fixed boundary [86,97-99,106] and

hence uniform displacement increments over the cross-section are imposed and chosen such that the resultant of the nodal forces over the cross-section is zero.

IV.3.3 Interpolation Technique

As previously discussed in the fixed mesh finite element analysis, it is necessary to determine the state of stress of the body-points momentarily occupying the integration points in the beginning of each incremental step for the calculations of the components of the material tensor ${}^2D_{ijkl}$. The displacements of the body-points which occupy the nodal points should also be known for the computations of the total stiffness matrix and the increments of the strain tensor. For this purpose, we utilize an imaginary finite element mesh. Consider a part of the mesh, for example, as illustrated in Figure (IV.5). Next, assume that the body-points occupying the integration points have moved within the incremental step. The state of the displaced body-points A', B', C', \dots , can then be determined by knowing the displacement increments. Now, to obtain the state of the body-points occupying the integration points A, B, C, \dots , after the incremental step, an imaginary finite element mesh is utilized through the displaced body-points as shown in Figure (IV.5). In this case, the isoparametric 4-node plane-strain element is employed. First, it is determined to which element each body-point (A, B, \dots) belongs. Then, the local coordinates r and s of the body-point are computed by knowing the global coordinates. The state of the stress of the body-point presently at the integration point, for example point B , can be calculated as follows:

$$({}^2\bar{\sigma})_B = \sum_{K=1}^4 h_K ({}^2\bar{\sigma})_K \quad (IV.40)$$

where $h_K(r,s)$ are the interpolation functions of the isoparametric 4-node plane strain element [5-7,9] and $({}^2\bar{\sigma})_K$ is the stress tensor at nodal point K .

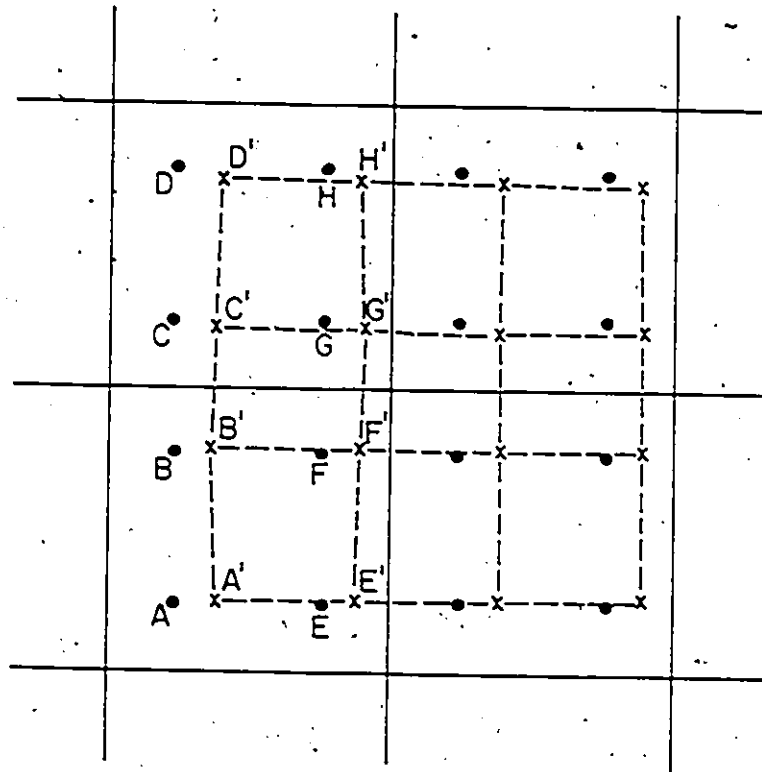


Figure (IV 5) A part of the fixed mesh showing the imaginary mesh.

From the numerical point of view, the above computational procedures are very expensive. On the other hand, owing to the nature of flow of the material in the extrusion process and also assuming small input incremental displacements imposed by the fictitious piston, we can assume, for example, that the point F lies on the side B'F'. This assumption results in $s = 1.0$, and easier computation of r . Therefore, the stress state of the body-point presently occupying the integration point F is given by

$$\bar{(\sigma)}_F = \frac{1}{2} (1 - r) \bar{(\sigma)}_B + \frac{1}{2} (1 + r) \bar{(\sigma)}_{F'} \quad (\text{IV.41})$$

In a similar procedure, the displacements of the body-points occupying the nodal points in the beginning of each incremental step are computed.

IV.3.4 Incompressibility Constraint

In problems of this class, where there are regions involving active plastic strains, the material can be considered approximately incompressible because in these regions the deformation is almost volume conserving (isochoric deformation). In what follows, a brief discussion of the difficulties and the methods of treating the incompressibility in metal-forming processes is presented, rather than, a comprehensive survey of this particular topic. For further details see [39,41,51,122-125]. The numerical difficulties in treating nearly-incompressible materials, i.e. materials for which Poisson's ratio ν approaches one-half, are due to the existence of a singularity in the constitutive equations of such materials. In the finite element analysis the above point means that the approximation characteristics of the element can be entirely lost and the condition of the numerical calculation of stiffness matrices may deteriorate indefinitely. There are three main approaches to deal with the problem of incompressibility.

(i) Direct Imposition of Incompressibility on the Displacement Field

Apparently, the most logical method for incorporating the incompressibility constraint is to directly restrict the displacement field to be an incompressible one. Nagtegaal et al. [122], Nayler [123], Fried [126], and others show that finite element formulations, in which the incompressibility constraint is directly imposed on the displacement field, are sensitive to the type of element, element arrangement, total degrees of freedom, and its relation to total number of constraints as well as to other factors. Nagtegaal et al. [122] present a simple analytical discussion of the idea of "mesh locking" or "locking of degree of freedom" by direct imposition of the incompressibility constraint on the displacement field. It is shown that such limitation in some cases enforces a uniform strain state over all the body regardless of the boundary conditions, and also imposes unrealistic constraints on the kinematics of the body. As a result of the study given in [122], it is recommended to use: 1) constant-strain triangular element with specific mesh arrangement in which each four triangles form a quadrilateral and its diagonals; 2) 6-node linear strain triangle element; 3) perhaps the isoparametric 8-node plane element.

Owing to the difficulties mentioned above in imposing the incompressibility constraint on the displacement field within the element, Nagtegaal et al. [122] propose an alternative of using a mixed variational principle which includes the dilational strain as an auxiliary field. It is, however, significant to notice that the treatment given in [122] is carried out for specific element types with specific forms of interpolating functions for the auxiliary field.

(ii) Lagrangian Multiplier or Multi-Field Principle

The incompressibility constraint can be incorporated by the Lagrangian multiplier method [39,41,124,125]. In this case, the mean stress (or the hydrostatic pressure) is used as a

Lagrangian multiplier to account for the compressibility constraint. The advantage of using the Lagrangian multiplier, or the multi-field principle, in the numerical analysis of incompressible materials, is the elimination of the difficulties discussed above which appear when using single-field principle. However, in this case, the number of the unknowns are increased owing to the introduction of the nodal hydrostatic pressures, or the nodal generalized pressures as additional unknowns. Furthermore, the positive definiteness of the resulting global stiffness matrix of the continuum is no longer guaranteed even though it is for the original compressible material. This may cause difficulties in the numerical solution.

(iii) Reduced-Selective Integration Technique

The reduced-selective integration technique is an effective approach for treating the incompressibility constraint. Naylor [123] presents a series of numerical experiments in which he uses numerical integration in evaluating the stiffness of the parabolic isoparametric elements for the analysis of incompressible materials. In these experiments, Naylor finds that using the isoparametric 8-node with the exact integration of order 3x3 Gaussian points gives futile results when compared with the result of the reduced integration of order 2x2 Gaussian points. It was also found that when the reduced integration is used, the results are completely independent of Poisson's ratio over the range 0.49 to 0.499999. In [127] Zienkiewicz et al. utilize the reduced integration scheme for calculating the dilatation contribution to the element stiffness matrix. Wertheimer [118] examines the use of different isoparametric elements in plane strain and axisymmetric analysis. Based on this study, it was determined that the three elements isoparametric 4-node, 8-node with exact integration order, and 8-node with reduced integration order could be used successfully in an elastoplastic analysis. However, the isoparametric 4-node element does not handle large stress

gradients and in the case of 8-node element with the exact integration order, the stiffness matrix will be overestimated, and it may give large oscillations in the solution.

Hughes [128] and Malkus [129] demonstrate an equivalence between the results of the multi-field variational principle and the single-field principle employing the reduced-selective integration technique.

Incompressibility Constraint in Metal-Extrusion Process

Based on the above discussion, we will examine the use of the above techniques to incorporate the incompressibility constraint in the metal-extrusion process. When the displacement field is restricted to be an incompressible one, only one reliable possibility exists which is used by Lee et al. [97-99] and Yamada et al. [106]: constant-strain triangular element with specific mesh arrangement. As discussed above, this may impose unrealistic constraints on the kinematic of the body. The Lagrangian multiplier method, or the multi-field principle is effective only in the region of active plastic deformation, usually a small region in the metal-extrusion process. However, the deformation of the billet away from the die and the unloading of the extrudate discharged by the process is elastic. Hence, the analysis becomes more complicated if the Lagrangian multiplier method is used. As already discussed above, the reduced-selective integration technique can be used for its computational effectiveness; therefore, it is employed in this study. The isoparametric 8-node plane strain element with the reduced integration of order 2x2 Gaussian points is used with Poisson's ratio equal to 0.495.

Numerical experiments (using the linear constitutive equations given by eqn. (IV.37), Jaumann stress rate given by eqn. (III.75), and changing the input incremental displacements imposed by the fictitious piston) showed that the inclusion of the stiffness matrix ${}^2K_{\alpha B}^{(2)}$, which corresponds to the initial displacement or the initial rotation stiffness

matrix, makes the structure unrealistically stiff and the corresponding response deviates considerably from the expected result (the results presented by Lee et al. [97-99] and Yamada et al. [106] using the updated Lagrangian formulation). Therefore, although this stiffness matrix and the corresponding terms in the increment of the strain tensor given by eqn. (IV.24) exist from the consistent formulation, they have been omitted in the numerical analysis.

IV.3.5 Numerical Results

Figures (IV.6-IV.8) give the steady-state distribution of the longitudinal, the shear, and the normal stresses respectively. With the centre-line of the billet taken to be the X-axis, each curve in the above Figures represents the stress variations for the body-points which pass through the centre-line of each row of the mesh. The steady-state is reached in 165 equal increments each of $(2 \times 10^{-2} a/3)$, where a is half the thickness of the original sheet. It can be seen from the results that large variation for all stresses occur along the die. Figures (IV.6-IV.8) also show that the longitudinal, the shear, and the normal stresses of the extrudate away from the die exit reach a constant value for each curve. This represents the residual stress distribution for the steady-state condition of the process. From Figure (IV.6) one observes that the maximum tensile stress appears near the surface just outside the die which represent the primary potential source of crack initiation and growth. The obtained results have the same trend similar to the results given by Yamada et al. [106], Figures (IV.9-IV.11), and by Lee et al. [99], Figures (IV.12-IV.13). In the results of Lee et al., the centre-line of the billet is taken to be the x axis, and each curve shows the distribution of the stresses of body-points which initially had the same relative ordinate in the billet. The lateral station dimensions indicated in Figures (IV.12-IV.13) are these ordinate divided by the half-width of the billet, a . In the results of Yamada et al. and Lee et al. the shear stresses at the free end of the extrudate are required to transform the longitudinal residual stresses to zero surface

traction since finite billet is used in their analysis. In the present work, this is not the case since we assume a very long billet. In the present analysis, however, a different element and a different technique for incorporating the incompressibility constraint are used. Furthermore, the finite element mesh used is rather coarse. In Yamada et al. [106] analysis, it is not clear physically why elements on the outer row should have tensile stresses before entering the die. Such results are not the case in the present analysis. Other available stress analyses for the extrusion process are based on the rigid-plastic material behaviour.

It is not our intention to claim that our results are more accurate than other results. The use of finer mesh and smaller incremental displacements would give more precise results. On the other hand, the analysis will be considerably more expensive.

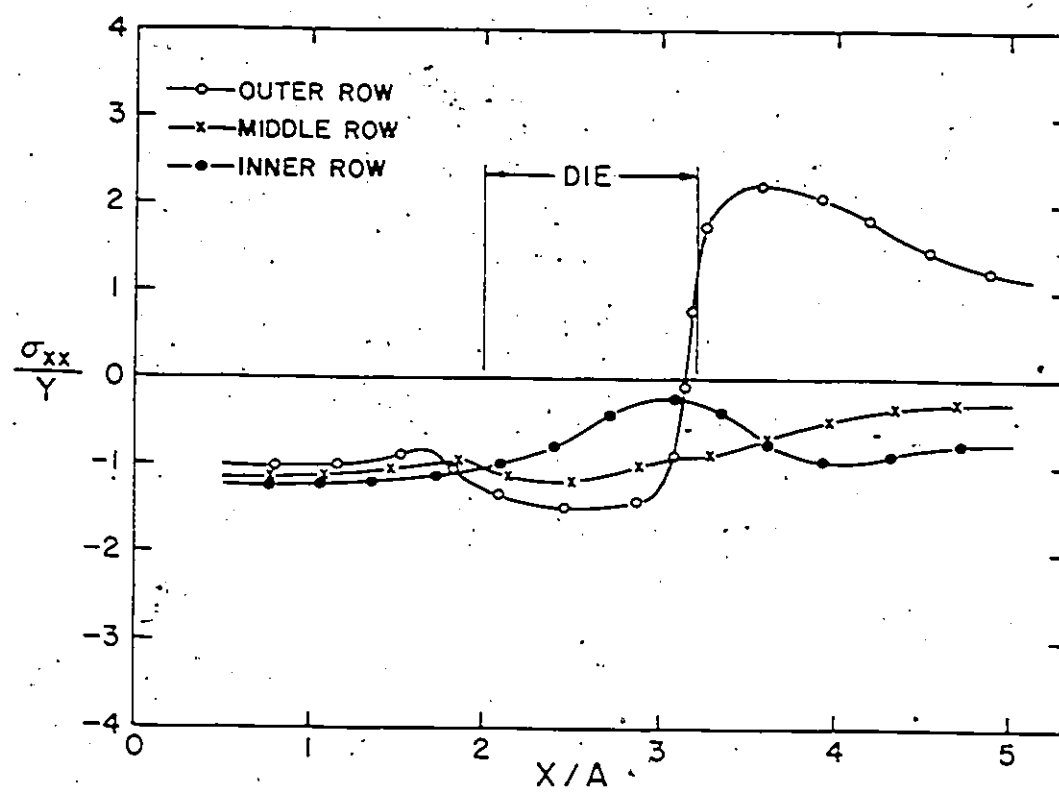


Figure (IV 6) The distribution of the longitudinal stress σ_{xx} at steady state

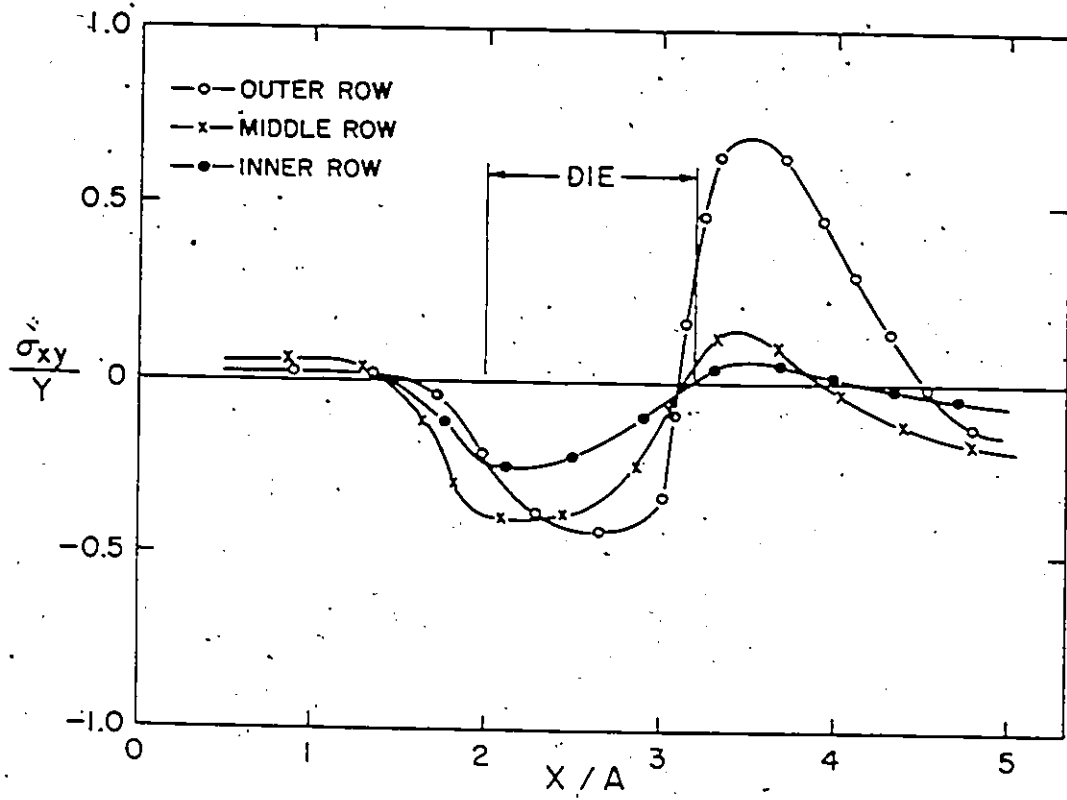


Figure (IV.7) The distribution of the shear stress σ_{xy} at steady state

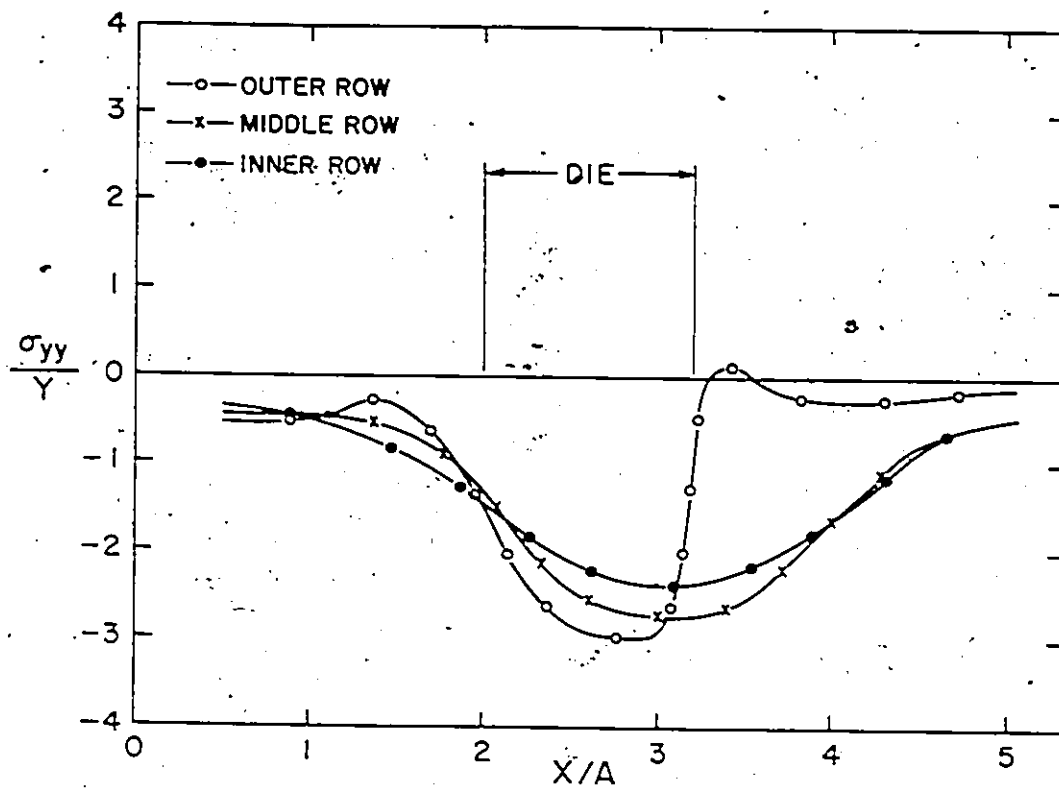


Figure (IV.8) The distribution of the normal stress σ_{yy} at steady state

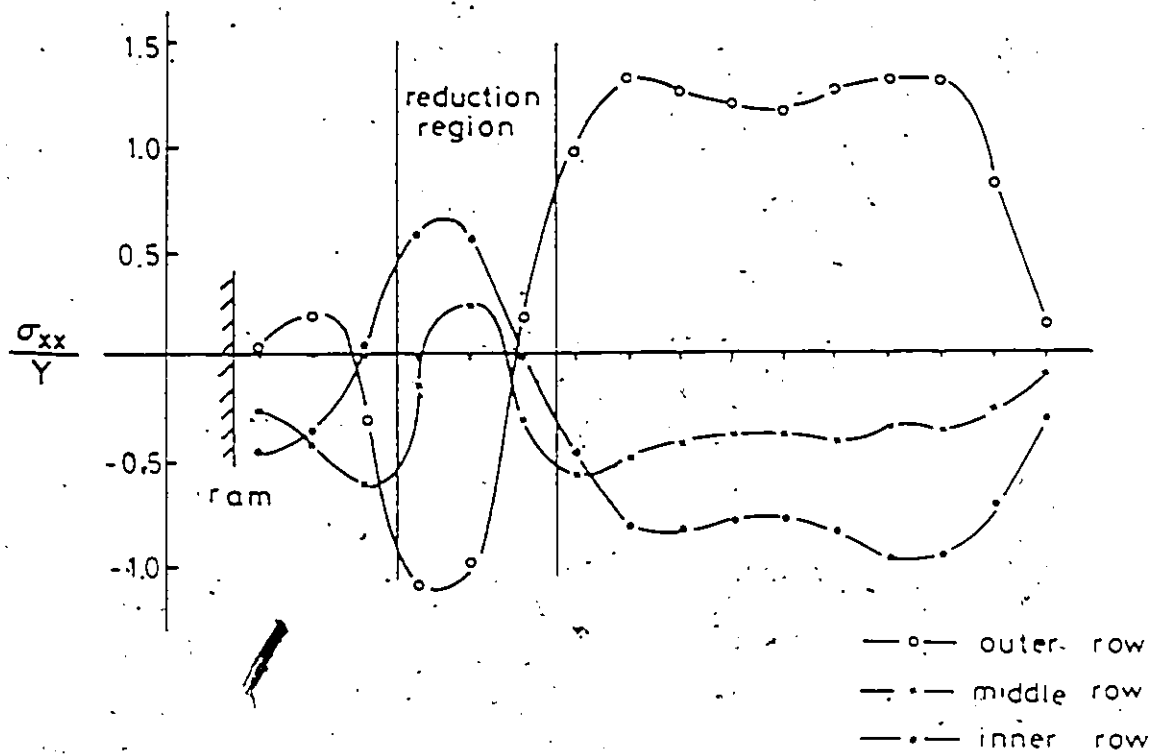


Figure (IV.9) The distribution of the longitudinal stress σ_{xx} at steady state
(Yamada et al. [106].)

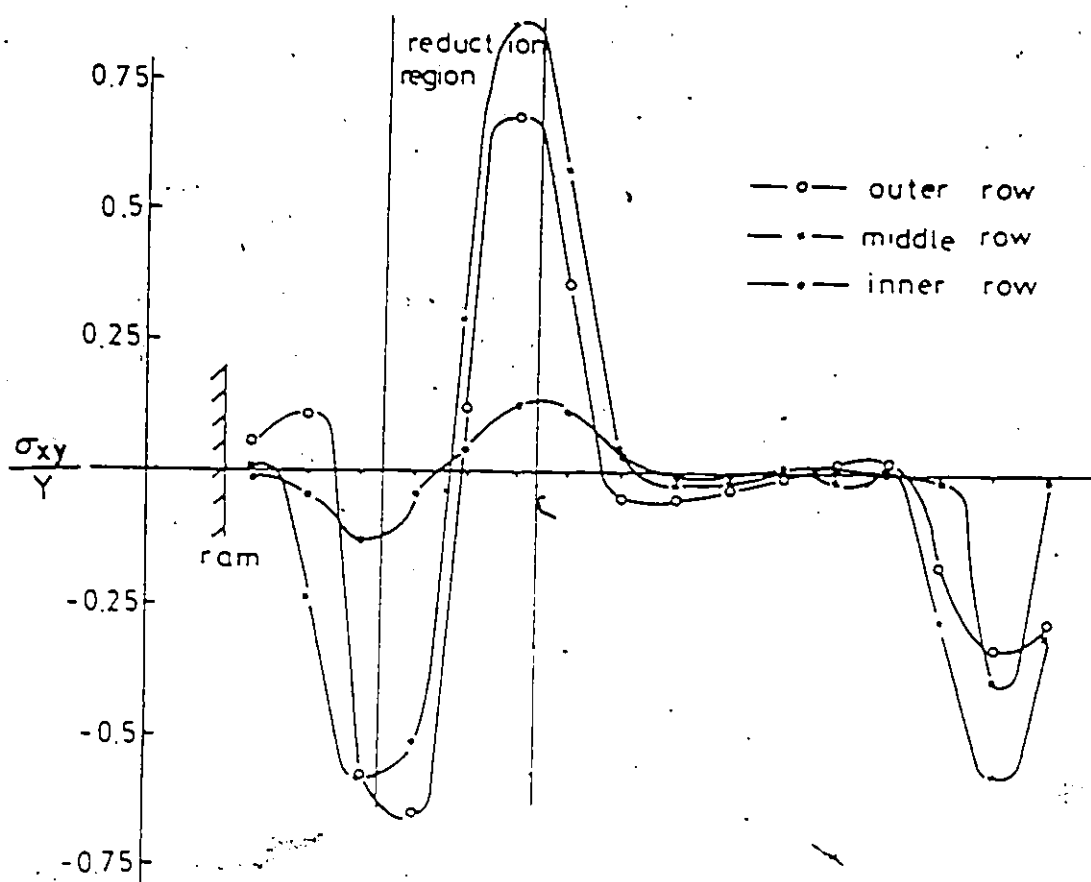


Figure (IV.10) The distribution of the shear stress σ_{xy} at steady state (Yamada et al. [106])

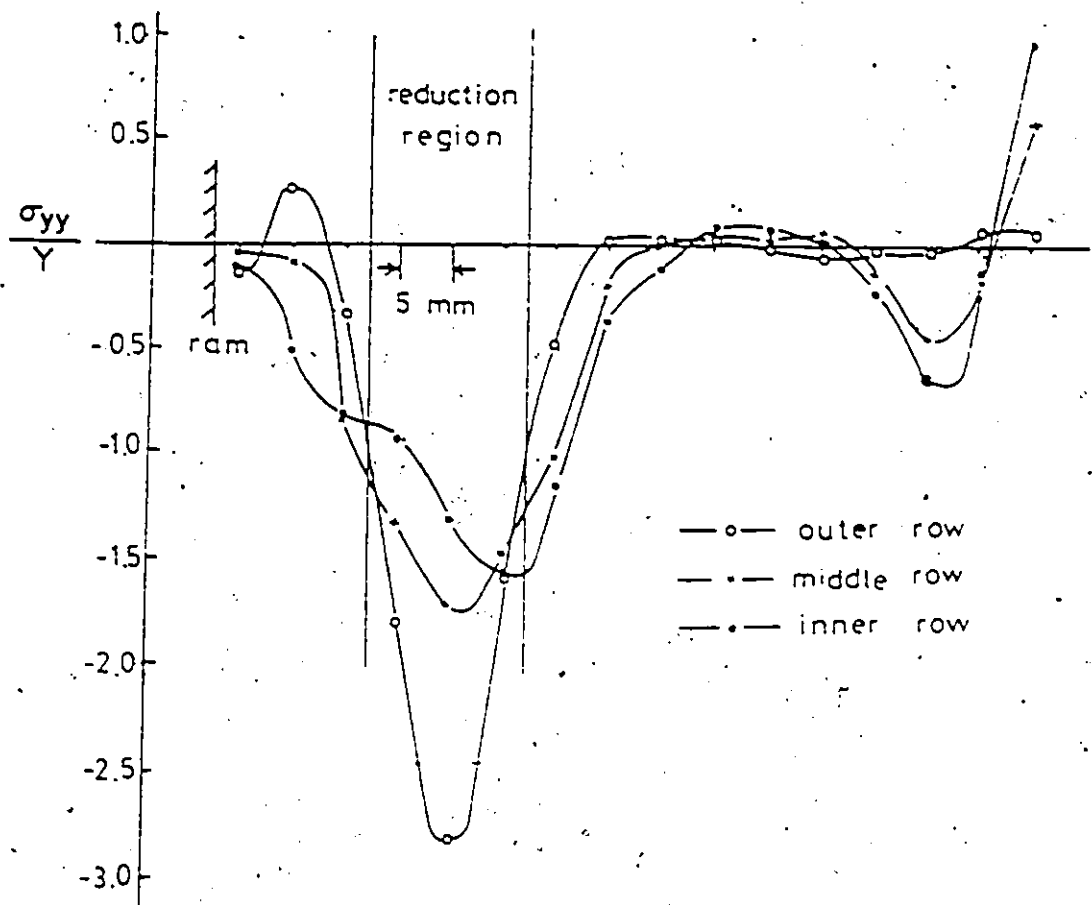


Figure (IV-11) The distribution of the normal stress σ_{yy} at steady state (Yamada et al. [106])

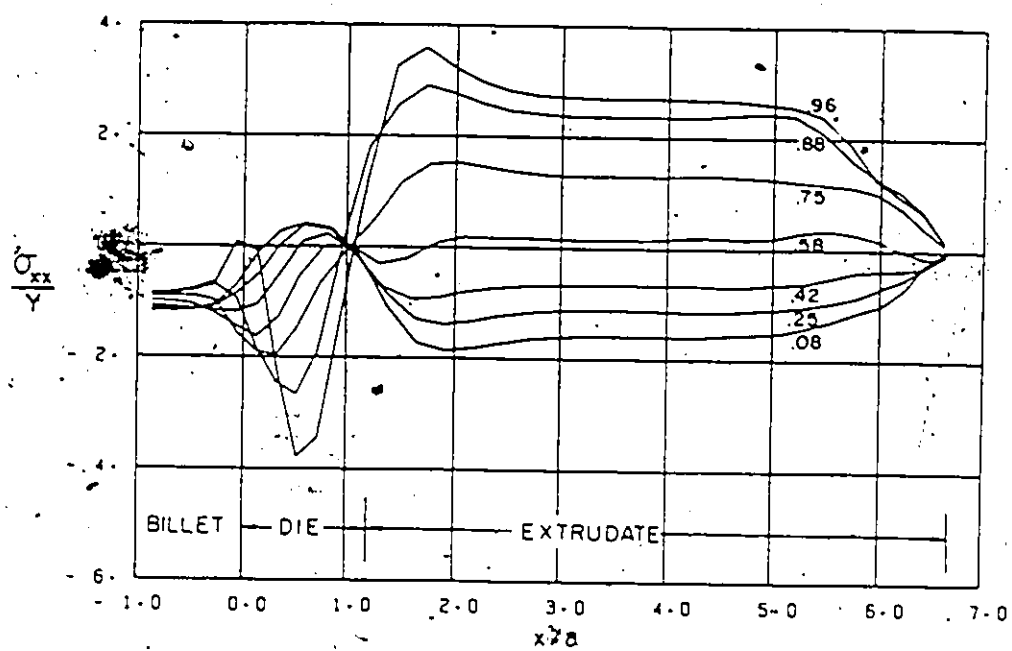


Figure (IV.12) The distribution of the longitudinal stress σ_{xx} at steady state (Lee et al. [99]).

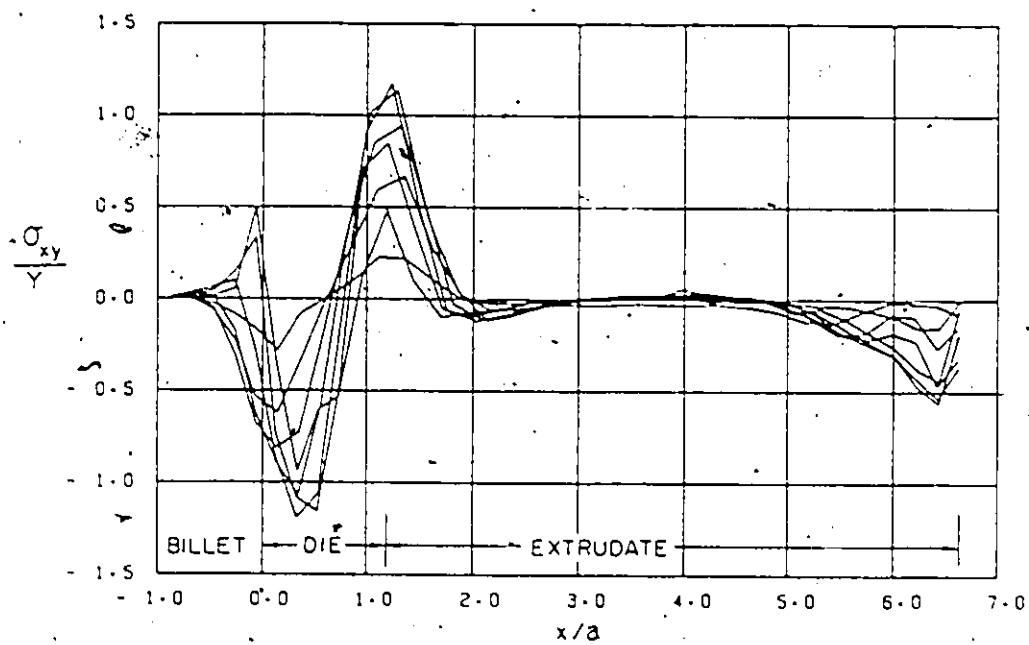


Figure (IV 13) The distribution of the shear stress σ_{xy} at steady state (Lee et al

1991)

CHAPTER V

CONCLUSIONS

A critical discussion of the formulation methods for the finite element analysis of nonlinear problems is given in this work. It is shown that many authors describe the relative or the updated Lagrangian formulation under the name of the Eulerian formulation. Hence, little effort has been devoted to the development of a consistent or detailed Eulerian formulation. Moreover, the attempts at Eulerian formulation include basic assumptions which impose a referential nature on the formulation.

Starting from the continuum mechanics principles, a consistent Lagrangian and updated Lagrangian formulations are derived in this work in explicit forms. The developed formulations are based on the virtual work principle expressed in the current configuration, and then transformed to the proper reference configuration. In the Lagrangian formulation the initial configuration is taken as the reference configuration whereas, in the updated Lagrangian formulation the reference configuration corresponds to the present (the last calculated) configuration. It is shown that the most general approach in deriving the formulations is to consider complete nonlinear kinematic relations within a linear increment. This leads to three stiffness matrices contributing to the total nonlinear stiffness matrix of the element: namely the usual small displacement or the incremental stiffness matrix, the initial stress or the geometric stiffness matrix, and the initial displacement or the initial rotation stiffness matrix.

A consistent transformation of the virtual work principle from the current configuration to both the Lagrangian and the updated Lagrangian configuration is provided. Such transformation eliminates the need for intuitive arguments for the development of the

load vector expression and provides a consistent development of the load-correction matrix. This matrix should be included for all types of loading. In the expressions of the load vector increment, it is found that the definition for the follower load increment resulted in a consistent formulation.

A consistent Eulerian formulation is derived on the basis of the virtual work principle expressed in the current configuration. In the formulation the expression for the increment of the load vector is independent of the deformation gradient tensor. This is not the case in both the Lagrangian and the updated Lagrangian formulation. The form of the load vector expression in the Eulerian formulation eliminates the existence of the load-correction matrix in comparison with the two Lagrangian formulations.

In the Eulerian formulation only two stiffness matrices contribute to the total stiffness matrix of the element. The use of the Cauchy stress tensor and the deformation tensor as the conjugate pair of variables eliminates the existence of the initial stress or the geometric stiffness matrix in the Eulerian formulation. A strict comparison between the Eulerian formulation and the two Lagrangian formulations may not be logical owing to the specific nature of each. However, an analogy between different formulations based on a comparison between linear and nonlinear parts in the expressions of the stress and the strain may be made. When such analogy is carried out, the two stiffness matrices in the Eulerian formulation correspond to the usual small displacement or the incremental stiffness matrix, and to the initial displacement or the initial rotation stiffness matrix of the two Lagrangian formulations.

In numerical applications, it is found that the inclusion of the load correction matrix in the developed Lagrangian formulation reduces the computational time by better than 35 percent. However, it should be observed that the effect of the load-correction matrix on the computational time is dependent on the nature of the particular application.

In the updated Lagrangian formulation, it is found that the predicted results deviate considerably from the results obtained using the Lagrangian formulation. However, invertible transformation between the two Lagrangian formulations ought to exist. When such transformation is carried out it is found that the two terms in the increment of the strain tensor which include the initial displacement effects do not conform with the transformation. Therefore, although these terms and the corresponding stiffness matrix (initial displacement stiffness matrix) come from the consistent formulation, they are omitted in the present updated Lagrangian formulation. In the literature, these terms have been discarded owing to imposition of certain assumptions on the kinematic relations or to restrictions on the displacement field. Some analysts used various stress-rates to describe the material behaviour within the increment to overcome such difficulty. The updated Lagrangian with omission of the initial displacement effects has the same computational efficiency as that of the present Lagrangian formulation. However, including the load-correction matrix in the analysis reduces the computational time by almost 10 percent. The effect of the load-correction matrix on the computational time is dependent on the nature of the application. The choice between the Lagrangian and the updated Lagrangian formulation is decided merely by their relative numerical effectiveness.

The nature of the Eulerian formulation is suitable for the study of flow problems. Therefore, the analysis of metal-forming processes which operate under steady-state condition such as extrusion, wire drawing, and rolling is then facilitated by the use of Eulerian fixed mesh finite element analysis based on the developed formulation. It has obvious advantages when compared with the updated Lagrangian formulation. In the extrusion analysis, however, it is found that the stiffness matrix which corresponds to the initial displacement stiffness matrix makes the structure unrealistically stiff and the corresponding results deviate considerably from the results of the updated Lagrangian

formulation. When this stiffness matrix and the corresponding two terms in the increment of the strain tensor were omitted in the formulation, it is found that the numerical results obtained using the Eulerian formulation compare well with that obtained using the updated Lagrangian formulation.

Finally, it is believed that the existence of the stiffness matrix which corresponds to the initial displacement stiffness matrix in the Eulerian formulation requires more investigation. This will be assessed by examining more numerical applications.

REFERENCES

1. C. Truesdell, 'The elements of continuum mechanics', Springer-Verlag, New York (1966).
2. C. Truesdell, 'A first course in rational continuum mechanics, Volume 1: General Concepts', Academic Press, New York (1977).
3. L.E. Malvern, 'Introduction to the mechanics of a continuous medium', Prentice-Hall, Englewood Cliffs, New Jersey (1969).
4. J.T. Oden, 'Finite elements of nonlinear continua', McGraw-Hill, New York (1972).
5. K.J. Bathe, 'Finite element procedure in engineering analysis', Prentice-Hall, Englewood Cliffs, New Jersey (1982).
6. O.C. Zienkiewicz, 'The finite element method', 3rd ed., McGraw-Hill, New York (1977).
7. B.M. Irons and S. Ahmad, 'Techniques of finite elements', Halsted Press, New York (1980).
8. D.R.J. Owen and E. Hinton, 'Finite Element in Plasticity: Theory and Practice', Pineridge Press, London (1980).
9. E. Hinton and D.R.J. Owen, 'Finite element programming', Academic Press, New York (1977).
10. C.S. Desai and J.F. Abel, 'Introduction to the finite element method', Van Nostrand Reinhold Co. (1972).
11. J.H. Argyris, E. Krempl and K.J. Willam, "Constitutive models and finite element solution of inelastic behaviour", In: Formulations and Computational Algorithms in Finite Element Analysis: U.S.-Germany Symposium, K.J. Bathe et al. (eds.), 1976, 353-392.
12. J.H. Argyris, M. Kleiber and W.C. Knudson, "Elasto-plastic analysis of finite deformation problems", In: Formulations and Computational Algorithms in Finite Element Analysis: U.S.-Germany Symposium, K.J. Bathe et al. (eds.), 1976, 440-467.
13. J.H. Argyris and A.S.L. Chan, "Static and dynamic elasto-plastic analysis by the method of finite elements in space and time", Int. Symp. on Foundation of Plasticity, A. Sawczuk (ed.), 1973, 147-175.
14. K.J. Bathe, "Finite element formulation, modeling and solution of nonlinear dynamic problems", Chapter in Numerical Methods for Partial Differential Equations, S.V. Parter (ed.), Academic Press, New York (1979).

15. K.J. Bathe, "An assessment of current finite element analysis of nonlinear problems in solid mechanics", In: Numerical Solution of Partial Differential Equation III, B. Hubbard (ed.), Academic Press, New York (1976), 117-164.
16. K.J. Bathe (ed.), "Nonlinear finite element analysis and ADINA", Computers & Structures, 17 (1983), No. 5/6.
17. K.J. Bathe, E. Ramm and E.L. Wilson, "Finite element formulations for large deformation dynamic analysis", Int. J. Num. Meth. Engng., 9 (1975), 353-386.
18. K.J. Bathe, H. Ozdemir and E.L. Wilson, "Static and dynamic-geometric and material nonlinear analysis", Report No. SESM 74-4, Dept. Civil Engng., Univ. of California, Berkeley, 1974.
19. K.J. Bathe and H. Ozdemir, "Elastic plastic large deformation static and dynamic analysis", Computers & Structures, 6 (1976), 81-92.
20. K.J. Bathe and S. Bolourchi, "Large displacement analysis of three dimensional beam structures", Int. J. Num. Meth. Engng., 14 (1979), 961-986.
21. K.J. Bathe and S. Bolourchi, "A geometric and material nonlinear plate and shell element", Computers & Structures, 11 (1980), 23-48.
22. E. Ramm, "A plate/shell element for large deflections and rotations", In: Formulations and Computational Algorithms in Finite Element Analysis: U.S.-Germany Symposium, K.J. Bathe et al. (eds.), 1976, 264-293.
23. W. Wunderlich, "Incremental formulations for geometrically nonlinear problems", In: Formulations and Computational Algorithms in Finite Element Analysis: U.S.-Germany Symposium, K.J. Bathe et al. (eds.), 1976, 193-240.
24. P.G. Bergan and R.W. Clough, "Large deflection analysis of plates and shallow shells using the finite element method", Int. J. Num. Meth. Engng., 5 (1973), 543-556.
25. S. Cescotto, F. Frey and G. Fonder, "Total and updated Lagrangian descriptions in nonlinear structural analysis: a unified approach", Chapter in Energy Methods in Finite Element Analysis, R. Glowinski et al. (eds.), John Wiley and Sons, 1979.
26. S. Cescotto, F. Frey and C. Massonnet, "On the effective finite element analysis of engineering structures in the nonlinear range", IUTAM (1980), 67-78.
27. F. Frey and S. Cescotto, "Some new aspects of the incremental total Lagrangian description in nonlinear analysis", Int. Conf. on Finite Element in Nonlinear Solid and Structural Mechanics, Geilo, Norway (1977), 323-343.
28. G.F. Carey, "A unified approach to three finite element theories for geometric nonlinearity", Comput. Meth. Appl. Mech. Engng., 4 (1974), 69-79.

29. C.S. Desai and H.V. Phan, "Three-dimensional finite element analysis including material and geometric nonlinearities", *Computational Methods in Nonlinear Mechanics*, Proc. TICOM 2nd Int. Conf., J.T. Oden (ed.), 1979, 205-224.
30. L.D. Hofmeister, G.A. Greenbaum and D.A. Evensen, "Large strain, elastic-plastic finite element analysis", *AIAA J.*, 9 (1971), 1248-1255.
31. T. Ishizaki and K.J. Bathe, "On finite element large displacement and elastic-plastic dynamic analysis of shell structures", *Computers & Structures*, 12 (1980), 309-318.
32. S. Klein, "The nonlinear dynamic analysis of shells of revolution with asymmetric properties by the finite element method", *ASME Trans., J. Pressure Vessel Tech.*, 97 (1975), 163-171.
33. J.A. Stricklin, W.A. von Rieseemann, J.R. Tillerson and W.E. Haisler, "Static geometric and material nonlinear analysis", *Advances in Computational Methods in Structural Mechanics and Design*, 2nd U.S.-Japan Seminar Matrix Meth. Str. Anal. and Design, Univ. of Alabama Press, J.T. Oden et al. (eds.), 1972, 301-324.
34. J.A. Stricklin, W.E. Haisler and W.A. von Rieseemann, "Evaluation of solution procedures for material and/or geometrically nonlinear structural analysis", *AIAA*, 11 (1973), 292-299.
35. J.R. Tillerson, J.A. Stricklin and W.E. Haisler, "Numerical methods for the solution of nonlinear problems in structural analysis", in *Numerical Solution of Nonlinear Structural Problems*, R.F. Hartung (ed.), ASME-AMD, 6 (1973), 67-101.
36. J.A. Stricklin, W.E. Haisler and W.A. von Rieseemann, "Comments on nonlinear transient structural analysis", *Finite Element Analysis of Transient Nonlinear Structural Behavior*, T. Belytschko et al. (eds.), ASME-AMD, 14 (1975), 157-177.
37. J.A. Stricklin and W.E. Haisler, "Formulations and solution procedures for nonlinear structural analysis", *Computers & Structures*, 7 (1977), 125-136.
38. Y. Yamada, "Incremental formulation for problems with geometric and material nonlinearities", *Advances in Computational Methods in Structural Mechanics and Design*, 2nd U.S.-Japan Seminar Matrix Meth. Str. Anal. and Design, Univ. of Alabama Press, J.T. Oden et al. (eds.), 1972, 325-355.
39. J.T. Oden and J.E. Key, "Numerical analysis of finite axisymmetric deformations of incompressible elastic solids of revolution", *Int. J. Solids & Structures*, 6 (1970), 497-542.
40. J.T. Oden and J.E. Key, "Analysis of finite deformations of elastic solids by finite element method", *Proc. IUTAM Symp. on High Speed Computing of Elastic Structures*, 1970, 65-103.
41. J.T. Oden and J.E. Key, "On some generalizations of the incremental stiffness relations for finite deformations of compressible and incompressible finite elements", *Nucl. Engng. and Design*, 15 (1971), 121-134.

42. T. Belytschko and B.J. Hsieh, "Nonlinear transient finite element analysis with convected co-ordinates", *Int. J. Num. Meth. Engng.*, 7 (1973), 255-271.
43. D.W. Murray and E.L. Wilson, "Finite-element large deflection analysis of plates", *ASCE Proc., J. Engng. Mech. Div.*, 95 (1969), 143-165.
44. P.K. Larsen and E.P. Popov, "A note on incremental equilibrium equations and approximate constitutive relations in large inelastic deformations", *Acta Mechanica*, 19 (1974), 1-14.
45. R.A. Brockman, "MAGNA: A finite element system for three-dimensional nonlinear static and dynamic structural analysis", *Computers & Structures*, 13 (1981), 415-423.
46. M.S. Gadala, G.AE. Oravas and M.A. Dokainish, "Geometric and material nonlinearity problems - formulation aspects", *Proc. 1st Int. Conf. on Numerical Methods for Nonlinear Problems, Swansea, U.K., Sept. (1980)*, 317-331.
47. M.S. Gadala, M.A. Dokainish and G.AE. Oravas, "Geometric and material nonlinearity problems - Lagrangian and updated Lagrangian formulations", *Proc. 2nd Int. Conf. on Numerical Methods in Fracture Mechanics, Swansea, U.K. (1980)*, 277-293.
48. M.S. Gadala, G.AE. Oravas and M.A. Dokainish, "Continuum bases and consistent numerical formulations of nonlinear continuum mechanics problems", *Solid Mechanics Archives*, 9 (1984), 1-52.
49. M.S. Gadala, M.A. Dokainish and G.AE. Oravas, "Formulation methods of geometric and material nonlinearity problems", *Int. J. Num. Meth. Engng.*, 20 (1984), 887-914.
50. M.S. Gadala, "Nonlinear structural analysis - survey of formulation and solution methods", Report No. 83-279-K, Ontario Hydro Research, Ontario, Canada (1983).
51. M.S. Gadala, "On numerical solution of nonlinear problems of continua", Ph.D. thesis, McMaster University, Hamilton, Ontario, Canada (1980).
52. H.D. Hibbit, P.V. Marcal and J.R. Rice, "A finite element formulation for problems of large strain and displacement", *Int. J. Solids & Structures*, 6 (1970), 1069-1086.
53. P.V. Marcal, "Large strain, large displacement analysis", In: *Lectures on Finite Element Methods in Continuum Mechanics*, J.T. Oden et al. (eds.), The University of Alabama Press, in Huntsville, Alabama (1973), 535-543.
54. P.V. Marcal, "On consistent matrices for finite displacements and stability analysis", *Proc. ASCE Joint Speciality Conf. on Optimization and Nonlinear Problems, Chicago, IL (1968)*, 45-47.
55. P.V. Marcal, "Finite-element analysis of combined problems of non-linear material and geometric behaviour", *Computational Approaches in Applied Mechanics, Comp. Conf.*, E. Sevin (ed.), Chicago, IL (1969), 133-149.

56. P.V. Marcal, "Finite element analysis with material nonlinearities theory and practice", Recent Advances in Matrix Meth. Struc. Anal. and Design, R.H. Gallagher et al. (eds.), Univ. of Alabama Press, 1971, 257-282.
57. R.H. Mallett and P.V. Marcal, "Finite element analysis of nonlinear structures", ASCE Proc., J. Struc. Div., 94 (1968), 2081-2105.
58. H.C. Martin, "Finite element and the analysis of geometrically nonlinear problems", Recent Advances in Matrix Meth. Struc. Anal. and Design, R.H. Gallagher et al. (eds.), Univ. of Alabama Press, 1971, 343-381.
59. T. Kawai, "Finite element analysis of the geometrically nonlinear problems of elastic plates", Recent Advances in Matrix Meth. Struc. Anal. and Design, R.H. Gallagher et al. (eds.), Univ. of Alabama Press, 1971, 383-414.
60. B.J. Hartz and N.D. Nathan, "Finite element formulation of geometrically nonlinear problems in elasticity", Recent Advances in Matrix Meth. Struc. Anal. and Design, R.H. Gallagher et al. (eds.), Univ. of Alabama Press, 1971, 415-437.
61. S. Yaghmai and E.P. Popov, "Incremental analysis of large deflections of shells of revolution", Int. J. Solids & Structures, 7 (1971), 1375-1393.
62. S. Yaghmai, "Incremental analysis of large deformation in mechanics of solids with application to axisymmetric shells of revolution", NASA Contractor Report 1350 (1969).
63. P. Sharifi and E.P. Popov, "Nonlinear finite element analysis of sandwich shells of revolution", AIAA J., 11 (1973), 715-722.
64. D.P. Mondkar and G.H. Powell, "Finite element analysis of non-linear static and dynamic response", Int. J. Num. Meth. Engng., 11 (1977), 499-520.
65. M.T.E. Tuomala and M.J. Mikkola, "Transient dynamic large deflection analysis of elastic viscoplastic plates by finite element method", Int. J. Mech. Sci., 22 (1980), 151-166.
66. J.W. Hutchinson, "Finite strain analysis of elasto-plastic solids and structures", In: Numerical Solution of Nonlinear Structural Problems, R.F. Hartung (ed.), ASME-AMD, 6 (1973), 17-29.
67. C.A. Felippa and P. Sharifi, "Computer implementation of nonlinear finite element analysis", In: Numerical Solution of Nonlinear Structural Problems, R.F. Hartung (ed.), ASME-AMD, 6 (1973), 31-49.
68. S. Nagarajan and E.P. Popov, "Non-linear finite element dynamic analysis of axisymmetric solids", Earthquake Engng. and Struc. Dyn., 3 (1975), 385-399.
69. R.F. Jones, Jr. and J.E. Roderick, "Incremental solution procedure for nonlinear structural dynamic problems", ASME Trans. J. Pressure Vessel Tech., 95 (1975), 95-100.

70. R.F. Jones, Jr. and M.G. Costello, "A solution procedure for nonlinear structural problems", In: Numerical Solution of Nonlinear Structural Problems, R.F. Hartung (ed.), ASME-AMD, 6 (1973), 157-169.
71. J.F. McNamara and P.V. Marcal, "Incremental stiffness method for finite element analysis of the nonlinear dynamic problems", In: Numerical and Computer Methods in Structural Mechanics, Fenves et al. (eds.), 1973, 353-376.
72. R.M. McMeeking and R.J. Rice, "Finite-element formulations for problems of large elastic-plastic deformation", Int. J. Solids & Structures, 11 (1975), 601-616.
73. J.C. Nagtegaal and J.E. de Jong, "Some computational aspects of elastic-plastic large strain analysis", Computational Methods in Nonlinear Mechanics, Proc. TICOM 2nd Int. Conf., J.T. Oden (ed.), 1979, 303-339.
74. J.C. Nagtegaal and J.E. de Jong, "Some computational aspects of elastic-plastic large strain analysis", Int. J. Num. Meth. Engng., 17 (1981), 15-41.
75. J.S. Gunasekera and J.M. Alexander, "Matrix analysis of the large deformation of an elastic-plastic axially symmetric continuum", Int. Symp. on Foundation of Plasticity, A. Sawczuk (ed.), 1973, 125-146.
76. E.L. Wilson, I. Forhoomand and K.J. Bathe, "Nonlinear dynamic analysis of complex structures", Earthquake Engng. and Struc. Dyn., 1 (1973), 241-252.
77. R.H. Gallagher, "Finite element analysis of geometrically nonlinear problems", Theory and Practice in Finite Element Struc. Anal., Y. Yamada et al. (eds.), Univ. Tokyo Press, 1973, 109-123.
78. R.H. Gallagher, "Geometrically nonlinear finite element analysis", Proc. of the Speciality Conf. on Finite Element Method in Civil Engng., Montreal, Canada (1972), 3-33.
79. S.W. Key, "A finite element procedure for the large deformation dynamic response of axisymmetric solid", Comp. Meth. Appl. Mech. Engng., 4 (1974), 195-218.
80. M. Hartzman and J.R. Hutchinson, "Nonlinear dynamics of solids by the finite element method", Computers & Structures, 2 (1972), 47-77.
81. M. Hartzman, "Nonlinear dynamics of solids by finite element method", University of California, Lawrence Radiation Laboratory UCRL-50779 (1969). Also Ph.D. thesis, University of California, Davis, CA, 1969.
82. S. Nemat Nasser and H.D. Shatoff, "A consistent numerical method for the solution of nonlinear elasticity problems at finite strains", SIAM J. Appl. Math., 20 (1971), 462-481.
83. W. Fengels, "The superimposition of the finite element solutions with respect to Lagrange's and Euler's reference system", Mech. Res. Comm., 5(6), 1978, 341-346.

84. Y. Yamada, "Formulation of a solution procedure for nonlinear material and structure behaviour - Theoretical basis for the program composite III", Proc. of Int. Conf. on Comut. Simul. for Mater. Appl. Nucl. Metal., Part 2, 20 (1976), 826-837.
85. M.S. Gadala, G.AE. Oravas and M.A. Dokainish, "A consistent Eulerian formulation of large deformation problems in static and dynamic", Int. J. Nonlinear Mechanics, 18 (1983), 21-35.
86. K.A. Derbalian, E.H. Lee, R.L. Mallett and R.M. McMeeking, "Finite element metal forming analysis with spacially fixed mesh", Application of Numerical Methods for Forming Processes, ASME-AMD, 28 (1978), H. Armen et al. (eds.), 39-47.
87. J. Huetink, "Analysis of metal forming processes based on a combined Eulerian Lagrangian finite element formulation", Numerical Methods in Industrial Forming Processes, J.F.T. Pittman et al. (eds.), Pineridge Press, Swansea, U.K. (1982), 501-509.
88. P.J.G. Schreurs, F.E. Veldpaus and W.A.M. Brekelmans, "An arbitrary Eulerian-Lagrangian finite element model for the simulation of geometrical non-linear hyper-elastic and elasto-plastic deformation processes", Numerical Methods in Industrial Forming Processes, J.F.T. Pittman et al. (eds.), Pineridge Press, Swansea, U.K. (1982), 491-500.
89. K. Mori, K. Osakada and M. Fukuda, "Simulation of severe plastic deformation by finite element method with spatially fixed elements", Int. J. Mech. Sci., 25 (1983), 775-783.
90. J.H. Biffle and S.W. Key, "Finite element formulations for transient dynamic problems in solids using explicit time integration", Comp. Meth. Appl. Mech. Engng., 12 (1977), 323-336.
91. R.W. Clough and E.L. Wilson, "Dynamic analysis of large structural systems with local nonlinearities", Comp. Meth. Appl. Mech. Engng., 17/18 (1979), 107-129.
92. S. Nemat-Nasser, "Continuum bases for consistent numerical formulations of finite strains in elastic and inelastic structures", Finite Element Analysis of Transient Nonlinear Structural Behavior, T. Belytschko et al. (eds.), ASME-AMD, 14 (1975), 85-98.
93. H.D. Hibbit, "Some follower forces and load stiffness", Int. J. Num. Mech. Engng., 14 (1979), 937-941.
94. J.T. Holden, "On the finite deflections of thin beams", Int. J. Solids & Structures, 8 (1972), 1051-1055.
95. M. Kielber, "Kinematics of deformation processes in materials subjected to finite elastic-plastic strains", Int. J. Engng. Sci., 13 (1975), 513-525.
96. A. Needleman, "Finite element for finite strain plasticity problems", Report No. MRLE 134, Material Research Laboratory, Brown University, 1981.

97. E.H. Lee, R.L. Mallett and R.M. McMeeking, "Stress and deformation analysis of metal-forming processes", IUTAM., Metal Forming plasticity, H. Lippmann et al. (eds.), 1979, 177-189.
98. E.H. Lee, R.L. Mallett and W.H. Yang, "Stress and deformation analysis of the metal extrusion process", Comput. Meth. Appl. Mech. Engng., 10 (1977), 339-353.
99. E.H. Lee, R.L. Mallett and R.M. McMeeking, "Stress and deformation analysis of metal-forming processes", Numerical Modeling of Manufacturing Processes, ASME, R.F. Jones, Jr. et al. (eds.), 1977, 19-33.
100. J.C. Nagtegaal and F.E. Veldpaus, "Analysis of metal forming problems with an improved finite strain plasticity formulation", In: Numerical Methods in Industrial Forming Processes, J.F.T. Pittman et al. (eds.), Pineridge Press, Swansea, U.K., 1982, 1-15.
101. E.H. Lee and R.M. McMeeking, "Concerning elastic and plastic components of deformation", Int. J. Solids & Structures, 16 (1980), 715-721.
102. E.H. Lee, "Some comments on elastic-plastic analysis", SUDAM No. 80-5, Metal Forming Report 9, Stanford University, Dept. of Mech. Engng., Div. of Appl. Mech., 1980.
103. V.A. Lubarda and E.H. Lee, "A correct definition of elastic and plastic deformation and its computational significance", SUDAM No. 80-1, Metal Forming Report 7, Stanford University, Dept. of Mech. Engng., Div. of Appl. Mech., 1980.
104. Y. Yamada, "Nonlinear matrices, their implications and applications in inelastic large deformation analysis", Comp. Meth. Appl. Mech. Engng., 33 (1982), 417-437.
105. Y. Yamada, A.S. Wifi and T. Hirakawa, "Analysis of large deformation and stress in metal forming processes by the finite element method", IUTAM Metal Forming Plasticity, H. Lippman et al. (eds.), 1979, 158-176.
106. Y. Yamada and H. Hirakawa, "Large deformation and instability analysis in metal forming process", Applications of Numerical Methods in Forming Processes, ASME AMD, 28 (1978), H. Armen (eds.), 27-38.
107. Y. Yamada, T. Hirakawa and A.S. Wifi, "Analysis of large deformation and bifurcation in plasticity by the finite element method", Int. Conf. Finite Element Nonlinear Solid and Structural Mechanics, Geilo, Norway (1977), Vol. 1, 393-417.
108. Y. Yamada and T. Sakurai, "Basic formulation and a computer program for inelastic large deformation analysis", Press Vessel Technol., I, ASME, 1977, 341-352.
109. Y. Yamada, "Constitutive modeling of inelastic behavior and numerical solution of nonlinear problems by the finite element method", Computers & Structures, 8 (1978), 533-543.

110. Y. Yamada, K. Takatsuka and K. Iwata, "Nonlinear analysis by the finite element method and some expository examples", *Theory and Practice in Finite Element Struc. Anal.*, Y. Yamada et al. (eds.), Univ. Tokyo Press, 1973, 125-138.
111. Y. Yamada, N. Yoshimura and T. Sakurai, "Plastic stress-strain matrix and its application for the solution of elastic-plastic problems by the finite element method", *Int. J. Mech. Sci.*, 10 (1968), 343-354.
112. P.Y. Marcal, "A stiffness method for elastic-plastic problems", *Int. J. Mech. Sci.*, 7 (1965), 229-238.
113. S.M. Ma and K.J. Bathe, "On finite element analysis of pipe-whip problems", *Nucl. Engng. and Design*, 37 (1976), 413-430.
114. K.J. Bathe and A.P. Cimento, "Some practical procedures for the solution of nonlinear finite element equations", *Comp. Meth. Appl. Meth. Engng.*, 22 (1980), 59-85.
115. K.J. Bathe, S. Bolourchi, S. Ramaswamy and M.D. Snyder, "Some computational capabilities for nonlinear finite element analysis", *Nucl. Engng. and Design*, 46 (1978), 429-455.
116. E.H. Lee, "Elastic-plastic deformation at finite strains", *ASME Trans., J. Appl. Mech.*, 36 (1969), 1-6.
117. J.H. Heifitz and C.J. Costantino, "Dynamic response of nonlinear media at large strains", *ASCE Proc., J. Engng. Mech. Div.*, 98 (1972), 1511-1528.
118. T.B. Wertheimer, "Problems in large deformation elastic-plastic analysis using the finite element method", Ph.D. thesis, Stanford University, Palo Alto, California, 1982.
119. O.C. Zienkiewicz and P.N. Godbole, "Flow of plastic and visco-plastic solids with special reference to extrusion and forming processes", *Int. J. Num. Meth. Engng.*, 8 (1974), 3-16.
120. O.C. Zienkiewicz, O.C. Jain and E. Onate, "Flow of solids during forming and extrusion: some aspects of numerical solutions", *Int. J. Solids & Structures*, 14 (1978), 15-38.
121. A. Chandra and S. Mukherjee, "A finite element analysis of metal-forming problems with an elastic-viscoplastic material model", *Int. J. Num. Meth. Engng.*, 20 (1984), 1613-1628.
122. J.C. Nagtegaal, D.M. Parks and J.R. Rice, "On numerically accurate finite element solutions in the fully plastic range", *Comp. Meth. Appl. Mech. Engng.*, 4 (1974), 153-177.
123. D.J. Naylor, "Stresses in nearly-incompressible materials by finite elements with application to the calculation of excess pore pressures", *Int. J. Num. Meth. Engng.*, 8 (1974), 443-460.

124. D.R. Dawson and E.G. Thompson, "Finite element analysis of steady-state elasto-visco-plastic flow by the initial stress-rate method", *Int. J. Num. Meth. Engng.*, 12 (1978), 47-57.
125. L.R. Herrman, "Elasticity equations for incompressible and nearly incompressible materials by variational theorem", *AIAA J.*, 3 (1965), 1896-1900.
126. I. Fried, "Finite element analysis of incompressible material by-residual energy balance", *Int. J. Solids & Structures*, 10 (1974), 993-1002.
127. O.C. Zienkiewicz and E. Hinton, "Reduced integration, function smoothing and non-conformity in finite element analysis", *J. Franklin Inst.*, 302 (1976), 443-461.
128. T.J.R. Hughes, "Equivalence of finite element for nearly incompressible elasticity", *ASME Trans., J. Appl. Mech.*, 44 (1977), 181-183.
129. D.S. Malkus, "A finite element displacement model valid for any value of the incompressibility", *Int. J. Solids & Structures*, 12 (1976), 731-738.
130. C. Truesdell and W. Noll, "The nonlinear field theories of mechanics", In: *Encyclopedia of Physics*, S. Flugge (ed.), vol. III/3, Springer-Verlag, 1975.
131. R. Hill, "A general theory of uniqueness and stability in elastic-plastic solids", *J. Mech. Phys. Solids*, 6 (1958), 236-249.
132. R. Hill, "Some basic principles in the mechanics of solids without a natural time", *J. Mech. Phys. Solids*, 7 (1959), 209-225.
133. R. Hill, "On constitutive inequalities for simple materials - I", *J. Mech. Phys. Solids*, 16 (1968), 229-242.
134. R. Hill, "On constitutive inequalities for simple materials - II", *J. Mech. Phys. Solids*, 16 (1968), 315-322.
135. Y. Yokoo, T. Nakamura and K. Uetani, "The incremental perturbation method for large displacement analysis of elastic-plastic structures", *Int. J. Num. Meth. Engng.*, 10 (1976), 503-525.
136. J.T. Oden and L.C. Wellford Jr., "Analysis of flow of viscous fluids by the finite method", *AIAA J.*, 10 (1972), 1590-1599.
137. J.T. Oden, "The finite element method in fluid mechanics", In: *Lectures on Finite Element Methods in Continuum Mechanics*, J.T. Oden et al. (eds.), The Univ. of Alabama Press in Huntsville (1973), 151-186.
138. K.J. Bathe and C.A. Almeida, "A simple and effective pipe elbow element-linear analysis", *ASME Trans., J. Appl. Mech.*, 47 (1980), 93-100.
139. N.W. Newmark, "A method of computation for structural dynamics", *Proc. ASCE, Engng. Mech. Div.*, 85 (1959), 67-94.

140. K.J. Bathe and E.L. Wilson, "Stability and accuracy analysis of direct integration methods", *Earthquake Engng. and Str. Dyn.*, 1 (1973), 283-291.
141. F. Brauer and J.A. Nohel, 'Ordinary differential equations: a first course', W.A. Benjamin, Inc., New York, 1967.
142. S. Nemat-Nasser et al. (eds.), "Theoretical foundation for large-scale computations of nonlinear material behavior", *Proc. Workshop on the Theor. Foun. of Large-Scale Comput. Nonlinear Material Behavior*, Martinus Nijhoff Publi., 1984.
143. E.H. Lee, "Finite deformation effects in plasticity analysis", In: *Numerical Methods in Industrial Forming Processes*, J.F.T. Pittman et al. (eds.), Pineridge Press, Swansea, U.K., 1982, 39-50.

APPENDIX A

TRANSFORMATION OF THE VIRTUAL WORK PRINCIPLE

The virtual work principle in the current deformed state is:

$$\int_{2V} \bar{\sigma} : \delta \bar{e} \, d^2V + \int_{2V} \rho \bar{a} \cdot \delta \bar{u} \, d^2V = \int_{2V} \rho \bar{b} \cdot \delta \bar{u} + \int_{2A} d^2\bar{\Lambda} \cdot \bar{\sigma} \cdot \delta \bar{u} \quad (\text{A.1})$$

where all individual terms are defined in Chapter I. The transformation of the virtual work principle from the current configuration to the reference configuration can be carried out term by term as follows:

• Strain energy,

$$\int_{2V} \bar{\sigma} : \delta \bar{e} \, d^2V$$

after substituting the transformations

$$\bar{\sigma} = \frac{1}{|J|} \bar{F} \cdot \bar{S} \cdot \bar{F}^T \text{ and } d^2V = |J| d^0V \quad (\text{A.2})$$

becomes

$$\int_{2V} \bar{\sigma} : \delta \bar{e} \, d^2V = \int_{0V} (\bar{F} \cdot \bar{S} \cdot \bar{F}^T) : \delta \bar{e} \, d^0V$$

From the definition of double-dot product of two second-order tensors, it can be proven that

$$\bar{B} : \bar{C} = (\bar{B} \cdot \bar{C}) : \bar{1} = (\bar{B} \cdot \bar{C}) : \bar{1} \quad (\text{A.3})$$

where \bar{B} and \bar{C} are general second order tensors and $\bar{1}$ is the identity tensor. Considering eqn.

(A.3) and utilizing the symmetry of $\delta \bar{e}$, we obtain

$$\begin{aligned}
\int_{2V} \bar{\sigma}^2 : \delta \bar{e}^2 &= \int_{0V} (\bar{F}^2 : \bar{S}^2 : \bar{F}^{2T}) : \delta \bar{e}^2 d^0V = \int_{0V} (\bar{F}^2 : \bar{S}^2) : (\bar{F}^{2T} : \delta \bar{e}^2) : \bar{I} d^0V \\
&= \int_{0V} (\bar{F}^2 : \bar{S}^2) : (\delta \bar{e}^2 : \bar{F}^2) d^0V \\
&= \int_{0V} (\bar{F}^2 : \bar{S}^2)^T : (\delta \bar{e}^2 : \bar{F}^2) : \bar{I} d^0V \\
&= \int_{0V} (\bar{S}^2 : \bar{F}^{2T}) : (\delta \bar{e}^2 : \bar{F}^2) : \bar{I} d^0V
\end{aligned}$$

where the symmetry of \bar{S}^2 has been employed

$$\begin{aligned}
&= \int_{0V} (\bar{S}^2 : \bar{F}^{2T} : \delta \bar{e}^2 : \bar{F}^2) : \bar{I} d^0V \\
&= \int_{0V} \bar{I} \bar{S}^2 : (\bar{F}^{2T} : \delta \bar{e}^2 : \bar{F}^2) : \bar{I} d^0V \\
&= \int_{0V} \bar{I} \bar{S}^2 : (\bar{F}^{2T} : \delta \bar{e}^2 : \bar{F}^2) d^0V
\end{aligned}$$

since

$$\delta_0 \bar{E}^2 = \bar{F}^{2T} : \delta \bar{e}^2 : \bar{F}^2$$

where $\delta_0 \bar{E}^2$ is the variation of the Green-Lagrange strain tensor, then

$$\int_{2V} \bar{\sigma}^2 : \delta \bar{e}^2 = \int_{0V} \bar{I} \bar{S}^2 : \delta_0 \bar{E}^2 d^0V \quad (\text{A.4})$$

* Inertia Force,

$$\int_{2V} \bar{\rho}^2 \bar{a}^2 : \delta \bar{u}^2 d^2V = \int_{0V} \bar{\rho}^0 \bar{a}^0 : \delta \bar{u}^0 d^0V \quad (\text{A.5})$$

* Body Force,

$$\int_{2V} \bar{\rho}^2 \bar{b}^2 : \delta \bar{u}^2 d^2V = \int_{0V} \bar{\rho}^0 \bar{b}^0 : \delta \bar{u}^0 d^0V \quad (\text{A.6})$$

• Surface Traction.

$$\int_{2_A} d^2 \bar{A} \cdot {}^2 \bar{\sigma} \cdot \delta^2 \bar{u}$$

$$= \int_{0_A} \left(d^0 \bar{A} \cdot \frac{d^2 \bar{A}}{d^0 \bar{A}} \right) \cdot {}^2 \bar{\sigma} \cdot \delta^2 \bar{u}$$

but

$$\frac{d^2 \bar{A}}{d^0 \bar{A}} = |{}_0^2 \bar{F}| {}_0^2 \bar{F}^{-1}$$

then

$$\int_{2_A} d^2 \bar{A} \cdot {}^2 \bar{\sigma} \cdot \delta^2 \bar{u} = \int_{0_A} (d^0 \bar{A} \cdot |{}_0^2 \bar{F}| {}_0^2 \bar{F}^{-1}) \cdot {}^2 \bar{\sigma} \cdot \delta^2 \bar{u}$$

$$= \int_{0_A} d^0 \bar{A} \cdot (|{}_0^2 \bar{F}| {}_0^2 \bar{F}^{-1} \cdot {}^2 \bar{\sigma}) \cdot \delta^2 \bar{u}$$

$$= \int_{0_A} d^0 \bar{A} \cdot {}_0^2 \bar{T} \cdot \delta^2 \bar{u}$$

where ${}_0^2 \bar{T}$ is the first Piola-Kirchhoff stress tensor, since

$${}_0^2 \bar{T} = {}_0^2 \bar{S} \cdot {}_0^2 \bar{F}^T$$

then

$$\int_{2_A} d^2 \bar{A} \cdot {}^2 \bar{\sigma} \cdot \delta^2 \bar{u} = \int_{0_A} d^0 \bar{A} \cdot {}_0^2 \bar{T} \cdot \delta^2 \bar{u} = \int_{0_A} d^2 \bar{A} \cdot {}_0^2 \bar{S} \cdot {}_0^2 \bar{F}^T \cdot \delta^2 \bar{u} \quad (\text{A.7})$$

Substituting eqns. (A.4-A.7) into eqn. (A.1), the virtual work principle referred to the initial (undeformed) configuration is:

$$\int_{0_V} {}_0^2 \bar{S} \cdot {}_0^2 \bar{E} + \int_{0_V} {}_0^p {}^2 \bar{a} \cdot \delta^2 \bar{u} \, d^0 V = \int_{0_V} {}_0^p {}^2 \bar{b} \cdot \delta^2 \bar{u} \, d^0 V$$

$$+ \int_{0_A} d^0 \bar{A} \cdot {}_0^2 \bar{S} \cdot {}_0^2 \bar{F}^T \cdot \delta^2 \bar{u} \quad (\text{A.8})$$

APPENDIX B

SHAPE FUNCTIONS AND SHAPE FUNCTION DERIVATIVES OF THE ISOPARAMETRIC 8-NODE PLANE ELEMENT

Starting with the expression of the displacement vector of a point in the element, eqn. (III.82), the components of the displacement vector ${}^t u_i$ may be expressed in the form

$${}^t u_i = \psi_{ia} \underline{{}^t u}_a \quad i = 1, 2 \quad (B.1)$$

where

$$\psi_{ia} = \begin{bmatrix} h_K & 0 \\ 0 & h_K \end{bmatrix} \quad (B.2)$$

for node K

are the shape functions, h_K are the interpolation function, and

$$\{\underline{{}^t u}_a\}^T = \{u_1^K, u_2^K\}, \quad K = 1, 2, 3, \dots, 8 \quad (B.3)$$

is the nodal displacements vector.

The displacement derivatives corresponding to the global axes ${}^t x_1$ and ${}^t x_2$, may be obtained as

$$\frac{\partial {}^t u_i}{\partial {}^t x_j} = \frac{\partial \psi_{ia}}{\partial {}^t x_j} \underline{{}^t u}_a \quad (B.4)$$

where

$$\begin{bmatrix} \frac{\partial \psi_{1a}}{\partial {}^t x_1} \\ \frac{\partial \psi_{1a}}{\partial {}^t x_2} \end{bmatrix} = \underline{{}^t J}^{-1} \begin{bmatrix} \frac{\partial h_K}{\partial r} & 0 \\ \frac{\partial h_K}{\partial s} & 0 \end{bmatrix} \quad \begin{bmatrix} \frac{\partial \psi_{2a}}{\partial {}^t x_1} \\ \frac{\partial \psi_{2a}}{\partial {}^t x_2} \end{bmatrix} = \underline{{}^t J}^{-1} \begin{bmatrix} 0 & \frac{\partial h_K}{\partial r} \\ 0 & \frac{\partial h_K}{\partial s} \end{bmatrix} \quad (B.5)$$

for node K

for node K

are the shape function derivatives, and $[J]^{-1}$ is the inverse of the Jacobian matrix. The Jacobian matrix relates the global derivatives to the local (natural) derivatives, and is defined as follows

$$[J]^{-1} = \begin{bmatrix} \frac{\partial^t x_1}{\partial r} & \frac{\partial^t x_2}{\partial r} \\ \frac{\partial^t x_1}{\partial s} & \frac{\partial^t x_2}{\partial s} \end{bmatrix} \quad (B.6)$$

APPENDIX C
THE RELATION BETWEEN HOOKEAN TENSOR AND
STRESS-STRAIN MATRIX

In this Appendix, the constitutive equations and the stress-strain relations are considered in general form which can be applied in both the Lagrangian formulation and the Eulerian formulation. As discussed in Section III.1.4, the constitutive equations may be written in the form

$$\Delta^1 \bar{\sigma} = {}_1 \bar{D} : \Delta^1 \bar{\epsilon} \quad (C.1)$$

where $\Delta^1 \bar{\sigma}$ and $\Delta^1 \bar{\epsilon}$ represent the increment of Cauchy stress and Euler strain tensors whereas, in both Lagrangian formulations $\Delta^1 \bar{\sigma}$ will be replaced by the increment of the second Piola-Kirchhoff stress tensor and $\Delta^1 \bar{\epsilon}$ will be the increment of the Green-Lagrange strain tensor. Equation (C.1) has the components

$$\Delta^1 \sigma_{ij} = {}_1 D_{ijkl} \Delta^1 \epsilon_{kl} \quad (C.2)$$

It should be observed that the tensor ${}_1 \bar{D}$ is symmetric in the following sense:

$${}_1 D_{ijkl} = {}_1 D_{ijlk} = {}_1 D_{jikl} = {}_1 D_{jilk}$$

Making use of this symmetry results in only 36 distinct values for the fourth order tensor, ${}_1 \bar{D}$, see, for example, reference [3]. On the other hand, for elastic and hyperelastic material, the stress-strain relation may be expressed as follows

$$\{\Delta^1 \sigma\} = [C] \{\Delta^1 \epsilon\} \quad (C.3)$$

or

$$\begin{bmatrix} \Delta^1 \sigma_{11} \\ \Delta^1 \sigma_{22} \\ \Delta^1 \sigma_{33} \\ \Delta^1 \sigma_{12} \\ \Delta^1 \sigma_{23} \\ \Delta^1 \sigma_{31} \end{bmatrix} = C_{ij} \begin{bmatrix} \Delta^1 \epsilon_{11} \\ \Delta^1 \epsilon_{22} \\ \Delta^1 \epsilon_{33} \\ \Delta^1 \gamma_{12} \\ \Delta^1 \gamma_{23} \\ \Delta^1 \gamma_{31} \end{bmatrix} \quad (C.4)$$

where C_{ij} is the matrix relating the stress vector $\{\Delta^1 \sigma\}$ to the strain vector $\{\Delta^1 \epsilon\}$. Comparing eqn. (C.2) with eqn. (C.4), we obtain a relationship between ${}_1 D_{ijkl}$ and C_{ij} , for example

$${}_1 D_{1111} = C_{11}, \quad {}_1 D_{1122} = C_{12}$$

$${}_1 D_{1112} \Delta \epsilon_{12} + {}_1 D_{1121} \Delta \epsilon_{21} = 2 C_{14} \Delta \epsilon_{12}$$

utilizing the symmetry of both the Hookean tensor ${}_1 \bar{D}$ and the strain tensor $\Delta^1 \epsilon_{kl}$, the above relation gives

$${}_1 D_{1112} = {}_1 D_{1121} = C_{14}$$

and so on.

Finally, owing to the symmetry of the matrix C_{ij} , the number of the independent constants in the Hookean tensor, ${}_1 \bar{D}$ is further reduced to 21 only

ELASTO-PLASTIC ANALYSIS

In this section, the basic laws governing elasto plastic material behaviour are briefly discussed, for more details see, for example [8,56,111,112]. In the following, the von Mises yield criterion and the associated flow rule have been employed. Once again, the equations presented in this section are applied to the Lagrangian, the updated Lagrangian, and the Eulerian formulation. According to the von Mises yield criterion, yielding begins when the effective stress σ exceeds the yield point, that is

$$\underline{\sigma} = \left[\frac{3}{2} (s_{ij}^1 s_{ij}^1) \right]^{1/2} \quad (C.5)$$

where s_{ij}^1 are the deviatoric stresses.

In general, after initial yielding the material behaviour will be partly elastic and partly plastic. During any incremental step, the resulting strain $\{\Delta^1 \epsilon\}$, can be linearly decomposed into elastic strain $\{\Delta^1 \epsilon\}_e$, and plastic strain $\{\Delta^1 \epsilon\}_p$, as

$$\{\Delta^1 \epsilon\} = \{\Delta^1 \epsilon\}_e + \{\Delta^1 \epsilon\}_p \quad (C.6)$$

Since the elastic part of the total strain is the only strain that can be associated with change in stresses, the increment of the stress vector is given by

$$\{\Delta^1 \sigma\} = [C] \{\Delta^1 \epsilon\}_e = [C] (\{\Delta^1 \epsilon\} - \{\Delta^1 \epsilon\}_p) \quad (C.7)$$

The flow rule or the Prandtl-Reuss relations state that

$$\{\Delta^1 \epsilon\}_p = \left\{ \frac{\partial g}{\partial s_{ij}^1} \right\} \Delta \underline{\epsilon}_p \quad (C.8)$$

where $\Delta \underline{\epsilon}_p$ is the effective plastic strain increment.

The von Mises yield criterion can be written in its incremental form as

$$\Delta \underline{\sigma} = \left\{ \frac{\partial g}{\partial s_{ij}^1} \right\}^T \{\Delta^1 \sigma\} \quad (C.9)$$

By multiplying eqn. (C.7) by $(\partial g / \partial s_{ij}^1)^T$ and using eqns. (C.8, C.9), we obtain an expression for the effective plastic strain increment $\Delta \underline{\epsilon}_p$

$$\Delta \underline{\epsilon}_p = \frac{\left\{ \frac{\partial g}{\partial s_{ij}^1} \right\}^T [C]}{H + \left\{ \frac{\partial g}{\partial s_{ij}^1} \right\}^T [C] \left\{ \frac{\partial g}{\partial s_{ij}^1} \right\}} \{\Delta^1 \epsilon\} = \{W\}^T \{\Delta^1 \epsilon\} \quad (C.10)$$

where H is the strain-hardening modulus and is defined as

$$H = \frac{d \underline{\sigma}}{d \underline{\epsilon}_p} = \frac{E E_t}{E - E_t} \quad (C.11)$$

in which E_t is the tangent modulus.

Substituting for the equivalent plastic strain, eqn. (C.10), into eqn. (C.8) and the result into eqn. (C.7), an incremental stress-strain relation may be obtained as

$$\{\Delta^1 \sigma\} = \left([C] - [C] \left\{ \frac{\partial \sigma}{\partial^1 \sigma_{ij}} \right\} \{W\}^T \right) \{\Delta^1 \epsilon\} = [C]_{ep} \{\Delta^1 \epsilon\} \quad (C.12)$$

where $[C]_{ep}$ is the elasto-plastic compliance matrix which can be used beyond the proportional limit.

APPENDIX D

SHAPE FUNCTIONS AND SHAPE FUNCTION DERIVATIVES OF THE ISOPARAMETRIC 3-NODE BEAM ELEMENT

Starting with the expression of the displacement vector of a point in the beam element; eqn (II.95), the components of the displacement vector ${}^t u_i$ may be put in the form

$${}^t u_i = \psi_{ia} {}^t \underline{u}_a \quad i = 1, 2, 3 \quad (D.1)$$

where

$$\psi_{ia} = \begin{bmatrix} h_K(1) & 0 & 0 & 0 & Q_3 & -Q_2 \\ h_K(0) & 1 & 0 & -Q_3 & 0 & Q_1 \\ h_K(0) & 0 & 1 & Q_2 & -Q_1 & 0 \end{bmatrix} \quad (D.2)$$

for node K

are the shape functions;

$$Q_j = \frac{s}{2} a_K {}^0 V_{sj}^K + \frac{t}{2} b_K {}^0 V_{tj}^K$$

and

$$\{ {}^t \underline{u}_a \}^T = \{ {}^t u_1^K \quad {}^t u_2^K \quad {}^t u_3^K \quad {}^t \theta_1^K \quad {}^t \theta_2^K \quad {}^t \theta_3^K \} \quad K = 1, 2, 3 \quad (D.4)$$

is the nodal displacements vector.

To calculate the global shape function derivatives, i.e., the derivatives corresponding to the global axes ${}^0 x_1$, ${}^0 x_2$ and ${}^0 x_3$, these derivatives are first obtained referred to the natural coordinates r, s, and t:

$$\begin{bmatrix} \frac{\partial t_{u_i}}{\partial r} \\ \frac{\partial t_{u_i}}{\partial s} \\ \frac{\partial t_{u_i}}{\partial t} \end{bmatrix} = \sum_{K=1}^3 \begin{bmatrix} \frac{\partial h_K}{\partial r} \left(1 & {}^0[g_{11}]^K & {}^0[g_{12}]^K & {}^0[g_{13}]^K \right) \\ h_K \left(0 & {}^0[\hat{g}_{11}]^K & {}^0[\hat{g}_{12}]^K & {}^0[\hat{g}_{13}]^K \right) \\ h_K \left(0 & {}^0[\bar{g}_{11}]^K & {}^0[\bar{g}_{12}]^K & {}^0[\bar{g}_{13}]^K \right) \end{bmatrix} \begin{bmatrix} t_{u_i}^K \\ t_{\theta_1}^K \\ t_{\theta_2}^K \\ t_{\theta_3}^K \end{bmatrix} \quad (D.4)$$

where

$${}^0[g_{ij}]^K = s {}^0[\hat{g}_{ij}]^K + t {}^0[\bar{g}_{ij}]^K \quad i, j = 1, 2, 3 \quad (D.5)$$

$${}^0[\hat{g}_{ij}]^K = \frac{1}{2} a_K \begin{bmatrix} 0 & {}^0V_{s3}^K & -{}^0V_{s2}^K \\ -{}^0V_{s3}^K & 0 & {}^0V_{s1}^K \\ {}^0V_{s2}^K & -{}^0V_{s1}^K & 0 \end{bmatrix} \quad (D.6)$$

and

$${}^0[\bar{g}_{ij}]^K = \frac{1}{2} b_K \begin{bmatrix} 0 & {}^0V_{t3}^K & -{}^0V_{t2}^K \\ -{}^0V_{t3}^K & 0 & {}^0V_{t1}^K \\ {}^0V_{t2}^K & -{}^0V_{t1}^K & 0 \end{bmatrix} \quad (D.7)$$

The displacement derivatives corresponding to the axes 0x_1 , 0x_2 and 0x_3 , are now obtained using the Jacobian transformation:

$$\begin{bmatrix} \frac{\partial t_{u_i}}{\partial {}^0x_1} \\ \frac{\partial t_{u_i}}{\partial {}^0x_2} \\ \frac{\partial t_{u_i}}{\partial {}^0x_3} \end{bmatrix} = \sum_{K=1}^3 {}^0[J]^{-1} \begin{bmatrix} \frac{\partial h_K}{\partial r} \left(1 & {}^0[g_{11}]^K & {}^0[g_{12}]^K & {}^0[g_{13}]^K \right) \\ h_K \left(0 & {}^0[\hat{g}_{11}]^K & {}^0[\hat{g}_{12}]^K & {}^0[\hat{g}_{13}]^K \right) \\ h_K \left(0 & {}^0[\bar{g}_{11}]^K & {}^0[\bar{g}_{12}]^K & {}^0[\bar{g}_{13}]^K \right) \end{bmatrix} \begin{bmatrix} t_{u_i}^K \\ t_{\theta_1}^K \\ t_{\theta_2}^K \\ t_{\theta_3}^K \end{bmatrix} \quad (D.8)$$

or

$$\frac{\partial {}^t u_i}{\partial {}^0 x_j} = \frac{\partial \psi_{ia}}{\partial {}^0 x_j} {}^t u_a$$

where

$$\frac{\partial \psi_{ia}}{\partial {}^0 x_j} = {}^0 [J]^{-1} \begin{bmatrix} \frac{\partial h_K}{\partial r} \left(1 & {}^0 [g_{11}]^K & {}^0 [g_{12}]^K & {}^0 [g_{13}]^K \right) \\ h_K \left(0 & {}^0 [\hat{g}_{11}]^K & {}^0 [\hat{g}_{12}]^K & {}^0 [\hat{g}_{13}]^K \right) \\ h_K \left(0 & {}^0 [\bar{g}_{11}]^K & {}^0 [\bar{g}_{12}]^K & {}^0 [\bar{g}_{13}]^K \right) \end{bmatrix} \quad (D.9)$$

for node K

are the shape function derivatives.

Starting with

$${}^{t+\Delta t} u_i = \sum_{K=1}^3 h_K {}^{t+\Delta t} u_i^K + \frac{\Delta t}{2} \sum_{K=1}^3 a_k h_k ({}^{t+\Delta t} v_{si}^K - {}^t v_{si}^K) + \frac{t}{2} \sum_{K=1}^3 b_k h_k ({}^{t+\Delta t} v_{ti}^K - {}^t v_{ti}^K)$$

and following procedures similar to the above, we obtain

$$\frac{\partial \psi_{ia}}{\partial {}^t x_j} = {}^t [J]^{-1} \begin{bmatrix} \frac{\partial h_K}{\partial r} \left(1 & {}^t [g_{11}]^K & {}^t [g_{12}]^K & {}^t [g_{13}]^K \right) \\ h_K \left(0 & {}^t [\hat{g}_{11}]^K & {}^t [\hat{g}_{12}]^K & {}^t [\hat{g}_{13}]^K \right) \\ h_K \left(0 & {}^t [\bar{g}_{11}]^K & {}^t [\bar{g}_{12}]^K & {}^t [\bar{g}_{13}]^K \right) \end{bmatrix} \quad (D.10)$$

for node K

0

APPENDIX E
 TRANSFORMATION OF THE SHAPE FUNCTION DERIVATIVES
 FROM THE GLOBAL AXES TO THE LOCAL AXES

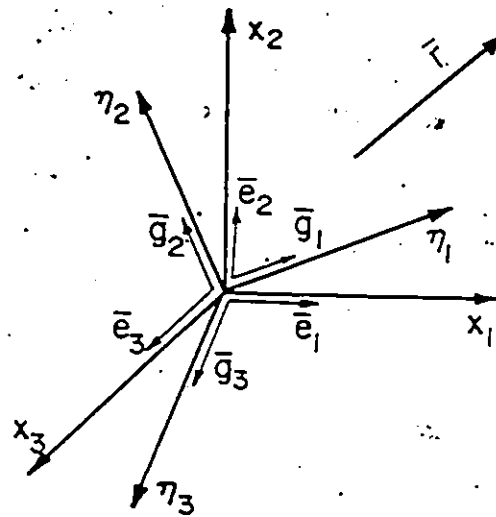


Figure (E.1)

Consider the two sets of axes - the global and the local axes x_i and η_i ($i = 1, 2, 3$) - at any integration point as shown in Figure (E.1). A general vector \bar{r} can be referred to the two orthonormal bases as follows:

$$\bar{r} = x_i \bar{e}_i = \eta_i \bar{g}_i \quad (E.1)$$

and

$$x_i = \eta_j (\bar{g}_j \cdot \bar{e}_i) \quad i, j = 1, 2, 3 \quad (E.2)$$

The local derivatives can be expressed as

$$\frac{\partial}{\partial \eta_j} = \frac{\partial x_i}{\partial \eta_j} \frac{\partial}{\partial x_i} \quad i, j = 1, 2, 3 \quad (\text{E.3})$$

from eqn. (E.2), we have

$$\frac{\partial x_i}{\partial \eta_j} = \bar{g}_j \cdot \bar{e}_i \quad (\text{E.4})$$

Therefore, the local derivatives become:

$$\frac{\partial}{\partial \eta_j} = (\bar{g}_j \cdot \bar{e}_i) \frac{\partial}{\partial x_i} \quad (\text{E.5})$$

Considering the invariance of the displacement vector:

$$\bar{u} = u_i \bar{e}_i = u_{\eta_i} \bar{g}_i$$

then

$$u_{\eta_i} = (\bar{g}_i \cdot \bar{e}_j) u_j \quad i, j = 1, 2, 3$$

Therefore, the local displacement vector derivatives can be written as

$$\frac{\partial u_{\eta_i}}{\partial \eta_j} = (\bar{g}_j \cdot \bar{e}_k) \left[(\bar{g}_i \cdot \bar{e}_\ell) \frac{\partial u_\ell}{\partial x_k} \right]$$

$k, j, k, \ell = 1, 2, 3$

In a similar procedure, the local shape function derivatives can be expressed as

$$\frac{\partial \psi_{ia}}{\partial \eta_j} = (\bar{g}_j \cdot \bar{e}_k) \left[(\bar{g}_i \cdot \bar{e}_\ell) \frac{\partial \psi_{\ell a}}{\partial x_k} \right]$$

It should be noticed that this transformation must be performed at each integration point. In the Lagrangian formulation, the direction cosines of the unit vectors \bar{g}_i with respect to the unit vector \bar{e}_i are calculated in each integration point around the circumference, whereas, in the updated Lagrangian formulation besides the transformation around the circumference, there is also a transformation due to the bend of the pipe element.